T.C.
DOKUZ EYLÜL UNIVERSITY
İZMİR INTERNATIONAL
BIOMEDICINE AND
GENOME INSTITUTE

INVESTIGATION OF ALTERATIONS CREATED BY NLRP3 ACTIVATION ON PERINEURONAL NETS

EMRE TARAKÇIOĞLU

MOLECULAR BIOLOGY AND GENETICS

PhD THESIS

İZMİR-2024

THESIS CODE: DEU.IBG.PhD-2017850010

T.C.
DOKUZ EYLÜL UNIVERSITY
İZMİR INTERNATIONAL
BIOMEDICINE AND
GENOME INSTITUTE

INVESTIGATION OF ALTERATIONS CREATED BY NLRP3 ACTIVATION ON PERINEURONAL NETS

MOLECULAR BIOLOGY AND GENETICS

PhD THESIS

EMRE TARAKÇIOĞLU

Advisor: Prof. Dr. Şermin GENÇ
Co-advisor: Assoc. Prof. Kemal Uğur TÜFEKCİ

(This research was supported by DEÜ BAP grant FDK-2022-2701
and TÜBİTAK 3501 grant 321S141)

THESIS CODE: DEU.IBG.PhD-2017850010

PhD Thesis Defense Examination Minutes

Dokuz Eylül University İzmir International Biomedicine and Genome Institute, Department Of Genomics And Molecular Biotechnology, Molecular Biology and Genetics Integrated PhD Programme student (number 2017850010) Emre Tarakçıoğlu's PhD thesis "**Investigation of Alterations Created by NLRP3 Activation on Perineuronal Nets**" was found successful following the defence examination held on 25/09/2024.

Prof. Dr. Şermin Genç
HEAD OF JURY

Assoc. Prof. Dr. Duygu Sağ
JURY MEMBER

Prof. Dr. Latife Arzu Aral
JURY MEMBER

Dr. Öğr. Üyesi Yavuz Oktay
JURY MEMBER

Dr. Öğr. Üyesi Ayşe Banu Demir
JURY MEMBER

DOKTORA TEZ SAVUNMA SINAVI TUTANAĞI

Dokuz Eylül Üniversitesi İzmir Uluslararası Biyotıp ve Genom Enstitüsü Genom Bilimleri ve Moleküler Biyoteknoloji Anabilim Dalı Moleküler Biyoloji ve Genetik Bütünleşik Doktora Programı 2017850010 numaralı öğrencisi Emre Tarakçıoğlu'nun "**NLRP3 inflamazom aktivasyonunun perinöronal ağlarda yarattığı değişikliklerin incelenmesi**" konulu Doktora tezi 25/09/2024 tarihinde yapılan savunma sınavı sonucunda başarılı bulunmuştur.

Prof. Dr. Şermin Genç
BAŞKAN

Doç. Dr. Duygu Sağ
JÜRİ ÜYESİ

Prof. Dr. Latife Arzu Aral
JÜRİ ÜYESİ

Dr. Öğr. Üyesi Yavuz Oktay
JÜRİ ÜYESİ

Dr. Öğr. Üyesi Ayşe Banu Demir
JÜRİ ÜYESİ

TABLE OF CONTENTS

TABLE OF CONTENTS i

Table Index iii

Figure Index iii

List of Abbreviations iv

Acknowledgement vi

1. INTRODUCTION AND AIM 3

1.1. The Problem Addressed in the Study 3

1.2. The Aim of the Study 4

1.3. The Hypotheses of the Study 4

2. CURRENT INFORMATION ON THE TOPICS 4

2.1. Neuroinflammation and Microglia 4

2.2. Inflammasomes 5

2.3. Perineuronal Nets 6

2.4. Relation Between Perineuronal Nets and Microglia 8

2.5. Inflammation and PNNs in the Neonatal Brain 9

3. MATERIALS AND METHODS 10

3.1. Type of Research 10

3.2. Location and Duration of Research 10

3.3. Sampling and Experimental Groups Used in the Research 10

3.4. Materials 11

3.4.1. Cell Lines 11

3.4.2. In Vivo Procedures 11

3.4.3. Consumable Materials 11

3.5. Variables in the Study 14

3.6. Means of Data Collection 15

3.6.1. Devices and Tools 15

3.6.2. Methods 15

3.6.2.1. Cell Culture 15
3.6.2.2. Neuronal Differentiation of N2a Cells 16
3.6.2.3. Neuronal Differentiation of CGR8 Cells 16
3.6.2.4. NLRP3 Inflammasome Activation Model 17
3.6.2.5. Coculture of N2a-derived Neuronal Cells and N9 Microglia 18
3.6.2.6. Coculture of CGR8-derived Neuronal Cells and N9 Microglia 19
3.6.2.7. Animal Maintenance and In Vivo Experimental Procedure 20
3.6.2.8. Behavioral Tests in Mice 22
3.6.2.9. RNA Isolation and Quantitative Real Time-PCR 23
3.6.2.10. Protein Isolation and Western Blot 24
3.6.2.11. Immunofluorescence Staining 25
3.7. Study Plan and Timeline 27
3.8. Data Analysis 28
3.9. Limitations of the Study 28
3.10. Ethics Committee Approval 28
4. RESULTS 29
4.1. Differentiation of N2a Cells Into PNN-positive Neurons 29
4.2. Microglial NLRP3 Inflammasome Activation 31
4.3. Coculture of Neuronal Cells with Inflammasome-activated Microglial Cells 32
4.4. Inflammasome Activation in Brains of Neonatal Mice 36
4.5. Assessment of PNN Presence in Neonatal Mouse Brains 37
4.6. Clinical Scoring and Behavioral Tests in Early Adult Mice 38
4.7. PNN Changes in Brains of Early Adult Mice 38
5. DISCUSSION 41
5.1. Connection of Findings to the Hypotheses and Possible Mechanistic Explanations 41
5.2. Other Observations and Limitations 44
5.3. Connection of Findings to Biomaterials and Tissue Engineering 45
6. CONCLUSION AND FUTURE PERSPECTIVES 46

6.1. Conclusion 46
6.2. Future perspectives 46
7. REFERENCES 47
8. APPENDICES 57
8.1. Ethical Approvals 57
8.2. Resume 59
8.3. Publications Linked to the Thesis 62

Table Index

Table 1: List of chemicals, reagents and kits used in the study 11
Table 2: List of antibodies used in western blot analyses 13
Table 3: List of antibodies used in immunofluorescent staining 14
Table 4: List of instruments used within the thesis study 15
Table 5: The experimental groups of mice for each experiment. 22
Table 6: List of primers used for RT-PCR 24

Figure Index

Figure 1: Timeline of N2a differentiation and coculture with N9 microglia 19
Figure 2: Timeline of CGR8 differentiation and coculture with N9 microglia 20
Figure 3: OFT set-up. 23
Figure 4: Timeline of the thesis study 27
Figure 5: Changes in mRNA expression of MAP2, NeuN and Neurocan in N2a cells at day 0, 3 and 4 of 10 μM RA treatment 29
Figure 6: Representative confocal microscopy images of WFA and MAP2 staining in N2a cells at Day 0 and 4 of neural differentiation via 10 μM RA treatment. 30
Figure 7: Proteins downstream of the NLRP3 inflammasome are increased with LPS+ATP treatment and this increase is reversed with MCC950 treatment in N9 cells. 31
Figure 8: Coculture with inflammasome-activated microglia reduces WFA+ neurons in N2a-derived neuronal cells 33

Figure 9: Coculture with inflammasome-activated microglia reduces WFA+ neurons in CGR8-derived neuronal cells 34
Figure 10: Coculture with inflammasome-activated microglia reduces neurocan+ neurons in N2a-derived neuronal cells. 35
Figure 11: Confirmation of NLRP3 inflammasome activation in WT mice and of inhibited NLRP3 inflammasome activation in NLKO mice. 36
Figure 12: Comparison of PNNs in neonatal and early adult mice. 37
Figure 13: Behavioral tests of mice at PND 60. 38
Figure 14: Comparisons of PNN+ neurons per area in the hippocampi of PND 60 mice. 39
Figure 15: Comparisons of PNN+ neurons per area in the primary somatosensory cortices of PND 60 mice. 40

List of Abbreviations

ATP: Adenosine triphosphate

BSA: Bovine serum albumin

CNS: Central nervous system

ECM: Extracellular matrix

FBS: Fetal bovine serum

FST: Forced swim test

IF: Immunofluorescence

IL: Interleukin

LPS: Lipopolysaccharide

NLKO: NLRP3 knockout

NLRP3: Nod-like receptor family pyrin domain containing 3

OFT: Open field test

PCR: Polymerase chain reaction

PBS: Phosphate buffered saline

PDL: Poly-D-lysine

PNN: Perineuronal net

PNN+: PNN-positive

qPCR: Quantitative real-time PCR

N2a: Neuro-2a

Neurocan+: Neurocan-positive

RA: Retinoic acid

SDS-PAGE: Sodium dodecyl sulfate–polyacrylamide gel electrophoresis

TST: Tail suspension test

WFA: *Wisteria floribunda* agglutinin

WFA+: WFA-positive

WT: Wildtype

Acknowledgement

I would like to express my gratitude to:

My advisor Prof. Şermin Genç for introducing me to the field of scientific publishing; my co-advisor Assoc. Prof. Kemal Uğur Tüfekci for inducing me to hone my skills as a scientist. All former and current members of Genç Lab that I knew for their physical, mental and moral support; and especially Bora Taştan, Burak Arıöz, Bilgesu Genç, Yusuf Güdücü, Batın Güleç, and Hüseyin Kocakuşak for their help with the experimental or analytic parts of this thesis.

My parents Hülya and Ahmet Tarakçıoğlu for all their moral and material support and their effort to keep me pursuing the path of a scientist.

Ece Uzun of the IBG Histopathology Unit and Aslı Seren of the IBG Optic Imaging Facility for their operation service of the cryostat and confocal microscopy, which helped generate the images that form the core of my thesis.

My thesis committee members Assoc. Prof. Duygu Sağ and Prof. Latife Arzu Aral for their time and effort in helping to fine tune my thesis.

I would also like to thank the following institutions for their financial support. The research presented in this thesis, as well as my postgraduate studies as a whole, were funded by:

- The Council of Higher Education (YÖK) under the PhD scholarship programme YÖK 100/2000
- Scientific and Technological Research Council of Turkey (TÜBİTAK) under the scholarship programme BİDEB 2211-A; and under the 3501 Career Development Program - grant code 321S141 (this grant has funded the in vivo studies and parts of the in vitro studies in this thesis)
- Dokuz Eylül University Scientific Research Projects (DEÜ BAP) Coordination Unit under grant code FDK-2022-2701 (this grant has funded parts of the in vitro studies in this thesis)

INVESTIGATION OF ALTERATIONS CREATED BY NLRP3 ACTIVATION ON PERINEURONAL NETS

Emre Tarakçıoğlu

İzmir International Biomedicine and Genome Institute, Dokuz Eylül University Health Campus, Mithatpaşa Cad. 58/5, 35340, Balçova, İzmir, Türkiye

ABSTRACT

Microglia and the NLRP3 inflammasome drive key inflammatory responses in the nervous system and are implicated in various neurodegenerative diseases. Perineuronal nets (PNNs) are extracellular structures that cover neuron bodies, stabilizing synapses and protecting neurons against oxidative stress. Clarifying how NLRP3-activated microglia impact PNNs could guide therapies that target inflammation selectively. This study examines whether microglial activation via inflammasomes can degrade PNNs in a neuron-microglia coculture model, investigates the role of NLRP3 inflammasome activation in microglia-mediated PNN loss both in vitro and in vivo, and assesses the long-term impact of neonatal microglial activation on PNN amount in the brain in early adulthood. In the study, neuronal differentiation was induced in the mouse N2a neuroblastoma cell line with retinoic acid and the presence of PNN components like neurocan and chondroitin sulfate proteoglycans was confirmed in N2a-derived neuronal cells. To investigate the role of the NLRP3 inflammasome, the mouse microglial cell line N9 was activated with LPS and ATP, and they were cocultured with the N2a-derived neurons. Results showed that activated microglia led to a significant reduction in PNN-positive neurons, an effect that was reversed by NLRP3 inhibition with the compound MCC950. In vivo studies in neonatal mice injected with LPS revealed a decrease in PNNs in the hippocampus and cortex by early adulthood, with preserved PNN presence observed in NLRP3 knockout mice. The findings highlight the role of NLRP3 in mediating PNN degradation and suggest that targeting NLRP3 could be a strategy to prevent PNN loss and associated cognitive impairments.

Keywords: NLRP3 inflammasome, microglia, perineuronal nets, coculture

NLRP3 İNFLAMAZOM AKTİVASYONUNUN PERİNÖRONAL AĞLARDA YARATTIĞI DEĞİŞİKLİKLERİN İNCELENMESİ

Emre Tarakçıoğlu

İzmir Uluslararası Biyotip Ve Genom Enstitüsü, Dokuz Eylül Üniversitesi Sağlık Yerleşkesi, Mithatpaşa Cad. 58/5, 35340, Balçova, İzmir, Türkiye

ÖZET

Mikroglia ve NLRP3 inflamazomu, sinir sisteminde temel inflamatuar tepkileri yönlendirir ve çeşitli nörodejeneratif hastalıklarda rol oynar. Perinöronal ağlar (PNN'ler) nöron gövdelerini örten, sinapsları stabilize eden ve nöronları oksidatif strese karşı koruyan hücre dışı yapılardır. NLRP3 ile aktive olan mikrogliaların PNN'leri nasıl etkilediğinin açıklığa kavuşturulması, enflamasyonu seçici olarak hedefleyen tedavilere rehberlik edebilecektir. Bu çalışma, inflamazom düzeyinde mikroglial aktivasyonun bir nöron-mikroglia kokültür modelinde PNN'leri yıkıp yıkmadığını incelemekte, NLRP3 inflamazom aktivasyonunun mikroglia aracılı PNN kaybındaki rolünü hem in vitro hem de in vivo olarak araştırmakta ve neonatal mikroglial aktivasyonun erken yetişkinlikte beyindeki PNN miktarı üzerindeki uzun vadeli etkisini değerlendirmektedir. Çalışmada, fare N2a nöroblastoma hücre hattında retinoik asit ile nöronal farklılaşma indüklenmiş ve N2a kökenli nöronal hücrelerde neurocan ve kondroitin sülfat proteoglikanları gibi PNN bileşenlerinin varlığı doğrulanmıştır. NLRP3 inflamazomunun rolünü araştırmak için, fare mikroglial hücre hattı N9, LPS ve ATP ile aktive edilmiş ve N2a kökenli nöronlarla ortak kültüre alınmıştır. Sonucunda aktive edilmiş mikroglianın PNN-pozitif nöron sayısında önemli bir azalmaya yol açtığı ve bu etkinin MCC950 yoluyla NLRP3 inhibisyonu ile tersine çevrildiği gösterilmiştir. LPS enjekte edilen yenidoğan farelerle yapılan in vivo çalışmalar, bu farelerde erken yetişkinlik döneminde hipokampus ve korteksteki PNN'lerde azalma olduğunu; ve NLRP3 nakavt farelerde aynı model uygulandığında PNN sayılarının korunduğunu ortaya koymuştur. Bulgular, NLRP3'ün PNN yıkımına aracılık etmedeki kritik rolünü vurgulamakta ve NLRP3'ü hedeflemenin PNN kaybını ve buna bağlı bilişsel bozuklukları önlemek için terapötik bir strateji olabileceğini düşündürmektedir.

Anahtar sözcükler: NLRP3 inflamazomu, mikroglia, perinöronal ağlar, kokültür

1. INTRODUCTION AND AIM

1.1. The Problem Addressed in the Study

Microglia are immune cells in the central nervous system (CNS) that provide an immune protection to the tissue and give neurons and other glial cells molecular support. They maintain a healthy neuronal milieu by performing tasks such as releasing neural growth factors, pruning synapses, and removing cellular debris, pathogens and exogenous particles. Long-term microglial activation and unresolved microglial inflammation can upset this equilibrium and result in damage to neural structures.

Inflammasomes, especially the well-characterized Nod-like Receptor Family Pyrin Domain Containing Protein 3 (NLRP3) inflammasome, are important in inducing inflammatory reactions in a variety of CNS injuries and disorders. These multiprotein complexes initiate inflammatory pathways in response to harmful or pathogenic molecular signals. NLRP3 is known to contribute to inflammation-associated CNS diseases like Alzheimer's disease, multiple sclerosis and meningitis

Perineuronal nets (PNNs) encircle the somas of a subset of neurons —mainly interneurons— in the CNS and maintain neuronal integrity, shielding neurons from radical oxygen species and regulating their synaptic connections. Because of these synapse-stabilizing and antioxidant roles, PNNs are critical for memory retention and long-term health of the neurons they surround.

Inflammatory microglia are known to degrade PNNs; however, the role of inflammasomes in this degradation remains unclear. If it becomes clear that the role of a specific inflammasome in this process is substantial, this would lead to drug discovery efforts towards targeting the inflammasome instead of inflammation in general; and thus, generation of therapies with limited disruption of the immune system.

Moreover, inflammation-induced PNN degradation has not been demonstrated in cell lines thus far. Creating an in vitro coculture model that replicates microglial degradation of PNNs would be beneficial in studying the use of contemporary and future anti-inflammatory drugs for treating inflammation-induced PNN loss.

Finally, it is also not known whether microglial PNN degradation has a lasting effect when it occurs during the neonatal developmental stage of the brain. This question is important because both perineuronal net formation and microglia numbers are at beginning stages during the neonatal period, and the inflammation-induced degradation's effect may not be as strong once the insult is removed.

1.2. The Aim of the Study

In line with the problem presented above, the aims of this thesis study are:

1. Investigating whether an inflammasome-activated microglial cell line can degrade PNNs of neurons generated from a cell line.
2. Determining the role of NLRP3 inflammasome activation in microglia-mediated PNN degradation in vitro and in vivo
3. The effects of microglial activation during the neonatal period to abundance of PNNs during early adulthood

1.3. The Hypotheses of the Study

H1: Inflammatory activation in a microglial cell line results in degradation of PNNs of neurons generated from a cell line.

H2: NLRP3 has a significant role in microglia-mediated PNN degradation

H3: Microglial activation during neonatal period results in reduction of PNNs at early adulthood

2. CURRENT INFORMATION ON THE TOPICS

2.1. Neuroinflammation and Microglia

Inflammation in the brain is considered a major component of multiple psychiatric diseases, neurodegeneration, and brain injury. Microglia, the brain's resident immune cells of myeloid origin are predominantly responsible for many cases of neurodegenerative brain inflammation (Kim and Joh, 2006).

In homeostatic conditions, microglia tend to be in a resting state and they support the proper functioning of the nervous system. They exist in a ramified state, extending their moving processes to survey their surroundings in search of potential debris or pathogens (Colonna and Butovsky, 2017). Microglia are essential for the survival of certain neurons by providing them with growth factors (Colonna and Butovsky, 2017) (Ueno et al., 2013) and they also sculpt neuronal circuitries by pruning synapses (Filipello et al., 2018). When activated through their pattern recognition receptors like Triggering receptor expressed on myeloid cells 2 (TREM-2) or Toll-like receptors (TLRs), they assume an amoeboid shape and become more mobile (Wendimu and Hooks, 2022). In this form they start to clear cellular debris, apoptotic cells, aggregated proteins, foreign material, or infiltrating pathogens by engulfing and phagocytosing them (Hanke and Kielian, 2011; Neumann et al., 2009).

While these functions make microglia an indispensable part of the brain microenvironment, unresolved inflammation can lead to chronically active microglia which can damage neurons, glia or extracellular structures (Bachiller et al., 2018). Indeed, even acute inflammation can result in the release of an array of damaging factors (in addition to neuroprotective factors) like matrix metalloproteinases (MMPs), cytotoxic cytokines like tumor necrosis factor-α (TNFα), and reactive species like superoxide or nitric oxide (Kawabori and Yenari, 2015). Thus, active microglia are a double-edged sword in the context of brain maintenance. It is also hypothesized that heightened or repeated activations in some cases can prime microglia to be more alert to future stimuli and less responsive to anti-inflammatory feedback, thus turning microglia's defensive feature into a potential threat (Lima et al., 2022; Perry and Holmes, 2014).

2.2. Inflammasomes

Central to innate immunity are inflammasomes, which are multiprotein complexes that initiate several secretory and inflammatory pathways when they detect specific pathogens or damage-associated molecular patterns (Santoni et al., 2015).

The NLRP3 inflammasome is implicated in various CNS diseases and injuries (Eren and Ozoren, 2019; Wang and Hauenstein, 2020). Expression of NLRP3 is regulated by a prime mediator of inflammation, NF-κB, which is activated through TLRs by inflammatory signals such as lipopolysaccharide (LPS). NLRP3 can be activated by several molecular

signals, like extracellular ATP, pathogen-associated molecular patterns, particle aggregates, potassium efflux, and reactive oxygen species (ROS) (Jo et al., 2016; Latz et al., 2013). Upon activation by any of these cues, NLRP3 undergoes self-oligomerization through its ligand-sensing domain. This process recruits adaptor proteins called Apoptosis-associated Speck-like Protein (ASC). The ASC proteins clustered on the NLRP3 complex then recruit multiple pro-caspase-1 proteins, which undergo proximity-induced cleavage and become the active protease caspase-1. Caspase-1 cleaves (and as a consequence, activates) the pore-forming protein Gasdermin-D (GSDMD) and the inactive forms of the inflammatory cytokines Interleukin (IL)-1β and IL-18. These inflammatory mediators are released through pores in the cell membrane formed by active GSDMD, enabling paracrine signaling (Franklin et al., 2018; Voet et al., 2019).

2.3. Perineuronal Nets

Specialized sheath-like extracellular matrices (ECMs) surrounding certain neuron bodies in the nervous system have been given the name perineuronal nets (PNNs). These structures are composed of protein and carbohydrates, and envelop primarily parvalbumin(PV)-expressing and rapid-firing GABAergic interneurons. However, there also are PV negative neurons with PNNs (Morikawa et al., 2017). It is understood that these nets provide both stability to synapses and some amount of protection from free radicals to neuron bodies (Fawcett et al., 2019).

While PNNs across the brain can be heterogenous in protein composition, there are four components that are found in the majority of PNNs. First, hyaluronic acid (or hyaluronan) which is a non-sulfated glycosaminoglycan (GAG) consisting of repeating disaccharide units of N-glucuronic acid and N-acetylglucosamine, forms the backbone of many PNNs (Smith et al., 2015). Secondly, chondroitin sulfate proteoglycans (CSPGs), which are proteins with attached GAG side chains called chondroitin sulfates, are present in large numbers in PNNs and can bind to hyaluronan (Siebert et al., 2014). CSPGs are composed of repeating units of N-acetylgalactosamine and glucuronic acid, with carbons that tend to be sulfated. The lectican family of CSPGs is the most commonly studied, and it includes aggrecan, neurocan, brevican and versican (Smith et al., 2015). The N-acetylgalactosamine groups of CSPGs can be bound by a plant lectin called *Wisteria floribunda* agglutinin (WFA) (Hartig et al., 1992), which is very commonly used in immunofluorescence staining of PNNs. Thirdly, tenascin-R is an

essential protein that cross-links CSPGs to each other (Morawski et al., 2014). And the fourth critical component of PNNs is the family of hyaluronan and proteoglycan binding link proteins (HAPLNs) which connect CSPGs to hyaluronan (Fawcett et al., 2019).

The primary function assigned to PNNs is that they are inhibitors of plasticity and stabilizers of synaptic circuitry. This has been shown previously through experimental models where removal of PNN components results in increased plasticity (Bukalo et al., 2001; Pizzorusso et al., 2002) and susceptibility to memory erasure (Gogolla et al., 2009). Another role of perineuronal nets appears to be protection against oxidative stress, either through acting as antioxidants directly (Cabungcal et al., 2013; Campo et al., 2004; Morawski et al., 2004) or through free chondroitin sulfate groups inducing the expression of the antioxidant protein heme oxygenase-1 (Canas et al., 2007).

PNNs appear to be relevant in multiple psychiatric conditions, including schizophrenia, autism and bipolar disorder (BD) (Fawcett et al., 2019). A post-mortem study on human amygdalas reveal that PNN loss occurs in schizophrenia and BD patients (Pantazopoulos et al., 2015). Another study on prefrontal cortex showed a similar loss was observable in schizophrenia patients but not BD patients (Mauney et al., 2013). A third study of schizophrenia patient brains showed reduction in PNNs along with PV-positive neurons was visible in dorsolateral prefrontal cortices of schizophrenia patients (Enwright et al., 2016); possibly implying that PNNs are lost together with the PV-positive neurons they normally surround. PV-positive cells surrounded by PNNs and PNN density was found to be increased in the ventromedial prefrontal cortex of child abuse victims (Tanti et al., 2022), which is in line with the region's function in mediating extinction of fear responses (Szeska et al., 2022). In a histochemical study of Alzheimer's disease (AD) patient brains, PNNs reduction was not observed in cortices of AD cases; however, neurofibrillary tangles appeared to never coincide with PNN-positive (PNN+) neurons, implying a possible protective effect (Morawski et al., 2012). A different earlier study of AD brains showed a reduction of WFA-positive (WFA+) neurons in the frontal cortices of AD patients (Baig et al., 2005). A more recent study that stained for PNNs (in cortical tissue from the middle frontal gyrus) via aggrecan antibodies showed that PNN+ neurons were decreased and PNN staining was colocalized with microglia staining in AD patients, implying the disruptive role of microglia (Crapser et al., 2020). The variation of PNN-related results in the clinical field are likely due to a discrepancy between

brain regions examined, the exact method in staining PNNs, and how PNN loss is quantified (as it can be measured by reduction of WFA or antibody staining intensity, absolute loss of PNN+ neurons per area, absolute loss of PV+PNN+ neurons per area, or loss of PNN+ neurons within PV+ neurons and possibly in more ways). Thus, in a comprehensive review of PNN-associated clinical data, normalizing these measurements across studies could be considered.

Although PNN synthesis and maintenance is regulated in vivo by glia (especially astrocytes), it is not known whether glial presence is essential to PNN production (Fowke et al., 2017; Tewari et al., 2022). There has been an in vitro study of PNNs in HEK cells transfected with PNN-promoting proteins (Kwok et al., 2010); and the expression of the PNN protein neurocan has been demonstrated in the SH-SY5Y cell line (Sun et al., 2016). Furthermore, primary cortical neurons are documented as staining positive for hyaluronan and CSPGs (Fowke et al., 2017). These studies indicate that neurons cultured alone can produce some form of PNN although the composition and form may not necessarily represent the in vivo forms of PNN.

2.4. Relation Between Perineuronal Nets and Microglia

It is documented that PNNs are degraded in response to activated microglia (Cheung et al., 2024; Crapser et al., 2020; Tansley et al., 2022; Venturino et al., 2021; Wegrzyn et al., 2021) and that depletion of microglia can result in increased PNN numbers and density (Liu et al., 2021). It is thought that a large role in this degradation is played by MMP-9, the expression of which increases in activated microglia (Cheung et al., 2024; Venturino et al., 2021; Wegrzyn et al., 2021).

To this date, the interplay between microglia and PNNs have only been shown in primary neurons generated by cocultured with astrocyte (Wegrzyn et al., 2021). One of the aims of this study was to test whether the interplay can be also demonstrated using cell lines, which are easier and more cost-effective to manipulate. Showing that it is possible to replicate the same “microglia-degrades-PNN” behavior in cell lines would accelerate drug development studies that inquire into the mechanisms of this degradation.

Moreover, while the fact that microglia can degrade PNNs has been mostly established, it is not known how much of a role NLRP3 inflammasome activation has in the role of

microglia in this degradation. The studies that have demonstrated active microglia results in PNN loss have used various inflammatory insults: ketamine and light (Venturino et al., 2021), ROS (Cheung et al., 2024), poly I:C (Wegrzyn et al., 2021), spared nerve injury (Tansley et al., 2022), and amyloid or tau aggregates (Crapser et al., 2020). None of these inflammatory triggers selectively affect NLRP3 and none of the studies have investigated NLRP3's function in the model with inhibitors or knockdown/knockout models. If we learn that in inflammatory scenarios where NLRP3 is triggered, NLRP3 bears most of the inflammatory burden and thus most of the degradation role, then NLRP3 can be chosen as a potential drug target instead of stronger anti-inflammatory drugs that can have undesirable side effects.

2.5. Inflammation and PNNs in the Neonatal Brain

In rodents, microglia numbers and PNN staining intensity in the brain are both considerably low (compared to adolescence and adulthood) in the first week after birth. According to immunofluorescence (IF) study performed on mice, microglia numbers in the hippocampus are near zero at birth, start to rise at postnatal day 7 (PND7), reach a peak of about 14 times the amount at birth at PND14, then fall to about half of that value and remain stable throughout early adulthood (Kim et al., 2015). Similarly, rats with microglial ablation at PND14 show less drastic changes in immune parameters compared to those with microglial ablation at PND7, where microglia numbers would be just beginning to rise (Soch et al., 2020).

According to a western blot of mouse brain homogenates on different postnatal days, the PNN components aggrecan, brevican and tenascin-R are either undetectable or visibly and significantly low at PND1 and PND15 compared to later ages (Miyata and Kitagawa, 2016); however, the CSPGs neurocan and phosphacan have relatively high levels across all ages through PND0 to PND45. In an IF study of PNN detection, WFA+ cells are near zero at PND10, start to rise at PND14 and stabilize around PND50. (Ye and Miao, 2013). Likewise, an imaging study in frontal association cortex, medial prelimbic cortex and amygdala of rats also shows that at PND7 there are no WFA+ cells detectable in any of these regions; whereas they begin to appear at PND21 (Paylor et al., 2016).

In view of this data, it would be of interest to see if PNN formation would be affected by early inflammation in a way that would reduce the number of PNN+ cells in adulthood. To

that end, we have planned a study where: (1) PND9 mice are injected with LPS and brains of PND60 mice are examined for changes in PNN levels; (2) a culture of neurons, neural progenitor cells and other stem cells developed from embryonic stem cells is cocultured with activated or resting microglia for 48 hours, and then examined for changes in PNN+ cell numbers.

3. MATERIALS AND METHODS

3.1. Type of Research

The research included in this thesis is an experimental study involving biological models.

3.2. Location and Duration of Research

The research for the thesis was performed in Izmir Biomedicine and Genome Center (IBG), mainly within laboratories dedicated to Genc Lab on Neurodegeneration and Neuroprotection. The research was performed from March 2022 to July 2024.

The research in the thesis involves results obtained from two projects. The first one is "*Investigation of alterations created by NLRP3 activation on perineuronal nets*" (code: FDK-2022-2701) and was supported by DEÜ BAP. The second one is "*Effects of microglial NLRP3 inflammasome activation on GABAergic interneuron differentiation, survival, and perineuronal nets*" (code: 321S141) and was supported by TÜBİTAK.

3.3. Sampling and Experimental Groups Used in the Research

In this study, for the in vitro part, mouse neuroblastoma cell line Neuro-2a and mouse microglial cell line N9 were used. For the in vivo part, C57BL/6 wildtype and NLRP3-knockout mice of both sexes were used.

3.4. Materials

3.4.1. Cell Lines

The cell lines used in the in vitro part of the study were N9, Neuro-2a and CGR8 mouse cell lines. N9 mouse microglial cell line, generated from primary brain cell cultures from mouse embryo (Righi et al., 1989), was provided by Dr. Paola Ricciardi-Castagnoli (Toscana Life Sciences Foundation, Italy). Neuro-2a (N2a) mouse neuroblastoma cell line was purchased from American Type Culture Collection (ATCC) (Catalog number: CCL-131). CGR8 mouse embryonic stem cells, established using the inner cell mass of a 3.5 day male mouse embryo, were purchased from the European Collection of Authenticated Cell Cultures (ECACC) (Catalog number: 07032901). Passages (P) used in the experiments for N9, N2a and CGR8 were respectively: P51-59, P12-14, P10-12.

3.4.2. In Vivo Procedures

The animals used in the in vivo part were C57BL/6J wildtype mice, provided by the IBG Vivarium; and transgenic NLRP3$^{-/-}$ mice (Strain name: B6.129S6-Nlrp3^{tm1Bhk}/J, Jackson Laboratory stock number: 021302) generated from the C57BL/6 strain (Kovarova et al., 2012), bought from The Jackson Laboratory by Prof. Dr. Serap Cilaker Mıçılı and transferred to the IBG Vivarium.

3.4.3. Consumable Materials

Table 1: List of chemicals, reagents and kits used in the study

Item	**Manufacturer**	**Catalog Number**
Ultrapure LPS (LPS from E. coli 0111: B4)	InvivoGen	tlrl-3pelps
LPS (LPS from E. coli 055: B5)	Sigma-Aldrich	L2880
Adenosine 5′ -triphosphate disodium salt hydrate (ATP)	Sigma-Aldrich	A6419
Fetal bovine serum (FBS)	ThermoFisher Scientific	16140071

Phosphate buffer saline (PBS)	Biowest	L0615
DMEM	ThermoFisher Scientific	11965084
RPMI-1640	ThermoFisher Scientific	11875093
L-Glutamine	ThermoFisher Scientific	A2916801
100 U/ml penicillin + 100 μg/ml streptomycin	ThermoFisher Scientific	15140148
Gelatin	Sigma-Aldrich	G1890
Triton X-100	BioShop	TRX777
Trypan Blue	Sigma-Aldrich	T8154
Leukemia inhibitory factor (LIF)	Biolegend	554006
CHIR99021	RayBiotech	331-10376-3
PD184352	MedChem Express	HY-50295
SU5402	MedChem Express	HY-10407
Poly-D-Lysine (PDL)	Sigma-Aldrich	P1149
Laminin	Sigma-Aldrich	L2020
Retinoic Acid (All Trans)	Cayman Chemical	11017
MCC950	MedChem Express	HY-12815A
TRI Reagent	Zymo Research	R2050-1-200
Chloroform	Merck-Millipore	1.02445
Isopropanol	ISOLAB	961.023

Ethanol	ISOLAB	920.027
High Capacity cDNA Reverse Transcription Kit	Applied Biosystems	4368813
Luna Universal qPCR Master Mix	New England Biolabs	M3003E
RIPA cell lysis buffer	ThermoFisher Scientific	89900
Halt Protease and Phosphatase Inhibitor Cocktail	ThermoFisher Scientific	78447
BCA Protein Colorimetric Assay Kit	Elabscience	E-BC-K318-M
SuperSignal™ West Pico PLUS Chemiluminescent Substrate	ThermoFisher Scientific	34577
Prolong Glass mounting medium	ThermoFisher Scientific	P36980
Anti-Fade Fluorescence Mounting Medium	Abcam	ab104135
Paraformaldehyde (PFA)	Sigma-Aldrich	P6148
Optimal cutting temperature (OCT) compound	Tissue-Tek	4583

Table 2: List of antibodies used in western blot analyses

Antibody	**Manufacturer**	**Catalog Number**	**Dilution**	**Solution type**
Anti-NLRP3	Adipogen	AG-20B-0014	1:800	3% Bovine serum albumin (BSA)
Anti-Actin	Cell Signaling Technology	8457s	1:1000	3% BSA
Anti-caspase-1	Adipogen	AG-20B-0042	1:400	1% Milk
Anti-IL-1β	Abcam	ab9722	1:400	1% Milk

Anti-Mouse IgG	Cell Signaling Technology	7076S	1:1000	3% Milk
Anti-Rabbit IgG	Jackson ImmunoResearch	111-035-144	1:1000	3% Milk

Table 3: List of antibodies used in immunofluorescent staining

Antibody	**Manufacturer**	**Catalog Number**	**Dilution or Concentration**
WFA-Fluorescein	ThermoFisher Scientific	L32481	1:300
Anti-MAP2	ThermoFisher Scientific	PA1-10005	1:800-1:1000
Anti-Neurocan	Affinity Biosciences	DF4236	1:300
Anti-rabbit IgG, Alexa Fluor™ 488	ThermoFisher Scientific	A-21206	1:800-1:1000
Anti-Chicken IgY, Alexa Fluor™ 568	ThermoFisher Scientific	A78950	1:800-1:1000
Hoechst 33342	AppliChem	A0741	1 µg/ml

3.5. Variables in the Study

For the in vitro part of the study, the independent variables are the LPS+ATP treatment; and the inhibition of NLRP3. The dependent variable is the percentage of PNN+ neurons. For the in vivo part, the independent variables are the injection of PBS or LPS; and the absence or presence of a coding NLRP3 gene. The dependent variable is the amount of PNN+ neurons per area in the photographed brain sections.

3.6. Means of Data Collection

3.6.1. Devices and Tools

Table 4: List of instruments used within the thesis study

Item	**Manufacturer**	**Catalog / Model Number**
Class II Biological Safety Cabinet	ThermoFisher Scientific	Safe 2020
CO2 Incubator	Memmert	INCO 153
Multiskan™ FC Microplate Photometer	ThermoFisher Scientific	51119000
Spectrophotometer	ThermoFisher Scientific	ND-2000
SimpliAmp™ Thermal Cycler	Applied Biosystems	A24811
ABI 7500/7500 Fast Real-Time PCR System	Applied Biosystems	-
Lyophilizer (Freeze Dryer)	ThermoFisher Scientific	MODULYOD-230
Fluorescent Microscope	Olympus	BX-61
Confocal Microscope	Zeiss	LSM 880
Centrifuge	Eppendorf	5810R
Microtube Centrifuge	ThermoFisher Scientific	MicroCL 17R
ChemiDoc MP Imaging System	Bio-Rad	-
Cryostat	Leica	CM 1950

3.6.2. Methods

3.6.2.1. Cell Culture

N2a cells were cultured in Dulbecco's MEM (DMEM) supplemented with 10% fetal bovine serum (FBS), 2 mM L-glutamine, 100 U/ml penicillin + 100 µg/ml streptomycin. N9

cells were cultured in RPMI 1640 with 10% FBS, 2 mM L-glutamine, 100 U/ml penicillin and 100 μg/ml streptomycin. CGR8 mouse embryonic stem cells were cultured in 0.2% gelatin-coated cell culture flasks in DMEM medium supplemented with 10% FBS, 2 mM glutamine, 2 mM sodium pyruvate, 10 mM HEPES, 100 μM non-essential amino acids, 50 μM β-mercaptoethanol, and differentiation inhibitors (1000 U/ml leukemia inhibitory factor, 2 μM SU5402, 0.8 μM PD184352, 3 μM CHIR99021). For brevity, this medium is abbreviated as "CGR8 medium" throughout the text. For gelatin coating, 0.2% gelatin solution in distilled sterile water was applied at 0.14 ml/cm^2 (0.28 mg/cm^2) for 1-24 hours at 37°C and the solution was aspirated completely before cell seeding.

N9 and N2a cells were maintained with medium changes every 2-3 days and were passaged at 50-90% confluency. CGR8 cells were maintained with daily medium changes and passaged at 30-50% confluency (before colony contact occurs). All cells were cultured at 37°C and 5% CO2.

3.6.2.2. Neuronal Differentiation of N2a Cells

For the differentiation of N2a cells, methods from previous literature were combined (Namsi et al., 2018; You et al., 2020). N2a cells were seeded on poly-D-lysine (PDL) coated glass coverslips placed inside cell culture plates at 18—20 × 10^3 cells/cm^2 for differentiation. For coating, PDL solution in distilled sterile water was applied at 5 μg/cm^2 on the coverslips for 2 hours at 37°C; then the solution was washed two times with distilled sterile water before cell seeding. Differentiation was started one day after seeding, using DMEM containing 1% FBS, 2 mM glutamine, and 10 μM retinoic acid (RA). The medium was changed every two days. For coculture experiments, N2a cells differentiated for four days were used.

3.6.2.3. Neuronal Differentiation of CGR8 Cells

To determine whether microglial activation can also affect PNNs in developing neurons, we also devised a model where neurons generated from embryonic stem cells were used in a neuron-microglia cocultured setting; and for that, CGR8 mouse embryonic stem cells were used.

For neuronal differentiation, embryoid body (EB) formation was used (Shin et al., 2012). CGR8 cells were seeded at a density of 10^5 cells/ml in non-adherent cell culture dishes and

grown suspended in CGR8 medium without differentiation inhibitors. The media of these cells were changed every two days and RA was added at a dose of 2.5 μM for induction of neuronal differentiation on days 4 and 6 after seeding. During EB formation procedure, coverslips were placed in empty 24-well-plates and coated with PDL (5 μg/cm2) and laminin (1.5 μg/cm2). For coating, initially an appropriate dilution of PDL in distilled sterile water was applied at room temperature for 2-24 hours; then the wells were aspirated and washed once with distilled sterile water. After drying for 15-20 minutes, laminin solution in distilled sterile water was applied at 37°C for 2-24 hours. Laminin was aspirated shortly before cell seeding.

On day 8 of EB formation, EBs were dissociated by trypsin treatment for 10 minutes. The cells were then centrifuged at 500 × g for 5 minutes and the media was replaced with N2B27 medium (1:1 mix of DMEM/F-12 and Neurobasal Medium supplemented with 50 μg/ml BSA, 1X N2 supplement, 1X B27 supplement, 2 mM L-Glutamine, 100 μM β-mercaptoethanol, 7.5 μg/ml insulin and 100 U/ml penicillin + 100 μg/ml streptomycin mixture). Suspended cells were filtered through 70 μm pore-sized cell strainers to separate cell clumps. The filtered cells were plated on PDL and laminin coated glass coverslips at a density of 3 x 10^4 cells/cm^2. The medium was replaced the next day; and every two days afterwards. For coculture experiments, CGR8-derived neuronal cells at day 5 of coverslip-seeding (day 13 of differentiation) were used. This day was chosen because before day 5, the number of neurited cells on the coverslips was too limited; and beyond day 13 the proliferation of non-neuronal cells in the culture was excessively elevated.

3.6.2.4. NLRP3 Inflammasome Activation Model

NLRP3 inflammasome activation was induced by treatment with LPS for priming of the TLR4/NF-κB signalling pathway and with ATP for activation of NLRP3, as described previously (Tarakcioglu et al., 2022). N9 microglial cells were seeded at 35—40 × 10^3 cells/cm^2 on cell culture flasks, dishes or transwell inserts; with N9 culture medium without antibiotics. The next day, the medium was replaced with RPMI 1640 with 2 mM L-glutamine (without serum or antibiotics).

In experiments, N9 cells were divided into the following groups:

Control (Ctrl): N9 cells without any intervention other than medium replacement

LPS+ATP (LA): N9 cells treated with LPS and ATP

CtrlMCC: Control N9 cells additionally treated with MCC950 (a selective inhibitor of NLRP3 inflammasome (Coll et al., 2015))

LAMCC: LPS+ATP N9 cells additionally treated with MCC950

In experiments without MCC950, only the first two groups were used. The following experimental procedure is followed: The LA and LAMCC groups were treated with 1 μg/ml Ultrapure LPS. After 3 hours, the CtrlMCC and LAMCC groups were treated with MCC950 at a concentration of 0.1 μM. Following one-hour treatment with MCC950, the LA and LAMCC groups were treated with 5 mM ATP, and cells were incubated for 1 hour. In all groups, the previously introduced molecules were maintained at the same concentration at each stage.

3.6.2.5. Coculture of N2a-derived Neuronal Cells and N9 Microglia

Upon completion of inflammasome activation, plates containing N9 transwell inserts were centrifuged at 300 × g for one minute to settle any detached cells. Subsequently, the medium was removed and substituted with DMEM medium that included 2 mM glutamine and 1% FBS. N2a cells were also given the same medium following aspiration of the RA-containing medium before coculture. Using sterile forceps, the transwell inserts containing N9 cells were placed on the 4-day-differentiated N2a wells. The coculture system was incubated at 37°C for 24 hours. At the end of the 24-hour period, the N2a cells were used for further analyses (**Figure 1**). The neuronal cells in the coculture experiment are divided into five groups:

noCC (no coculture): N2a cells cultured alone

Ctrl: N2a cells cultured with Ctrl microglia

LA: N2a cells cultured with LA microglia

CtrlMCC: N2a cells cultured with CtrlMCC microglia

LAMCC: N2a cells cultured with LAMCC microglia

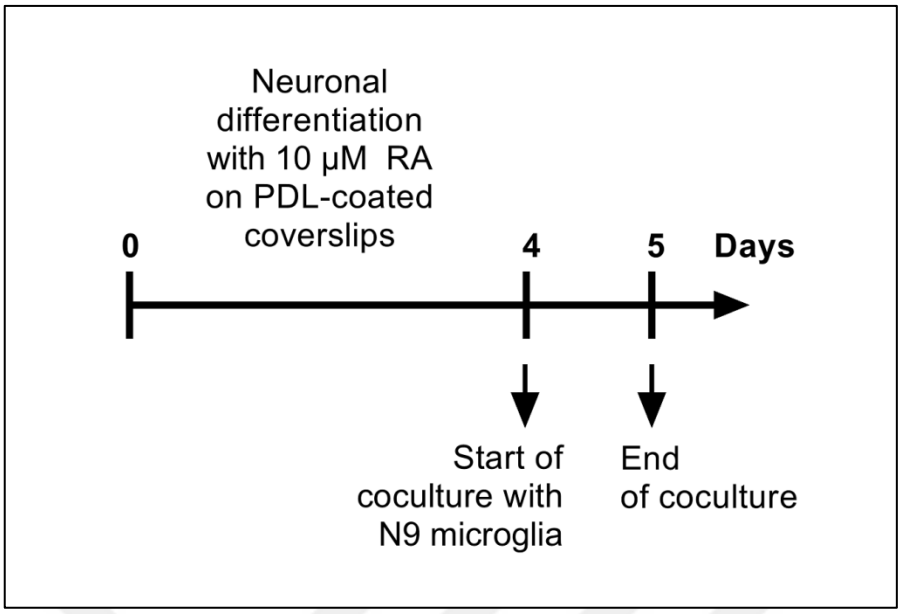

Figure 1: Timeline of N2a differentiation and coculture with N9 microglia

3.6.2.6. Coculture of CGR8-derived Neuronal Cells and N9 Microglia

Upon completion of inflammasome activation, plates containing N9 transwell inserts were centrifuged at 300 × g for one minute to settle any detached cells. Subsequently, the medium was removed and substituted with N2B27 medium. The medium of neuronal cells was also renewed shortly before coculture. Using sterile forceps, the transwell inserts containing N9 cells were placed on the wells with neuronal cells. The coculture system was incubated at 37°C for 48 hours. At the end of the 48-hour period, the neuronal cells were used for further analyses (**Figure 2**). The neuronal cells in this coculture experiment were divided into three groups: noCC, Ctrl and LA (with the same conditions given above). This coculture set-up was not repeated with MCC950 due to shortage in materials.

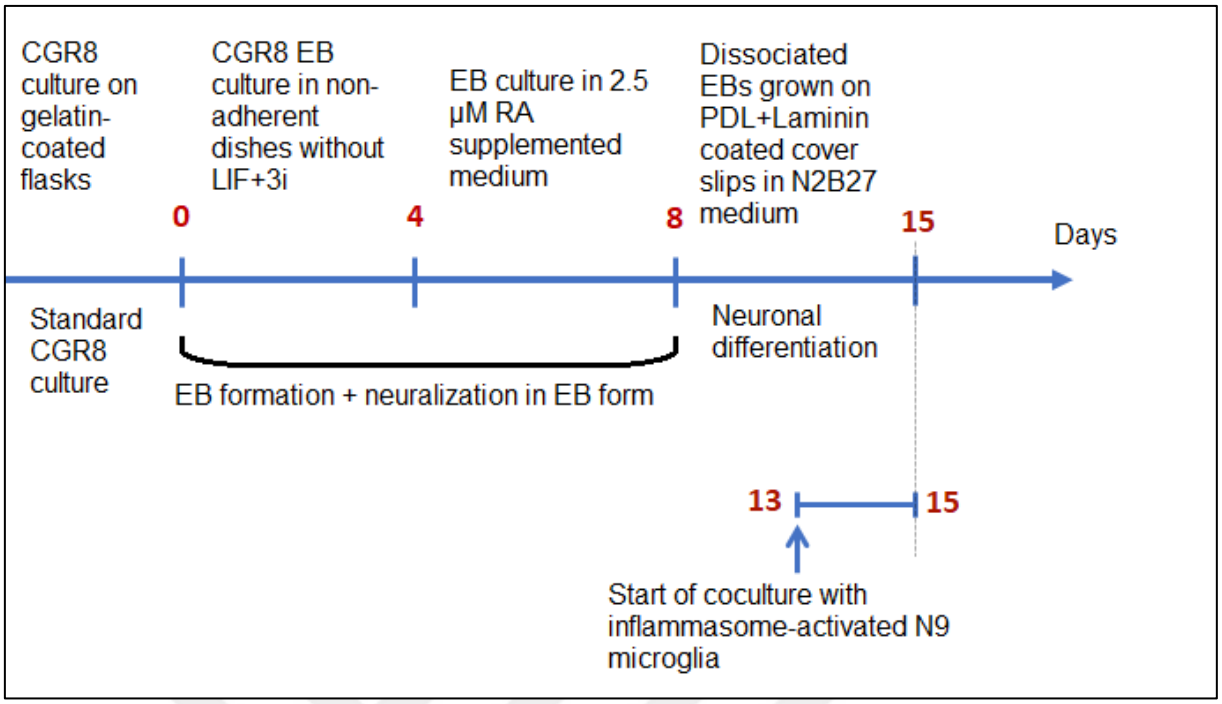

Figure 2: Timeline of CGR8 differentiation and coculture with N9 microglia

3.6.2.7. Animal Maintenance and In Vivo Experimental Procedure

The animal maintenance and experiments were conducted in the IBG Vivarium. Wildtype mice of C57BL/6J strain obtained from the vivarium and NLRP3 knockout mice obtained from The Jackson Laboratory (strain: B6.129S6-Nlrp3^{tm1Bhk}/J) were used. All animals were housed in standard animal housing rooms with 22±2°C temperature, ad libitum water and feed. The animal rooms were designed to have a 12 hour light and 12 hour dark cycle. Both male and female mice were used in every group at equal or close to equal numbers.

The NLRP3 inflammasome activation model in neonatal mice was performed on PND9 with an intraperitoneal injection of 1 mg/kg LPS (with an equal volume of PBS injected in the control group) (Lalancette-Hebert et al., 2017). On the next day of LPS administration, a portion of the mice were terminated for confirmation of inflammasome activation by decapitation after transcardial PBS perfusion under isoflurane anaesthesia (n=5).

In our in vivo NLRP3 activation model, a ligand (like ATP) that directly activates NLRP3 is not necessary since LPS alone can elevate proteins downstream of NLRP3 in the brain (Arioz et al., 2019). It is possible that in this LPS-only model, endogenous ATP released

from inflammatory or damaged cells that are affected by LPS can induce NLRP3 activation (Bodin and Burnstock, 1998; Sakaki et al., 2013). It is also possible that non-canonical NLRP3 activation (where LPS alone triggers caspase-11 activation, which in turn induces NLRP3 inflammasome assembly) contributes to the activation of the NLRP3 inflammasome in this model (Kayagaki et al., 2011; Smith and Creagh, 2022).

To investigate the long-term effect of inflammasome activation, the same model was applied in a separate set of mice (n=5) at PND9 and these mice were sacrificed by decapitation after transcardial cold PBS perfusion under anaesthesia after clinical scoring and behavioural experiments at PND60. For clinical scoring, animals were scored for symptoms of lethargy (decreased mobility), huddling (curled body posture) and ptosis (drooping eyelids) and each symptom was recorded as one point (one symptom = 1 point; two symptoms = 2 points; three symptoms = 3 points). The wildtype (WT) and NLRP3 knockout (NLKO) mice were divided into a total of eight groups for this study, where a part of the mice are sacrificed at neonatal stage (PND10) for confirmation of inflammasome activation post-injection, and a part are sacrificed in early adulthood (PND60) for examination of PNN in brain sections. For the WT mice, a part of the mice from each group was sacrificed at PND12 to assess early inflammatory damage to the brain. The late-sacrifice groups (PND60) were weaned from their mothers at PND21-26 and moved into new sex-separated cages. The described grouping is given in **Table 5**.

Table 5: The experimental groups of mice for each experiment.

	Sacrifice Day	Injection	Number
WT	**PND10**	PBS	5
		LPS	5
	PND12	PBS	3
		LPS	3
	PND60	PBS	5
		LPS	5
NLKO	**PND10**	PBS	5
		LPS	5
	PND60	PBS	5
		LPS	5

Brains obtained from the sacrificed mice were divided into two hemispheres (excluding the cerebellum and olfactory bulb), the right hemispheres were frozen in liquid nitrogen and stored at -80°C for further potential downstream analyses, the left hemispheres were immersed in 4% paraformaldehyde in PBS (4% PFA) to fix the tissue for immunofluorescent staining. The hemispheres were kept in 4°C overnight then prepared further for immunofluorescent staining (see: the section “Immunofluorescence Staining”).

3.6.2.8. Behavioral Tests in Mice

For measuring anxiety-like and depressive-like behavior, three commonly used tests were employed on PND60 mice before their sacrifice: forced swim test (FST), tail suspension test (TST), and open field test (OFT) (Boyko et al., 2019).

In OFT, the mice were placed in 20 cm deep, 26 cm wide, 40 cm long transparent boxes divided with a marker from outside into 40 (5x8) equal sized squares. The movements of mice were recorded from above for 8 minutes. Boxes were cleaned with 70% ethanol and dried between each mouse. Time spent in the central zone (the 3x6 square zone) (**Figure 3**) was recorded and used as a measure of reduced anxiety (Prut and Belzung, 2003).

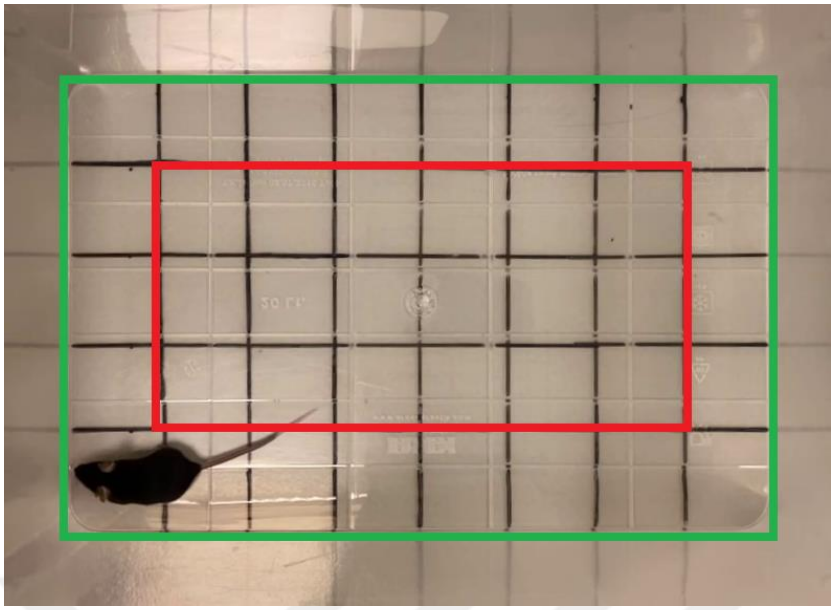

Figure 3: OFT set-up. The whole box is outlined in green and the area termed the central zone is outlined in red.

In TST, the tail of the mouse is place inside a small plastic cylinder, and the cylinder together with the tail is taped to a shelf and mice are allowed to hang freely while being recorded for 8 minutes. In FST, mice are placed inside a large beaker (25 cm tall with 15 cm diameter) filled 3/4 with room temperature (~23°C) tap water and were recorded for 8 minutes. The water was changed between each mouse, and the mice were dried with paper towels in their cages. In these two tests the latency to immobility was measured, as it is inversely related with depressive state (Castagne et al., 2011). The immobility time was set at 5 seconds, meaning that the first instance of a mouse stopping movement (except for small vibrations of head or paws) for 5 seconds or longer was taken to be the latency to immobility timestamp. In all behavioral tests, large cardboards were placed between mice to prevent them from seeing each other during the testing procedure.

3.6.2.9. RNA Isolation and Quantitative Real Time-PCR

RNA from N2a cells was extracted using TRI Reagent to lyse the cells. Lysates from each 24-well plate well was combined with lysates from the neighboring well for each group, adding up to a total of four samples from eight wells. Briefly: each sample was lysed in 600 µl of TRI Reagent and vortexed; 120 µl chloroform was added per sample, tubes were shaken vigorously. Tubes were then centrifuged at 12000 × g for 15 min at 4°C. The aqueous phase

was transferred to a new tube and mixed with 300 µl isopropanol; afterwards tubes were centrifuged at 12000 × g for 10 min at 4°C. After the supernatant was discarded, the pellet was resuspended in 600 µl of 75% ethanol and centrifuged at 7500 × g for 5 min at 4°C. After aspirating the supernatant, the pellet was allowed to air dry for five to ten minutes. The pellet was then dissolved in 25 µl of RNAse-free water, and concentration of RNA was measured with Nanodrop 2000.

cDNA from the extracted RNA was produced using Applied Biosystems High Capacity cDNA Reverse Transcription Kit according to the instructions of the manufacturer. For the quantitative real time-PCR (qPCR) reactions, Luna Universal qPCR Master Mix was used in line with the manufacturer's instructions. The reaction was performed in Applied Biosystems 7500/7500 Fast Real-Time PCR System. Primers used in this section are listed in **Table 3**. Relative expression levels of the quantified RNA were measured by the $2^{-\Delta\Delta ct}$ method (Livak and Schmittgen, 2001) with *Gapdh* as the housekeeping gene.

Table 6: List of primers used for RT-PCR

Primer	Sequence (5'→3')
Map2 Forward	GCCAGCCTCGGAACAAACA
Map2 Reverse	GCTCAGCGAATGAGGAAGGA
Ncan Forward	GGGTGTCATTGCCTGCTTATC
Ncan Reverse	AGCGAAGGTCAGCGCATAG
Rbfox3 (NeuN) Forward	GCTGAGATTTATGGAGGCTATGC
Rbfox3 (NeuN) Reverse	CCGATGGTGTGATGGTAAGGAT
Gapdh Forward	TGGCCTTCCGTGTTCCTAC
Gapdh Reverse	GAGTTGCTGTTGAAGTCGCA

3.6.2.10. Protein Isolation and Western Blot

Protein extraction from N9 cells was performed by scraping the cells and centrifuging them at 500 x g at the end of the inflammasome model. After this initial centrifuge, the supernatants (cell medium) were transferred into other tubes and lyophilized for 24 hours. To lyse the cell pellets, RIPA cell lysis solution containing 1% Halt Protease and phosphatase inhibitor cocktail was used. After 30 minutes of vortexing on ice, lysed cells were centrifuged

at 12,000 x g. The aqueous portions of the final centrifuge were acquired and kept at -80°C. The lyophilized cell media was resuspended in RIPA + inhibitor cocktail after the lyophilization, to measure the amounts of released caspase-1 and IL-1β.

Cell lysis from mouse brains was performed with an electro-mechanical homogenizer after they were placed in RIPA + inhibitor solution. The homogenized brain tubes were kept on ice for 2 hours and then centrifuged at 16,000 x g at 4°C to acquire the protein in the supernatant. BCA Protein Colorimetric Assay Kit was used to assess the protein contents in lysates, cell media and brain homogenates.

For the western blots, the proteins were separated on polyacrylamide gels using SDS-PAGE. Subsequently, proteins were transferred from the gels to PVDF membranes and blocked with TBST (Tris-buffered saline with 0.01% Tween-20) containing 3% milk. Following blocking, membranes were treated with relevant primary antibodies. The following day, after three TBST washes, one hour incubation with suitable secondary antibodies coupled with horseradish peroxidase, and three further TBST washes, the membranes were imaged using a chemiluminescent substrate utilizing the ChemiDoc MP Imaging System. The Image Studio Lite program (LI-COR Biosciences) was used to assess the protein band intensities.

3.6.2.11. Immunofluorescence Staining

For PNN detection in vitro via immunofluorescence (IF), neuronal cells at the end of their coculture periods were fixed with 4% paraformaldehyde in PBS for 10 minutes at room temperature and washed three times with PBS. The cells were then kept at room temperature for one hour with a blocking and permeabilization (block/perm) solution containing 2% FBS and 0.2% Triton-X 100 in PBS. Subsequently, primary antibodies (anti-MAP2 or anti-neurocan) or fluorescein-conjugated WFA was added to the coverslips (in block/perm solution) and the cells were incubated in dark at 4°C overnight. The following day, after three PBS washes, corresponding Alexa Fluor conjugated secondary antibodies and Hoechst 33342 dye (for nuclear staining) were applied to the cells in the block/perm solution, and the cells were kept in dark at room temperature for one hour. After three PBS washes, the coverslips were removed from the plates and placed on slides with mounting medium. After curing,

slides were sealed with nail polish and imaging was performed on a fluorescence or confocal microscope.

PFA-immersed brains were placed in 15% sucrose solution in PBS for dehydration of tissue. After the brains sunk to the bottom of the solution (after 20-40 hours at 4°C), they were moved into a 30% sucrose solution. After approximately 24 hours at 4°C, the brains that sank to the bottom of 30% sucrose solution were removed and placed in plastic cuvettes filled with optimal cutting temperature (OCT) compound and frozen at -80°C. Afterwards, 10 µm thick coronal sections of the hippocampus and neighboring areas were cut and transferred onto adhesive slides (the sections were stored for some days at -20°C before immunofluorescence staining). For post-sectioning IF procedures, the dried OCT was removed from slides and samples were bordered with a PAP-pen. The samples were then fixed and permeabilised with cold acetone at -20°C for 10 minutes, washed shortly in PBS, and kept in a block/perm solution of 5% donkey serum and 0. 2% Triton-X-100 (in PBS) for one hour. Afterwards, primary antibodies or WFA was added on samples in 1% donkey serum, 0.2% Triton-X-100 in PBS ("in vivo antibody solution") and the slides were kept overnight in humidified chambers at 4°C. The next day, slides were washed three times with PBS, kept for one hour at room temperature with secondary antibodies in the same solution and Hoechst, washed three times with PBS and finally with distilled water and dried briefly. Slides were then covered with coverslips after applying an anti-fade mounting medium. After curing in the dark (for half an hour or a day depending on mounting medium) slides were sealed with nail polish. They were then visualised with a fluorescence or confocal microscope.

Analysis and processing of the images were performed using Fiji/ImageJ. In line with previous literature, PNN-component-positive cells were to assess PNN integrity. Cells with somas covered with neurocan or WFA staining were considered "neurocan-positive" (neurocan+) or "WFA-positive" (WFA+), respectively (Tansley et al., 2022; Venturino et al., 2021). For every coverslip with (in vitro) neuronal cells, at least three microscope images were acquired and all cells were counted in each image. For every mouse, at least three sections were used and images of hippocampal cornu Ammonis 1, 2, 3 (CA1,2,3) and of the primary somatosensory cortex were taken for each section. In IF procedures, MAP2

antibodies were used to stain for mature neurons; neurocan antibodies and WFA was used to stain for PNNs.

3.7. Study Plan and Timeline

Literature research for the thesis topic, decision on thesis topic and approval of the thesis proposal was finished in the first half of 2021. Writing of grant/project proposals for supporting the thesis study was finished in the second half of 2021. The projects were approved in the first months of 2022. The timeline of the following dates are given in **Figure 4**.

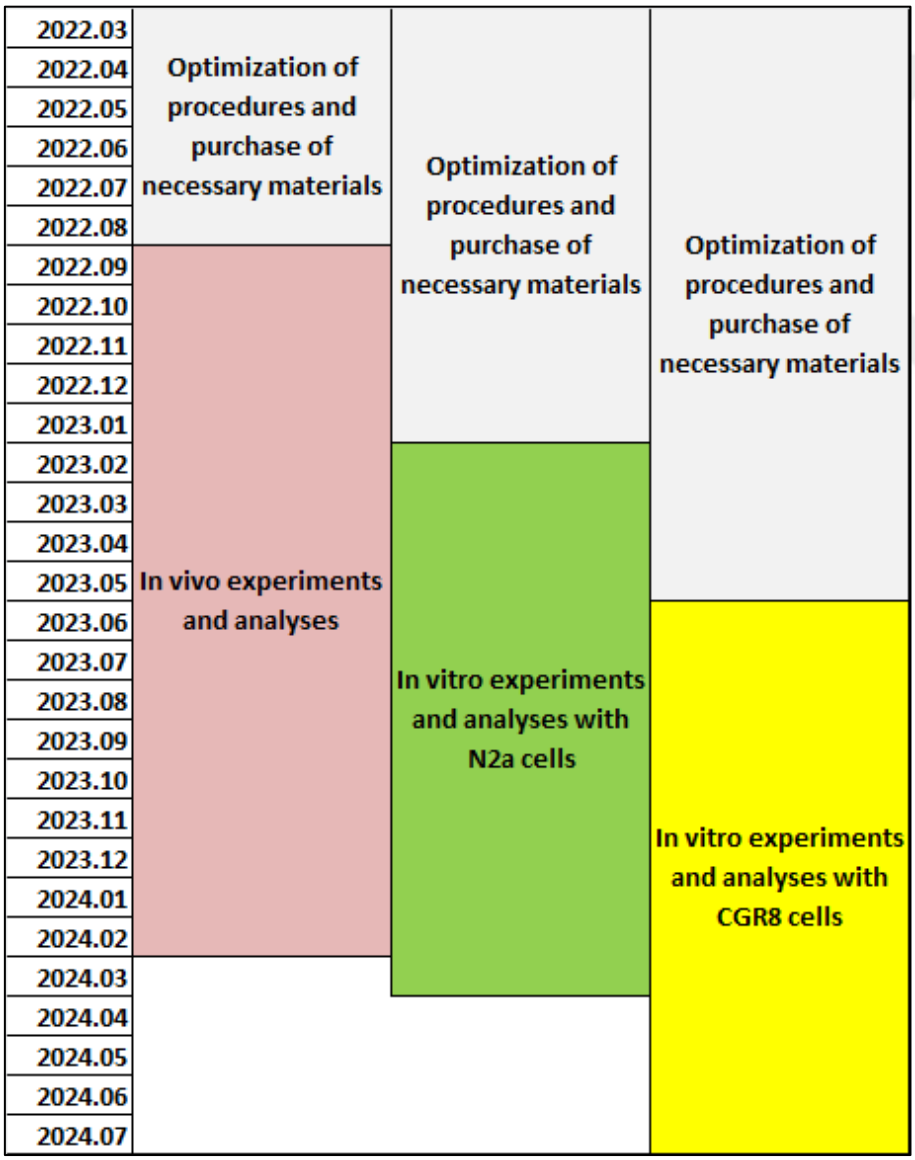

Figure 4: Timeline of the thesis study

3.8. Data Analysis

Statistical analyses were performed in GraphPad Prism 8.0. Data are presented as mean ± SEM. Normality of each data set was assessed by Shapiro–Wilk test. Comparisons between two groups where both group's distributions are normal were analyzed by Student's t-test. Comparisons between two groups where at least one distribution is non-normal were analyzed with the Mann–Whitney U-test. A p-value less than 0.05 was considered statistically significant in all comparisons. In graphical representations within the thesis $p<0.05$, $p<0.01$ and $p<0.001$ and $p<0.0001$ are represented respectively by *, **, *** and ****.

3.9. Limitations of the Study

There were several limitations in our study. Firstly, since neuroglia (and especially astrocytes) have big roles in organismal production of PNNs; PNNs created in in vitro culture of only neurons might not reflect the in vivo environment well enough. Furthermore, while the presence of PNN+ cells was investigated via staining for WFA-binding groups or neurocan in this study, these targets do not necessarily represent the entirety of a PNN, and it is possible that some PNNs without neurocan and WFA-binding groups exist. Additionally, determining the change (if any) of all common PNN proteins via immunoblotting could have contributed to the study. The mechanism (like proteinases contributing to the degradation) and time course (when PNNs begin to be degraded) of NLRP3-induced microglial PNN degradation could also be investigated through additional experiments. However, due to budget limitations, these additional protein detections and experiments could not be included in the thesis study.

3.10. Ethics Committee Approval

This thesis study has been approved by the Izmir Biomedicine and Genome Center Non-Interventional Research Ethics Committee with the protocol number 2021-016 and the Izmir International Biomedicine and Genome Institute Local Ethics Committee for Animal Experiments (IBG-AELEC) with protocol number 2022-002. The committee approval decisions are presented in the appendices section.

4. RESULTS

4.1. Differentiation of N2a Cells Into PNN-positive Neurons

The mouse N2a neuroblastoma cell line was used to create a model of neuronal differentiation in order to determine whether PNNs are present in N2a-derived neurons in vitro. To stimulate neuronal development, the cells were treated with 10 μM RA for three and four days. The mRNA levels of mature neuron markers *Map2* (long *Map2* transcripts that code for MAP2A and MAP2B, which are the predominant form in mature neurons) and *Rbfox3* (NeuN) increased on the third and fourth days in comparison to undifferentiated cells (**Figure 5A**). *Ncan*, the gene that codes for the PNN protein neurocan, was also tested to see when it increased in expression and it was highly elevated on the third and fourth days (**Figure 5B**).

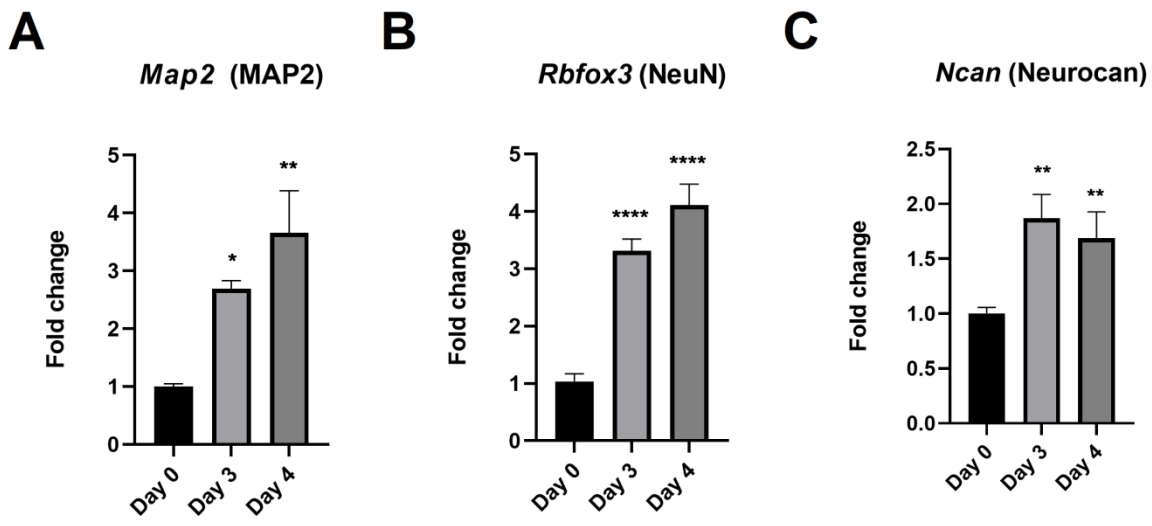

Figure 5: Changes in mRNA expression of MAP2, NeuN and Neurocan in N2a cells at day 0, 3 and 4 of 10 μM RA treatment. A: Fold change in *Map2* expression. B: Fold change in *Rbfox3* expression. C: Fold change in *Ncan* expression. (n=4; * = $p<0.05$; ** = $p<0.01$; **** = $p<0.0001$ compared to Day 0)

To further investigate if PNNs were present in differentiated N2a cells, we used immunostaining with WFA-fluorescein (which binds to PNN CSPGs) and neurocan antibody on undifferentiated N2a cells and N2a cells at day 4 of differentiation, also utilizing MAP2 antibody to stain for neurons. When comparing day 4 to day 0, the immunofluorescence

pictures revealed an increase in WFA+ and neurocan+ neurons (**Figure 6**). Day 4 was selected as the initial time point for our coculture model due to the significant rise in mature neuron markers, Ncan mRNA expression, and PNN component staining at that timepoint.

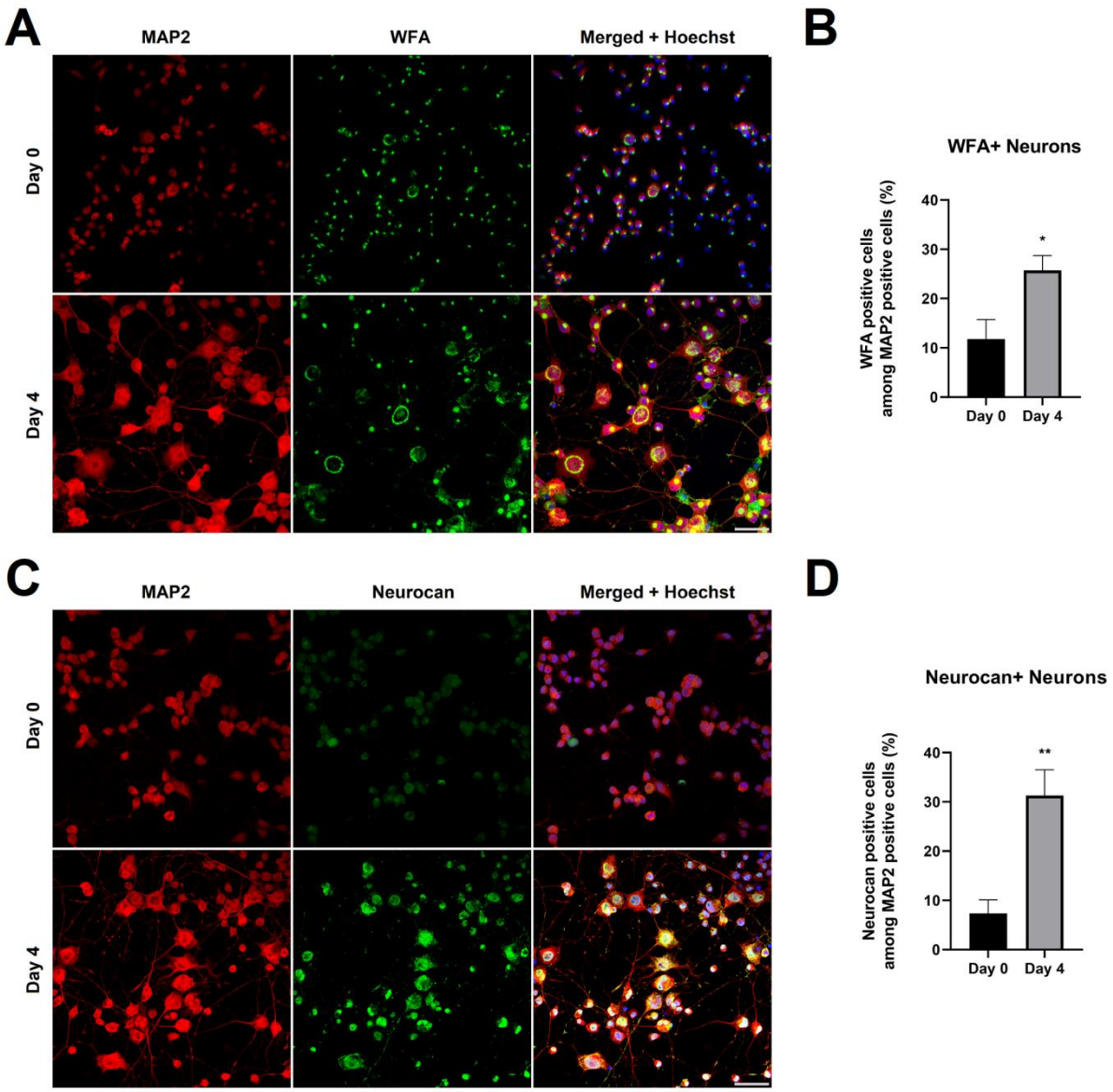

Figure 6: Representative confocal microscopy images of WFA and MAP2 staining in N2a cells at Day 0 and 4 of neural differentiation via 10 µM RA treatment. A: Images of WFA (green) and MAP2 (red) IF staining. B: Percentages of WFA+ neurons among all neurons. C: Images of neurocan and MAP2 IF staining. D: Percentages of Neurocan+ neurons among all neurons. (Scalebar = 50 µm; n=3; * = $p<0.05$ compared to Day 0, ** = $p<0.01$ compared to Day 0)

4.2. Microglial NLRP3 Inflammasome Activation

N9 microglial cells were cultured with LPS and ATP (with and without the NLRP3 inhibitor MCC950) in order to activate the NLRP3 inflammasome. At the end of the model, the microglial cells were moved into a coculture with neurally differentiated N2a or CGR8 cells. Immunoblotting analysis was used to verify the inflammasome model and inhibitor efficiency after the identical experimental setup was carried out independently on culture flasks. In the LA group, the inflammasome model led to a rise in NLRP3 (in cell homogenates), cleaved IL-1β and cleaved caspase-1 (in cell media). NLRP3 inhibition counteracted this effect, indicating that the increase in caspase-1 and IL-1β in our model is NLRP3-dependent (**Figure 7**).

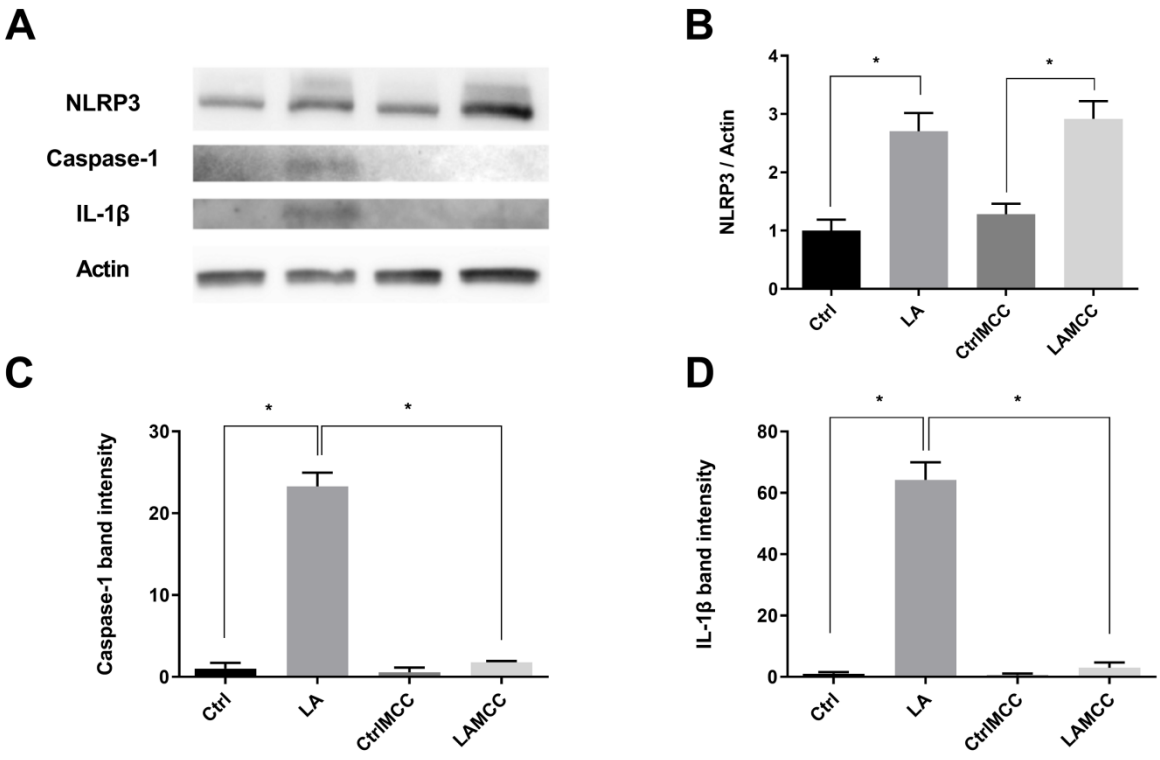

Figure 7: Proteins downstream of the NLRP3 inflammasome are increased with LPS+ATP treatment and this increase is reversed with MCC950 treatment in N9 cells. A) Representative

bands from the western blot analyses for NLRP3, caspase-1 and IL-1β. B) Normalized band intensity for NLRP3 in N9 lysates. C) Band intensity quantification of cleaved caspase-1 in cell media. D) Band intensity quantification of cleaved IL-1β in cell media. (n=4; * = $p<0.05$)

4.3. Coculture of Neuronal Cells with Inflammasome-activated Microglial Cells

PNNs on neuronal cells were photographed using fluorescein-tagged WFA at the end of the coculture phase. The percentage of neurons in the LA group that were WFA+ was lower compared to all other groups, both for N2a-derived neurons (**Figure 8)** and for CGR8-derived neurons (**Figure 9**). In N2a-derived neurons, IF staining was performed also for neurocan, a significant CSPG in PNNs. Similar PNN levels across groups were visible in this staining, with the exception of the LA group, which had a noticeably decreased number of neurocan+ neurons (**Figure 10**). Consequently, the decrease in WFA+ or neurocan+ neurons was reversed when NLRP3 inhibition was present in microglia cocultured with N2a-derived neurons.

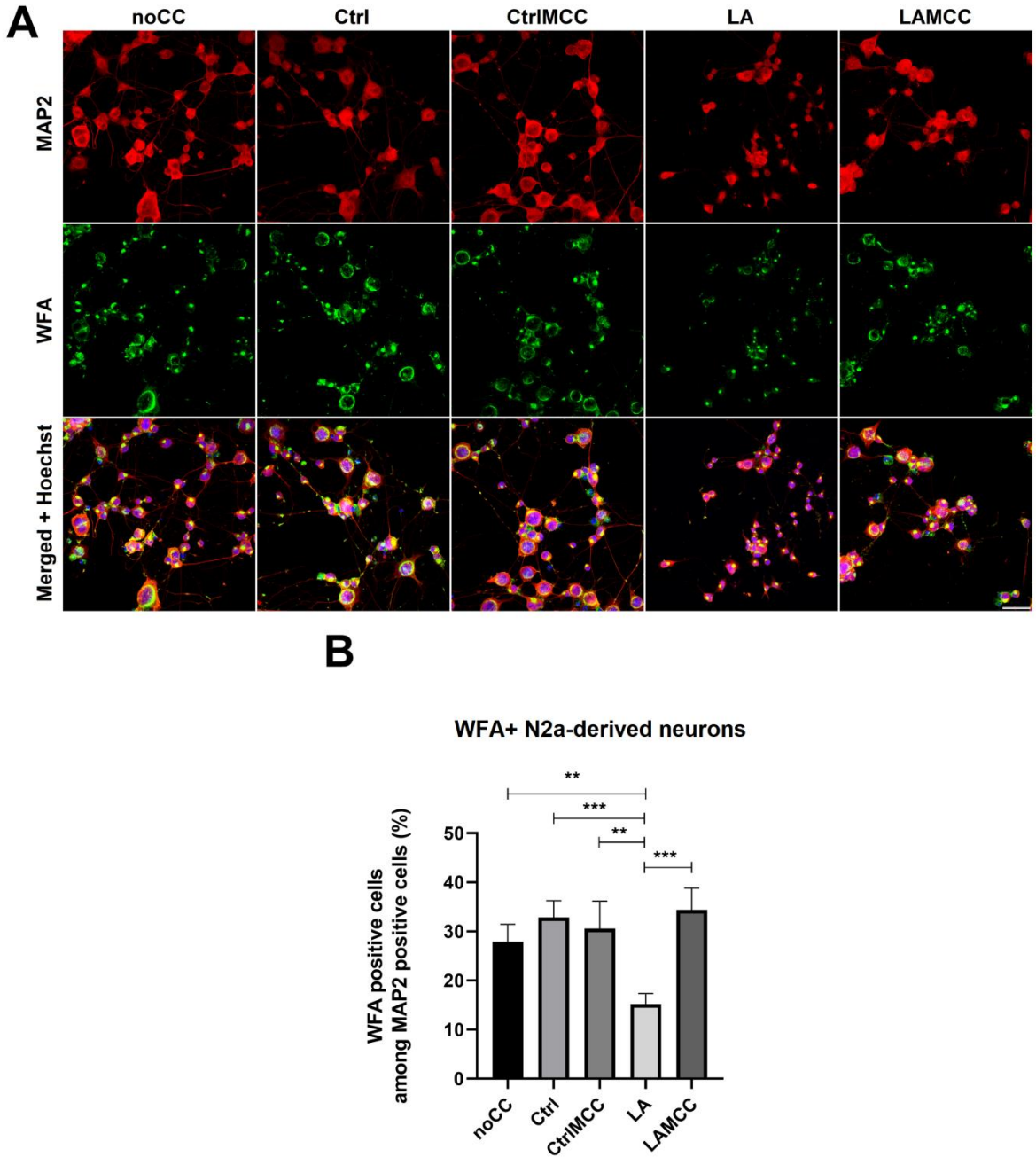

Figure 8: Coculture with inflammasome-activated microglia reduces WFA+ neurons in N2a-derived neuronal cells A) Representative confocal microscopy images of WFA (green) and MAP2 (red) staining in N2a-derived neuronal cells at the end of the coculture period. B) Quantification of the percentages of WFA+ neurons among all neurons. (n=3; scalebar = 50 µm; ** = $p<0.01$; *** = $p<0.001$)

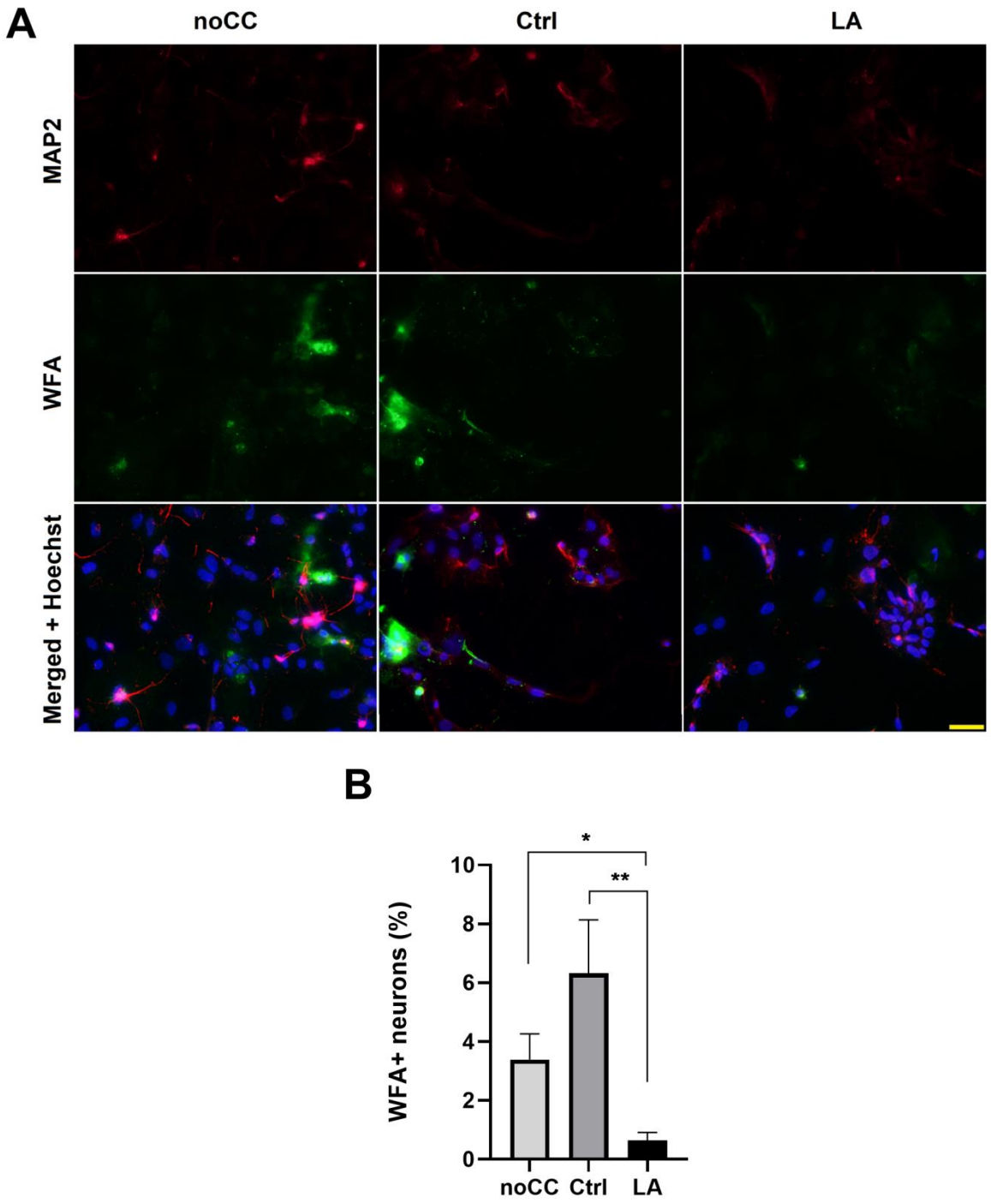

Figure 9: Coculture with inflammasome-activated microglia reduces WFA+ neurons in CGR8-derived neuronal cells A) Representative fluorescence microscopy images of WFA (green) and MAP2 (red) staining in CGR8-derived neuronal cells at the end of the coculture period. B) Quantification of the percentages of WFA+ neurons among all neurons. (n=3; scalebar = 20 µm; ** = $p<0.01$; *** = $p<0.001$)

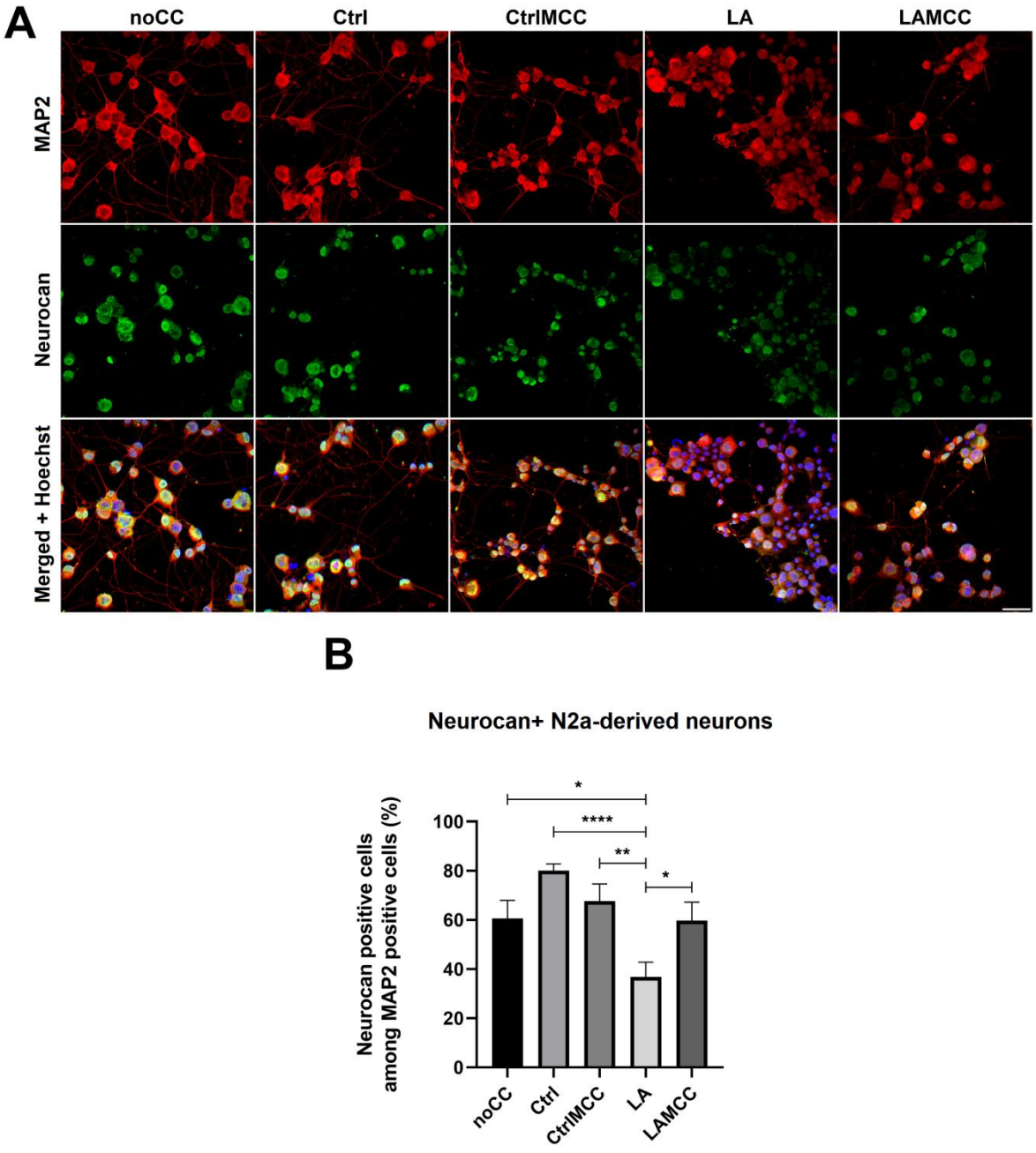

Figure 10: Coculture with inflammasome-activated microglia reduces neurocan+ neurons in N2a-derived neuronal cells. A) Representative confocal microscopy images of neurocan (green) and MAP2 (red) staining in N2a-derived neuronal cells at the end of the coculture period. B) Quantification of the percentages of neurocan+ neurons among all neurons. (Scalebar = 50 µm; n=3; * = $p<0.05$; ** = $p<0.01$; **** = $p<0.0001$)

4.4. Inflammasome Activation in Brains of Neonatal Mice

Mice injected on PND9 were sacrificed on the next day and levels of NLRP3 and IL-1β were determined in their brain homogenates. NLKO mice had no NLRP3 protein expression in their brains. And the levels of IL-1β in NLKO mice were similar to the levels in WT mice injected with PBS (**Figure 11**).

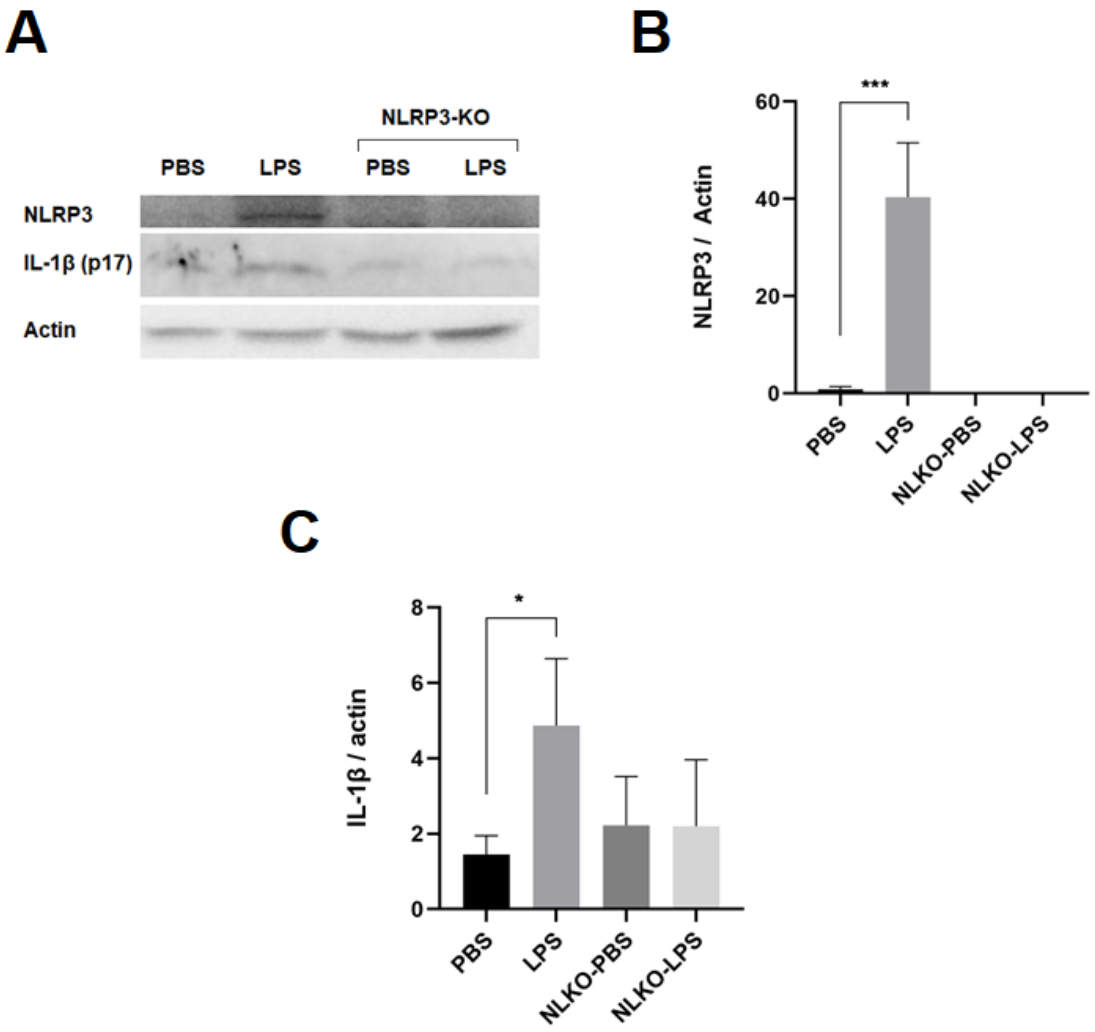

Figure 11: Confirmation of NLRP3 inflammasome activation in WT mice and of inhibited NLRP3 inflammasome activation in NLKO mice. A) Representative bands from the western blot analyses for NLRP3 and IL-1β. B) Normalized band intensity for NLRP3 in PND10 mouse brains. C) Normalized band intensity for IL-1β in PND10 mouse brains. (n=4; * = $p<0.05$; *** = $p<0.001$)

4.5. Assessment of PNN Presence in Neonatal Mouse Brains

To determine whether PNNs are present and are affected by inflammation in the first few days after the LPS injection, we also used PND12 mice to assess presence of PNNs by WFA staining. IF visualization of these brains revealed that there were no WFA+ cells in the brains of PND12 mice. A comparison of PND12 and PND60 WFA staining is given in **Figure 12.**

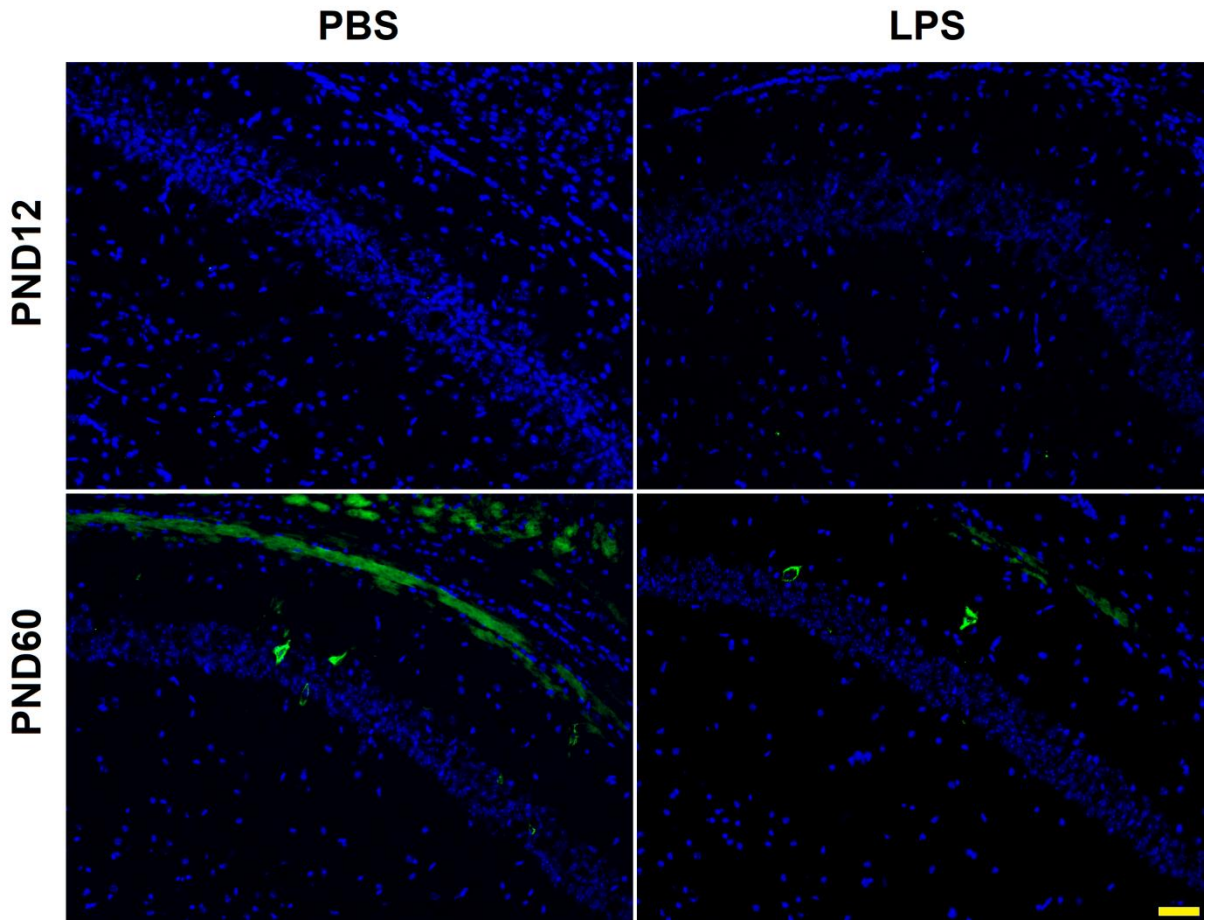

Figure 12: Comparison of PNNs in neonatal and early adult mice. The representative images show WFA (green) and Hoechst (blue) staining of the hippocampi (CA1 regions) of PND12 and PND60 mice injected with PBS or LPS at PND9. (Scalebar = 50 μm)

4.6. Clinical Scoring and Behavioral Tests in Early Adult Mice

Before early adult mice were sacrificed on PND60, they were clinically scored for symptoms of lethargy, huddling and ptosis (with presence of each symptom considered 1 point). All mice had a score of 0 on this measure, meaning that their behavior appeared normal. However, two of the three female NLKO-LPS mice each had a patch of hair loss on their backs (about 0.5 to 1.5 cm in diameter). The levels of anxiety- and depressive-like behavior of the mice were measured by the open field, tail suspension and forced swim tests. WT LPS-injected mice spent less time in the central zone in the open field, and had lower latency to immobility when suspended or swimming. This behavior was not replicated between NLKO mice, where both injections resulted in similar behavior (**Figure 13**). Latency to immobility of NLKO mice in general in TST was visibly less than that of WT mice, but the phenomenon was not explored further as it is not relevant to the topic of research.

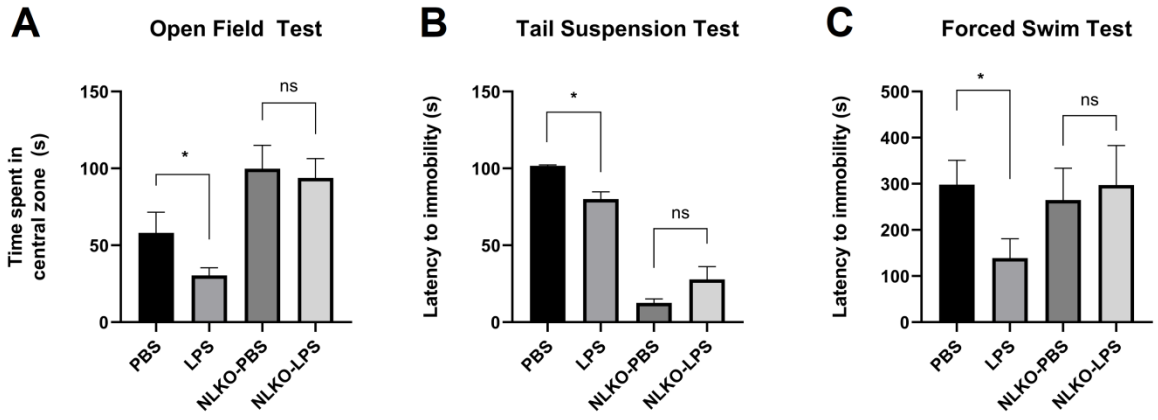

Figure 13: Behavioral tests of mice at PND 60. A) Inter-group comparisons of the time spent in the central zone of the box in OFT. B) Inter-group comparisons of time spent until first immobility in TST. C) Inter-group comparisons of the time spent until first immobility in FST. (n=5; * = $p<0.05$, ns = not significant)

4.7. PNN Changes in Brains of Early Adult Mice

PND60 mouse brain sections were stained with anti-MAP2 for neurons and WFA for PNNs. Visualization and counting of PNN+ cells in the hippocampus (**Figure 14**) and primary somatosensory cortex (**Figure 15**) revealed that LPS mice had lower number of PNN+ cells, implying that the neonatal systemic LPS exposure reduces PNNs in these areas.

Moreover, it was also seen in the microscopy images that NLKO-LPS mice did not have the same level of decrease in PNN+ cells seen between LPS and PBS injected WT mice.

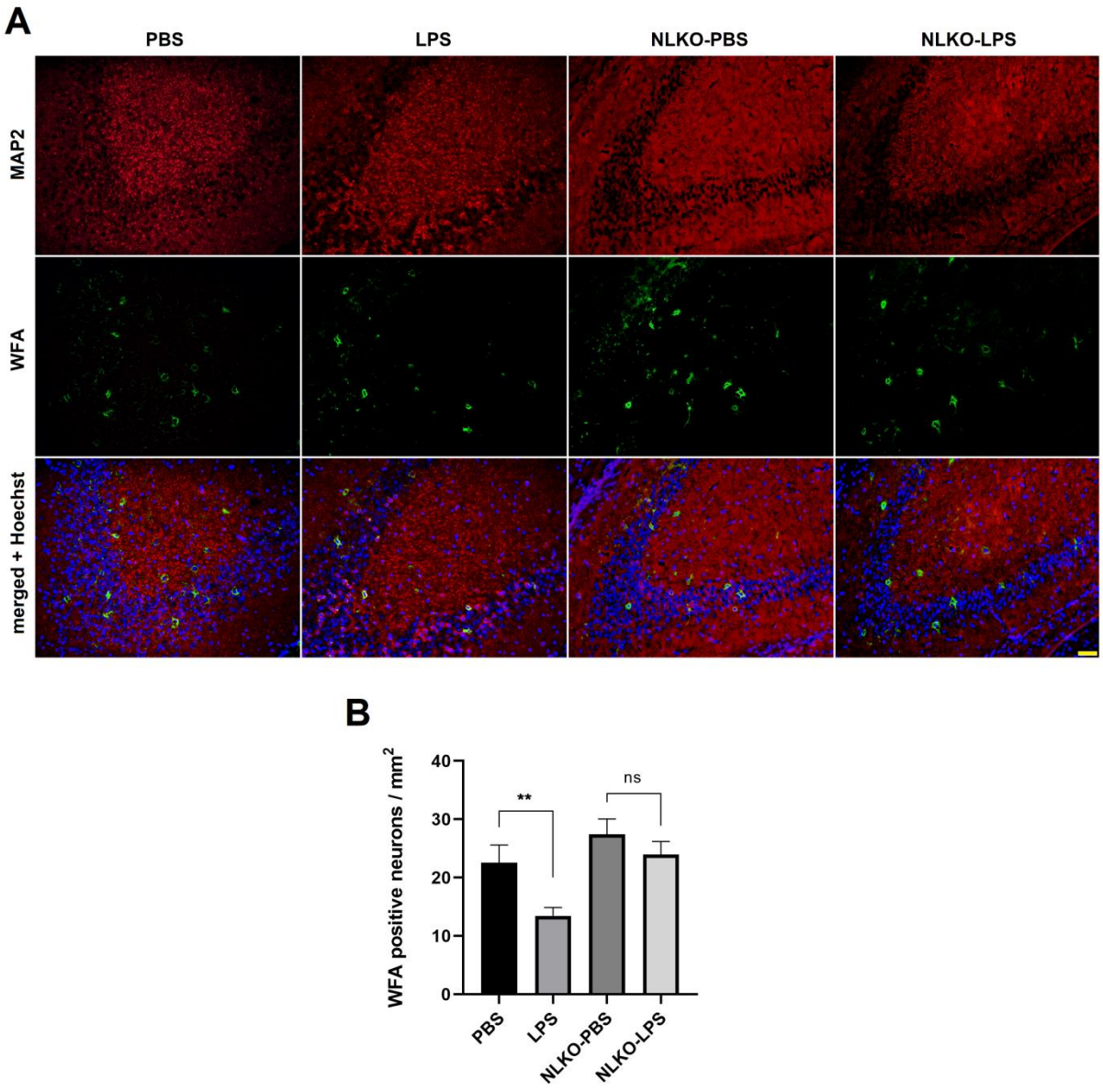

Figure 14: Comparisons of PNN+ neurons per area in the hippocampi of PND 60 mice. A) Representative images of MAP2 (red) and WFA (green) staining of the hippocampi (CA3 regions) of mice from the four groups. B) Graphical representation of the WFA+ neurons/mm^2 quantification in the hippocampal images (images from CA1, CA2 and CA3). (n=5; ** = $p<0.01$, ns = not significant)

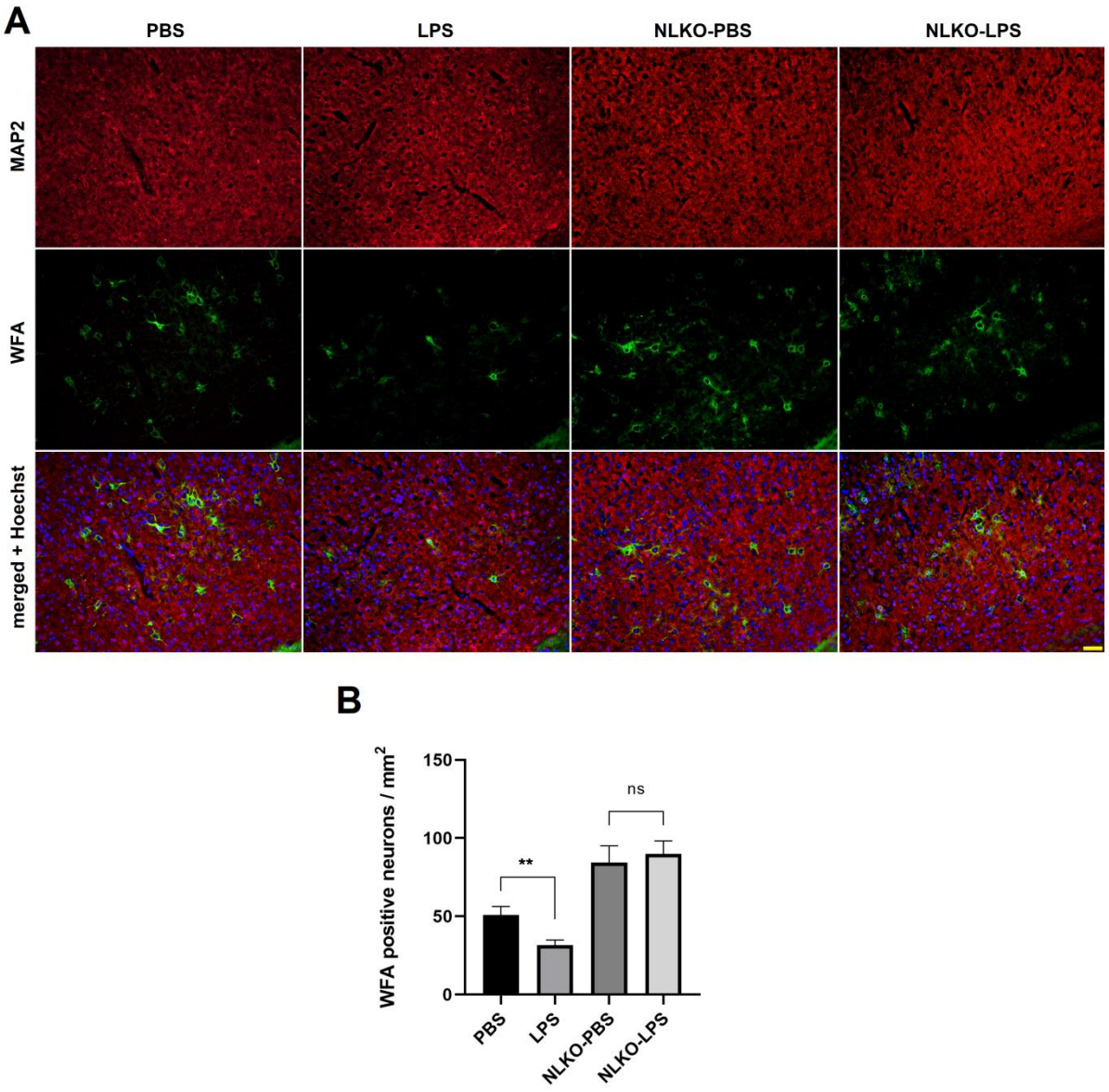

Figure 15: Comparisons of PNN+ neurons per area in the primary somatosensory cortices of PND 60 mice. A) Representative images of MAP2 (red) and WFA (green) staining of the cortices of mice from the four groups. B) Graphical representation of the WFA+ neurons/mm^2 quantification in the cortex images. (n=5; ** = $p<0.01$, ns = not significant)

5. DISCUSSION

5.1. Connection of Findings to the Hypotheses and Possible Mechanistic Explanations

The findings of the coculture experiments confirm that microglial activation (via LPS and ATP) leads to a significant reduction in PNN+ neurons generated from cell lines (**hypothesis 1**). This is evidenced by decreased WFA and neurocan staining in N2a and CGR8 derived neurons cocultured with LPS+ATP activated N9 microglia. Inhibition of NLRP3 with MCC950 in the N2a cocultures reversed this effect, confirming the role of NLRP3 inflammasome activation in the degradation process (**Figure 8, Figure 9, Figure 10**). This finding also supports the hypothesis that NLRP3 activation in microglia contributes significantly to PNN disruption (**hypothesis 2**). The in vivo data, where genetically knocking out NLRP3 protected neurons from losing PNNs, strongly supports the second hypothesis as well. These findings highlight NLRP3's pivotal role in initiating the inflammatory cascade that disrupts PNN integrity (at least in the cases of inflammatory insult via LPS/gram-negative bacteria).

Our in vivo model of neonatal LPS injection resulted in increased anxiety-like and depressive-like behavior in early adulthood (**Figure 13**), which is in line with previous mouse studies where early life inflammation (Dinel et al., 2014) or stress (Qin et al., 2021) creates similar rises in anxiety-like or depressive-like behavior later in life. Although this change in behavior is not necessarily caused by the reduction in PNNs, depressive-like behavior was previously shown in another model of PNN loss where rats exposed to chronic unpredictable mild stress had both reduced PNNs and increased depressive-like behavior (Yu et al., 2020). It remains to be seen whether protection of PNNs while keeping inflammation's other effects intact would revert this phenomenon.

Furthermore, our in vivo IF results support **hypothesis 3**: that postnatal/early brain inflammation might lead to reduced PNNs (**Figure 14, Figure 15**). We demonstrate that early-life inflammation mediated by NLRP3 activation can have lasting effects on PNN distribution in neurons. The hippocampal decrease in PNN+ neurons would indicate a lower amount of synaptic stability and thus likely reduced amount of memory consolidation (Schapiro et al., 2019). The PNN reduction in the primary somatosensory cortex could lead to problems in sensory input, which might eventually lead to dysfunctional motor output (Borich

et al., 2015). Our finding supports the idea that neonatal brain inflammation is particularly detrimental to PNN formation and maintenance during brain development, when microglia are low in number and PNNs are still forming. Similar PNN alterations in the CGR8-derived neuronal cells also suggest that microglia can affect the number of PNN+ neurons in an environment where mature neurons are present together with neural progenitor cells and neural stem cells.

However, it is important to note that while our results in mice show a reduction in PNN+ neurons, this does not necessarily imply that PNNs of neurons have been degraded. Because the inflammatory insult was in the neonatal period, it is possible that neurons that would normally develop PNNs do not develop them due to a transcriptome and/or proteome alteration by inflammatory (microglial or otherwise) factors. Similarly, it is not clear whether microglia in our CGR8-derived neuronal culture model degrade PNNs on mature neurons or prevent neural progenitor cells from developing into PNN-forming mature neurons. This line of thought is also consistent with a previous study in rats. In the study, rats born from female rats injected with the immunostimulant polyinosinic:polycytidylic acid (poly I:C) during gestation and those born from female rats injected with saline have similar levels of PNN per area at PND7-to-35. But the poly I:C rats eventually exhibited reduced numbers of PNN per area once the PNN levels reached its peak in control groups (at PND90) (Paylor et al., 2016). This implicates that rather than direct microglial degradation, the inflammation at embryonic stage had a more subtle effect on the capacity of neurons to form PNNs. Corroborating this, the rat study also records unchanged microglial numbers between the control and poly I:C groups at all ages. Likewise, in our neonatal LPS injection model too, the microglia might simply be downregulating proteins in neurons that would later contribute to PNN formation (or simply selectively eliminating neurons that would generate PNNs, although this seems less probable). Another finding that suggests PNNs were prevented from forming rather than degraded appears in our study: IF visualization of PND12 mouse brain sections showed an absence of WFA staining in both groups (**Figure 12**); meaning that there would be no PNNs (or at least WFA+ PNNs) for microglia to degrade in the first few days after LPS injection.

Regarding the importance of NLRP3 in the in vivo model, the explanation for the LPS-induced decrease in PNN+ neurons seen in brain sections of WT mice but not in NLKO mice may be given in two ways. In our in vivo model of NLRP3 activation, since LPS injection is

not made directly into the brain, activation in the brain is thought to occur with the help of inflammatory factors in the periphery (Skrzypczak-Wiercioch and Salat, 2022). Therefore, the lack of PNN decrease in the brain of NLKO mice may be associated with reduced NLRP3-induced inflammation in the periphery; hence reduced inflammatory factors reaching the brain. Alternatively —or additionally— the absence of NLRP3 in microglia in the brain may have limited the effect of LPS on microglia (the same could also be said for astrocytes, which also express NLRP3 (Tastan et al., 2021; Tufekci et al., 2021)). Further studies examining PNN components and the LPS-induced immune factors in the brain and other tissues over time are required to elucidate the reason why NLRP3 was critical in the long-term reduction of PNNs. A potential avenue of study could be a conditional knockout models where NLRP3 is knocked out specifically in CNS cells or only in microglia; and models where LPS is injected directly into the brain. These models would help determine the specific tissue level at which NLRP3 is responsible and identify the cell types that play the most significant role in PNN loss.

While it is unclear whether the effect of microglial NLRP3 activation on developmental period PNNs are through direct extracellular degradation or indirect influence on PNN genes, the effect might be more straightforward in the N2a part of the study. This is because the time between indirect microglia-neuron contact and neuron fixation is relatively short and an effect is still visible. It is thus probable there is degradation at work in this model. As for the mechanism of this degradation, the arrows point to inflammasome-associated proteases. The activation of the NLRP3 inflammasome has been connected to the upregulation of multiple MMPs, including MMP-2 (Unamuno et al., 2021), MMP-9 (Ren et al., 2020) and MMP-13 (Liu et al., 2023), which could be connected to the degradation of PNNs. Indeed, it was demonstrated in the knee cartilage of mice that an increase in IL-1β, a marker of inflammasome activation, occurred simultaneously with an increase in MMP-13 and a decrease in aggrecan (Liu et al., 2023). It was also suggested or reported in previous studies that MMP-9 can degrade PNN components (Cheung et al., 2024; Kelly et al., 2015; Murase et al., 2017; Venturino et al., 2021; Wegrzyn et al., 2021). Furthermore, it has been revealed that cathepsin S degrades neurocan in rats (Petanceska et al., 1996), and cathepsins are also linked to the activation of the NLRP3 inflammasome (Campden and Zhang, 2019). Therefore, in our coculture model too, the degradation of PNNs may be caused by MMPs or cathepsins secreted from microglial cells.

5.2. Other Observations and Limitations

In our coculture models, there appears to be a slight but insignificant rise in PNN+ neurons in Ctrl groups compared to noCC groups, which (if it can be replicated and shown to be significant in a larger sample) might indicate that factors from homeostatic microglia can induce PNN formation.

One drawback of our research is that WFA may stain more than extracellular chondroitin sulfates due to its affinity for chondroitin sulfate groups: certain cells in our IF images have high-intensity WFA-stained circles around the nucleus, which indicates intracellular staining. WFA may be binding to nuclear perlecan, a proteoglycan that can also contain side chains of chondroitin sulfate (Gomes et al., 2002; Hayes and Melrose, 2021). The presence of isolated high-intensity WFA specks in some of the N2a-derived neurons in our study can also be explained by this intracellular staining.

A second potential limitation is that in our in vitro model, there seems to be a difference in the proportion of WFA+ and neurocan+ N2a-derived neurons: in both the differentiation and coculture models, the neurocan+ neurons are more abundant than the WFA+ neurons. This could be explained by the increased affinity of WFA for some CSPGs and the diversity of components between PNNs of individual cells. For instance, it has been observed that while the neurons of mice lacking aggrecan still stain positively for other PNN components, they do not stain positively for WFA (Giamanco et al., 2010), perhaps because of the high number of chondroitin sulfate side chains in aggrecan.

A more evident limitation is that the number of WFA+ neurons (and neurons in general, as indicated by the neurite-to-nucleus ratio in IF images) are markedly low in our CGR8-derived neuronal coculture model. This is probably to be attributed to the inefficiency of trypsin dissociation, as the process had a large leftover of non-dissociated cell masses. Moreover, the length of the procedure also seemed to be toxic to cells that were dissociated, as a large number of dead cells were visible in final cell counts with trypan blue. The cells that dissociated and survived the process tended to be more stem-like and non-neuronal. To create an ideal coculture model with “developing neurons”, the generation of neurons from CGR8 EBs has to be refined further.

Another drawback is the lack of glial cells in our neuronal culture models. Since glia (especially astrocytes) contribute to the formation and maintenance of PNNs (Tewari et al., 2022), their role is disregarded in a model with only neurons. Nonetheless, the ability to observe PNN fate without the extra complexity of maintaining multiple cell cultures is both time-efficient and cost-effective.

5.3. Connection of Findings to Biomaterials and Tissue Engineering

This research supports the development of biomaterials aimed at protecting neuronal integrity. For example, biomaterials that can respond to inflammation levels, releasing therapeutic agents like MCC950 when NLRP3 activation is detected, could also be used in the clinic, especially for favoring implant integration and biocompatibility during grafts, since NLRP3 can also be activated as a result of tissue damage (Menu and Vince, 2011). Coatings that inhibit NLRP3 could prevent inflammation-induced degradation of nearby neural structures and PNNs, preserving functionality and minimizing adverse immune reactions over time.

Findings from this study also show that neuron-microglia interaction includes not only the cell contents but also the ECM. This could improve in vitro models, allowing for more realistic and reliable study of neuron-microglia interactions, neural inflammation, and ECM dynamics under controlled conditions.

Furthermore, the PDL and laminin coatings used in this study were optimized multiple times for creating an ideal growth environment for cell adhesion and neural differentiation. For instance, washing wells after PDL coating once, rather than two or more times, resulted in enhanced adhesion of neuronal cells. Additionally, maintaining trace moisture in the wells was more effective for cell adhesion than drying the wells completely. The insights gained from this study could inform the future development of biomaterial surfaces for clinical and cell culture applications.

6. CONCLUSION AND FUTURE PERSPECTIVES

6.1. Conclusion

Our study's results align with its hypotheses, demonstrating that NLRP3 inflammasome activation plays a critical role in microglia-mediated PNN loss. Our study shows that **(1)** inflammatory activation in a microglial cell line results in the reduction of PNN+ neurons in a neuronal cell cultures derived from cell lines; **(2)** NLRP3 has a significant role in microglia-mediated PNN degradation (or reduction of PNN+ cells in the long-term) as evidenced both in vitro via MCC950 inhibition and in vivo via NLRP3 knockout mice; and **(3)** microglial activation during neonatal period results in reduction of PNNs at early adulthood. Our data indicate that soluble molecules from microglia, such as proteins, induce a reduction in PNN-positive neurons. This suggests that in cases of acute neuroinflammation due to microglial activation, drugs that target NLRP3 directly might be desirable options to prevent PNN degradation, considering the importance of PNNs in memory retention and synaptic stability. Inflammatory insults to PNNs would thus be mitigated without the use of broad-spectrum anti-inflammatory drugs like steroids, which may cause unintended effects at high doses.

6.2. Future perspectives

Future studies in this area of PNN and inflammasome research could include in vitro and in vivo studies that focus on:

- Effects of microglia-mediated (or possibly simply enzymatic) PNN degradation on learning and memory in animals.
- The timing of microglia-mediated PNN degradation (i.e., when degradation begins after the inflammatory insult).
- Whether degradation occurs at neonatal stages, and if not, identifying transcriptomic or proteomic changes that may indicate a reduced neuronal propensity to form PNNs.
- Identifying which proteases, among those induced by inflammation and inflammasome activation, play the most critical role in PNN degradation.

7. REFERENCES

Arioz, B.I., Tastan, B., Tarakcioglu, E., Tufekci, K.U., *et al.* (2019). Melatonin Attenuates LPS-Induced Acute Depressive-Like Behaviors and Microglial NLRP3 Inflammasome Activation Through the SIRT1/Nrf2 Pathway. Frontiers in immunology; *10*: 1511.

Bachiller, S., Jimenez-Ferrer, I., Paulus, A., Yang, Y., *et al.* (2018). Microglia in Neurological Diseases: A Road Map to Brain-Disease Dependent-Inflammatory Response. Frontiers in cellular neuroscience; *12*: 488.

Baig, S., Wilcock, G.K., and Love, S. (2005). Loss of perineuronal net N-acetylgalactosamine in Alzheimer's disease. Acta neuropathologica; *110*: 393-401.

Bodin, P., and Burnstock, G. (1998). Increased release of ATP from endothelial cells during acute inflammation. Inflammation research : official journal of the European Histamine Research Society [et al]; *47*: 351-354.

Borich, M.R., Brodie, S.M., Gray, W.A., Ionta, S., *et al.* (2015). Understanding the role of the primary somatosensory cortex: Opportunities for rehabilitation. Neuropsychologia; *79*: 246-255.

Boyko, M., Kutz, R., Grinshpun, J., Zvenigorodsky, V., *et al.* (2019). The effect of depressive-like behavior and antidepressant therapy on social behavior and hierarchy in rats. Behavioural brain research; *370*: 111953.

Bukalo, O., Schachner, M., and Dityatev, A. (2001). Modification of extracellular matrix by enzymatic removal of chondroitin sulfate and by lack of tenascin-R differentially affects several forms of synaptic plasticity in the hippocampus. Neuroscience; *104*: 359-369.

Cabungcal, J.H., Steullet, P., Morishita, H., Kraftsik, R., *et al.* (2013). Perineuronal nets protect fast-spiking interneurons against oxidative stress. Proceedings of the National Academy of Sciences of the United States of America; *110*: 9130-9135.

Campden, R.I., and Zhang, Y. (2019). The role of lysosomal cysteine cathepsins in NLRP3 inflammasome activation. Archives of biochemistry and biophysics; *670*: 32-42.

Campo, G.M., Avenoso, A., Campo, S., D'Ascola, A., *et al.* (2004). The antioxidant and antifibrogenic effects of the glycosaminoglycans hyaluronic acid and chondroitin-4-sulphate in a subchronic rat model of carbon tetrachloride-induced liver fibrogenesis. Chemico-biological interactions; *148*: 125-138.

Canas, N., Valero, T., Villarroya, M., Montell, E., *et al.* (2007). Chondroitin sulfate protects SH-SY5Y cells from oxidative stress by inducing heme oxygenase-1 via phosphatidylinositol 3-kinase/Akt. The Journal of pharmacology and experimental therapeutics; *323*: 946-953.

Castagne, V., Moser, P., Roux, S., and Porsolt, R.D. (2011). Rodent models of depression: forced swim and tail suspension behavioral despair tests in rats and mice. Current protocols in neuroscience; *Chapter 8*: Unit 8 10A.

Cheung, S.W., Bhavnani, E., Simmons, D.G., Bellingham, M.C., *et al.* (2024). Perineuronal nets are phagocytosed by MMP-9 expressing microglia and astrocytes in the SOD1G93A ALS mouse model. Neuropathology and applied neurobiology; *50*.

Coll, R.C., Robertson, A.A., Chae, J.J., Higgins, S.C., *et al.* (2015). A small-molecule inhibitor of the NLRP3 inflammasome for the treatment of inflammatory diseases. Nature medicine; *21*: 248-255.

Colonna, M., and Butovsky, O. (2017). Microglia Function in the Central Nervous System During Health and Neurodegeneration. Annual review of immunology; *35*: 441-468.

Crapser, J.D., Spangenberg, E.E., Barahona, R.A., Arreola, M.A., *et al.* (2020). Microglia facilitate loss of perineuronal nets in the Alzheimer's disease brain. EBioMedicine; *58*: 102919.

Dinel, A.L., Joffre, C., Trifilieff, P., Aubert, A., *et al.* (2014). Inflammation early in life is a vulnerability factor for emotional behavior at adolescence and for lipopolysaccharide-induced spatial memory and neurogenesis alteration at adulthood. Journal of neuroinflammation; *11*: 155.

Enwright, J.F., Sanapala, S., Foglio, A., Berry, R., *et al.* (2016). Reduced Labeling of Parvalbumin Neurons and Perineuronal Nets in the Dorsolateral Prefrontal Cortex of Subjects

with Schizophrenia. Neuropsychopharmacology : official publication of the American College of Neuropsychopharmacology; *41*: 2206-2214.

Eren, E., and Ozoren, N. (2019). The NLRP3 inflammasome: a new player in neurological diseases. Turkish journal of biology = Turk biyoloji dergisi; *43*: 349-359.

Fawcett, J.W., Oohashi, T., and Pizzorusso, T. (2019). The roles of perineuronal nets and the perinodal extracellular matrix in neuronal function. Nature reviews Neuroscience; *20*: 451-465.

Filipello, F., Morini, R., Corradini, I., Zerbi, V., *et al.* (2018). The Microglial Innate Immune Receptor TREM2 Is Required for Synapse Elimination and Normal Brain Connectivity. Immunity; *48*: 979-991 e978.

Fowke, T.M., Karunasinghe, R.N., Bai, J.Z., Jordan, S., *et al.* (2017). Hyaluronan synthesis by developing cortical neurons in vitro. Scientific reports; *7*: 44135.

Franklin, B.S., Latz, E., and Schmidt, F.I. (2018). The intra- and extracellular functions of ASC specks. Immunological reviews; *281*: 74-87.

Giamanco, K.A., Morawski, M., and Matthews, R.T. (2010). Perineuronal net formation and structure in aggrecan knockout mice. Neuroscience; *170*: 1314-1327.

Gogolla, N., Caroni, P., Luthi, A., and Herry, C. (2009). Perineuronal nets protect fear memories from erasure. Science; *325*: 1258-1261.

Gomes, R., Kirn-Safran, C., Farach-Carson, M.C., and Carson, D.D. (2002). Perlecan: an important component of the cartilage pericellular matrix. Journal of musculoskeletal & neuronal interactions; *2*: 511-516.

Hanke, M.L., and Kielian, T. (2011). Toll-like receptors in health and disease in the brain: mechanisms and therapeutic potential. Clinical science; *121*: 367-387.

Hartig, W., Brauer, K., and Bruckner, G. (1992). Wisteria floribunda agglutinin-labelled nets surround parvalbumin-containing neurons. Neuroreport; *3*: 869-872.

Hayes, A.J., and Melrose, J. (2021). What Are the Potential Roles of Nuclear Perlecan and Other Heparan Sulphate Proteoglycans in the Normal and Malignant Phenotype. International journal of molecular sciences; *22*.

Jo, E.K., Kim, J.K., Shin, D.M., and Sasakawa, C. (2016). Molecular mechanisms regulating NLRP3 inflammasome activation. Cellular & molecular immunology; *13*: 148-159.

Kawabori, M., and Yenari, M.A. (2015). The role of the microglia in acute CNS injury. Metabolic brain disease; *30*: 381-392.

Kayagaki, N., Warming, S., Lamkanfi, M., Vande Walle, L., *et al.* (2011). Non-canonical inflammasome activation targets caspase-11. Nature; *479*: 117-121.

Kelly, E.A., Russo, A.S., Jackson, C.D., Lamantia, C.E., *et al.* (2015). Proteolytic regulation of synaptic plasticity in the mouse primary visual cortex: analysis of matrix metalloproteinase 9 deficient mice. Frontiers in cellular neuroscience; *9*: 369.

Kim, I., Mlsna, L.M., Yoon, S., Le, B., *et al.* (2015). A postnatal peak in microglial development in the mouse hippocampus is correlated with heightened sensitivity to seizure triggers. Brain Behav; *5*.

Kim, Y.S., and Joh, T.H. (2006). Microglia, major player in the brain inflammation: their roles in the pathogenesis of Parkinson's disease. Experimental & molecular medicine; *38*: 333-347.

Kovarova, M., Hesker, P.R., Jania, L., Nguyen, M., *et al.* (2012). NLRP1-dependent pyroptosis leads to acute lung injury and morbidity in mice. Journal of immunology; *189*: 2006-2016.

Kwok, J.C., Carulli, D., and Fawcett, J.W. (2010). In vitro modeling of perineuronal nets: hyaluronan synthase and link protein are necessary for their formation and integrity. Journal of neurochemistry; *114*: 1447-1459.

Lalancette-Hebert, M., Faustino, J., Thammisetty, S.S., Chip, S., *et al.* (2017). Live imaging of the innate immune response in neonates reveals differential TLR2 dependent activation patterns in sterile inflammation and infection. Brain, behavior, and immunity; *65*: 312-327.

Latz, E., Xiao, T.S., and Stutz, A. (2013). Activation and regulation of the inflammasomes. Nature reviews Immunology; *13*: 397-411.

Lima, M.N., Barbosa-Silva, M.C., and Maron-Gutierrez, T. (2022). Microglial Priming in Infections and Its Risk to Neurodegenerative Diseases. Frontiers in cellular neuroscience; *16*: 878987.

Liu, B., Wu, Y., Liang, T., Zhou, Y., *et al.* (2023). Betulinic Acid Attenuates Osteoarthritis via Limiting NLRP3 Inflammasome Activation to Decrease Interleukin-1beta Maturation and Secretion. Mediators of inflammation; *2023*: 3706421.

Liu, Y.J., Spangenberg, E.E., Tang, B., Holmes, T.C., *et al.* (2021). Microglia Elimination Increases Neural Circuit Connectivity and Activity in Adult Mouse Cortex. Journal of Neuroscience; *41*: 1274-1287.

Livak, K.J., and Schmittgen, T.D. (2001). Analysis of relative gene expression data using real-time quantitative PCR and the 2(-Delta Delta C(T)) Method. Methods; *25*: 402-408.

Mauney, S.A., Athanas, K.M., Pantazopoulos, H., Shaskan, N., *et al.* (2013). Developmental pattern of perineuronal nets in the human prefrontal cortex and their deficit in schizophrenia. Biological psychiatry; *74*: 427-435.

Menu, P., and Vince, J.E. (2011). The NLRP3 inflammasome in health and disease: the good, the bad and the ugly. Clinical and experimental immunology; *166*: 1-15.

Miyata, S., and Kitagawa, H. (2016). Chondroitin 6-Sulfation Regulates Perineuronal Net Formation by Controlling the Stability of Aggrecan. Neural plasticity; *2016*.

Morawski, M., Bruckner, G., Jager, C., Seeger, G., *et al.* (2012). Involvement of perineuronal and perisynaptic extracellular matrix in Alzheimer's disease neuropathology. Brain pathology; *22*: 547-561.

Morawski, M., Bruckner, M.K., Riederer, P., Bruckner, G., *et al.* (2004). Perineuronal nets potentially protect against oxidative stress. Experimental neurology; *188*: 309-315.

Morawski, M., Dityatev, A., Hartlage-Rubsamen, M., Blosa, M., *et al.* (2014). Tenascin-R promotes assembly of the extracellular matrix of perineuronal nets via clustering of aggrecan. Philosophical transactions of the Royal Society of London Series B, Biological sciences; *369*: 20140046.

Morikawa, S., Ikegaya, Y., Narita, M., and Tamura, H. (2017). Activation of perineuronal net-expressing excitatory neurons during associative memory encoding and retrieval. Scientific reports; *7*: 46024.

Murase, S., Lantz, C.L., and Quinlan, E.M. (2017). Light reintroduction after dark exposure reactivates plasticity in adults via perisynaptic activation of MMP-9. eLife; *6*.

Namsi, A., Nury, T., Hamdouni, H., Yammine, A., *et al.* (2018). Induction of Neuronal Differentiation of Murine N2a Cells by Two Polyphenols Present in the Mediterranean Diet Mimicking Neurotrophins Activities: Resveratrol and Apigenin. Diseases; *6*.

Neumann, H., Kotter, M.R., and Franklin, R.J. (2009). Debris clearance by microglia: an essential link between degeneration and regeneration. Brain : a journal of neurology; *132*: 288-295.

Pantazopoulos, H., Markota, M., Jaquet, F., Ghosh, D., *et al.* (2015). Aggrecan and chondroitin-6-sulfate abnormalities in schizophrenia and bipolar disorder: a postmortem study on the amygdala. Translational psychiatry; *5*: e496.

Paylor, J.W., Lins, B.R., Greba, Q., Moen, N., *et al.* (2016). Developmental disruption of perineuronal nets in the medial prefrontal cortex after maternal immune activation. Scientific reports; *6*.

Perry, V.H., and Holmes, C. (2014). Microglial priming in neurodegenerative disease. Nature reviews Neurology; *10*: 217-224.

Petanceska, S., Canoll, P., and Devi, L.A. (1996). Expression of rat cathepsin S in phagocytic cells. The Journal of biological chemistry; *271*: 4403-4409.

Pizzorusso, T., Medini, P., Berardi, N., Chierzi, S., *et al.* (2002). Reactivation of ocular dominance plasticity in the adult visual cortex. Science; *298*: 1248-1251.

Prut, L., and Belzung, C. (2003). The open field as a paradigm to measure the effects of drugs on anxiety-like behaviors: a review. European journal of pharmacology; *463*: 3-33.

Qin, X., Liu, X.X., Wang, Y., Wang, D., *et al.* (2021). Early life stress induces anxiety-like behavior during adulthood through dysregulation of neuronal plasticity in the basolateral amygdala. Life sciences; *285*: 119959.

Ren, P., Wu, D., Appel, R., Zhang, L., *et al.* (2020). Targeting the NLRP3 Inflammasome With Inhibitor MCC950 Prevents Aortic Aneurysms and Dissections in Mice. Journal of the American Heart Association; *9*: e014044.

Righi, M., Mori, L., De Libero, G., Sironi, M., *et al.* (1989). Monokine production by microglial cell clones. European journal of immunology; *19*: 1443-1448.

Sakaki, H., Tsukimoto, M., Harada, H., Moriyama, Y., *et al.* (2013). Autocrine regulation of macrophage activation via exocytosis of ATP and activation of P2Y11 receptor. PloS one; *8*: e59778.

Santoni, G., Cardinali, C., Morelli, M.B., Santoni, M., *et al.* (2015). Danger- and pathogen-associated molecular patterns recognition by pattern-recognition receptors and ion channels of the transient receptor potential family triggers the inflammasome activation in immune cells and sensory neurons. Journal of neuroinflammation; *12*: 21.

Schapiro, A.C., Reid, A.G., Morgan, A., Manoach, D.S., *et al.* (2019). The hippocampus is necessary for the consolidation of a task that does not require the hippocampus for initial learning. Hippocampus; *29*: 1091-1100.

Shin, E., Palmer, M.J., Li, M., and Fricker, R.A. (2012). GABAergic neurons from mouse embryonic stem cells possess functional properties of striatal neurons in vitro, and develop into striatal neurons in vivo in a mouse model of Huntington's disease. Stem cell reviews and reports; *8*: 513-531.

Siebert, J.R., Conta Steencken, A., and Osterhout, D.J. (2014). Chondroitin sulfate proteoglycans in the nervous system: inhibitors to repair. BioMed research international; *2014*: 845323.

Skrzypczak-Wiercioch, A., and Salat, K. (2022). Lipopolysaccharide-Induced Model of Neuroinflammation: Mechanisms of Action, Research Application and Future Directions for Its Use. Molecules; *27*.

Smith, A.P., and Creagh, E.M. (2022). Caspase-4 and -5 Biology in the Pathogenesis of Inflammatory Bowel Disease. Frontiers in pharmacology; *13*: 919567.

Smith, P.D., Coulson-Thomas, V.J., Foscarin, S., Kwok, J.C., *et al.* (2015). "GAG-ing with the neuron": The role of glycosaminoglycan patterning in the central nervous system. Experimental neurology; *274*: 100-114.

Soch, A., Sominsky, L., Younesi, S., De Luca, S.N., *et al.* (2020). The role of microglia in the second and third postnatal weeks of life in rat hippocampal development and memory. Brain Behavior and Immunity; *88*: 675-687.

Sun, X., Ren, Z., Pan, Y., and Zhang, C. (2016). Antihypoxic effect of miR-24 in SH-SY5Y cells under hypoxia via downregulating expression of neurocan. Biochemical and biophysical research communications; *477*: 692-699.

Szeska, C., Punjer, H., Riemann, S., Meinzer, M., *et al.* (2022). Stimulation of the ventromedial prefrontal cortex blocks the return of subcortically mediated fear responses. Translational psychiatry; *12*: 394.

Tansley, S., Gu, N., Guzmán, A.U., Cai, W.H., *et al.* (2022). Microglia-mediated degradation of perineuronal nets promotes pain. Science; *377*: 80-+.

Tanti, A., Belliveau, C., Nagy, C., Maitra, M., *et al.* (2022). Child abuse associates with increased recruitment of perineuronal nets in the ventromedial prefrontal cortex: a possible implication of oligodendrocyte progenitor cells. Molecular psychiatry; *27*: 1552-1561.

Tarakcioglu, E., Tastan, B., Arioz, B.I., Tufekci, K.U., *et al.* (2022). Melatonin Alters the miRNA Transcriptome of Inflammasome Activation in Murine Microglial Cells. Neurochemical research; *47*: 3202-3211.

Tastan, B., Arioz, B.I., Tufekci, K.U., Tarakcioglu, E., *et al.* (2021). Dimethyl Fumarate Alleviates NLRP3 Inflammasome Activation in Microglia and Sickness Behavior in LPS-Challenged Mice. Frontiers in immunology; *12*: 737065.

Tewari, B.P., Chaunsali, L., Prim, C.E., and Sontheimer, H. (2022). A glial perspective on the extracellular matrix and perineuronal net remodeling in the central nervous system. Frontiers in cellular neuroscience; *16*: 1022754.

Tufekci, K.U., Eltutan, B.I., Isci, K.B., and Genc, S. (2021). Resveratrol Inhibits NLRP3 Inflammasome-Induced Pyroptosis and miR-155 Expression in Microglia Through Sirt1/AMPK Pathway. Neurotoxicity research; *39*: 1812-1829.

Ueno, M., Fujita, Y., Tanaka, T., Nakamura, Y., *et al.* (2013). Layer V cortical neurons require microglial support for survival during postnatal development. Nature neuroscience; *16*: 543-551.

Unamuno, X., Gomez-Ambrosi, J., Ramirez, B., Rodriguez, A., *et al.* (2021). NLRP3 inflammasome blockade reduces adipose tissue inflammation and extracellular matrix remodeling. Cellular & molecular immunology; *18*: 1045-1057.

Venturino, A., Schulz, R., De Jesús-Cortés, H., Maes, M.E., *et al.* (2021). Microglia enable mature perineuronal nets disassembly upon anesthetic ketamine exposure or 60-Hz light entrainment in the healthy brain. Cell Rep; *36*.

Voet, S., Srinivasan, S., Lamkanfi, M., and van Loo, G. (2019). Inflammasomes in neuroinflammatory and neurodegenerative diseases. EMBO molecular medicine; *11*.

Wang, L., and Hauenstein, A.V. (2020). The NLRP3 inflammasome: Mechanism of action, role in disease and therapies. Molecular aspects of medicine; *76*: 100889.

Wegrzyn, D., Freund, N., Faissner, A., and Juckel, G. (2021). Poly I:C Activated Microglia Disrupt Perineuronal Nets and Modulate Synaptic Balance in Primary Hippocampal Neurons in vitro. Frontiers in synaptic neuroscience; *13*: 637549.

Wendimu, M.Y., and Hooks, S.B. (2022). Microglia Phenotypes in Aging and Neurodegenerative Diseases. Cells; *11*.

Ye, Q., and Miao, Q.L. (2013). Experience-dependent development of perineuronal nets and chondroitin sulfate proteoglycan receptors in mouse visual cortex. Matrix biology : journal of the International Society for Matrix Biology; *32*: 352-363.

You, Q., Gong, Q., Han, Y.Q., Pi, R., *et al.* (2020). Role of miR-124 in the regulation of retinoic acid-induced Neuro-2A cell differentiation. Neural regeneration research; *15*: 1133-1139.

Yu, Z., Chen, N., Hu, D., Chen, W., *et al.* (2020). Decreased Density of Perineuronal Net in Prelimbic Cortex Is Linked to Depressive-Like Behavior in Young-Aged Rats. Frontiers in molecular neuroscience; *13*: 4.

8. APPENDICES

8.1. Ethical Approvals

İZMİR BİYOTIP VE GENOM MERKEZİ
GİRİŞİMSEL OLMAYAN ARAŞTIRMALAR ETİK KURULU (İBG-GOEK)
KARARI

Toplantı Tarihi	: 28/05/2021	**Toplantı Günü**	: Cuma
Toplantı Sayısı	: 6	**Toplantı Saati**	: 12:00

Sayın Prof. Dr. Şermin GENÇ,

2021-016 Protokol No'lu; sorumlusu olduğunuz "NLRP3 inflamazom aktivasyonunun perinöronal ağlarda yarattığı değişikliklerin incelenmesi" başlıklı araştırmanın uygulanmasında etik açıdan sakınca olmadığına oy birliği ile karar verilmiştir.

Bilgilerinizi ve gereğini rica ederiz.

Prof. Dr. H. Alper BAĞRIYANIK
Başkan

Pandemi süresince online ortamda gerçekleştirilen toplantımızda alınan kararlar tek imzalı olarak düzenlenmektedir. Pandemi sona erdikten sonra ıslak imzalı karar belgesi teslim edilecektir.

İZMİR BİYOTIP VE GENOM MERKEZİ
HAYVAN DENEYLERİ YEREL ETİK KURULU (İBG-HADYEK)
KARARI

Toplantı Tarihi	: 25/01/2022	**Toplantı Günü**	: Salı
Toplantı Sayısı	: 2	**Toplantı Saati**	: 15:30

Sayın Dr. Öğr. Üyesi Kemal Uğur TÜFEKCI,

2022-002 Protokol No'lu; yürütücüsü olduğunuz "Mikroglial NLRP3 inflamazom aktivasyonunun GABAerjik ara nöron farklılaşmasına, sağ kalımına ve perinöronal ağlara etkisinin incelenmesi" başlıklı projenin uygulanmasında etik açıdan sakınca olmadığına oy birliği ile karar verilmiştir.

Bilgilerinizi ve gereğini rica ederiz.

Dr. Gülçin ÇAKAN AKDOĞAN **Başkan**	**Vet. Hek. Kerem ESMEN** **Başkan Yardımcısı**
Prof. Dr. Ensari GÜNELİ **Üye**	**Doç. Dr. Güneş ÖZHAN** **Üye**
Doç. Dr. Kasım DİRİL **Üye** (Katılmadı)	**Dr. Yavuz DOĞAN** **Üye**
Vet. Hek. Umur KELEŞ **Üye**	**Vet. Hek. Ceren ÜLKER** **Üye**
Vet. Hek. Gizem ARALAN **Üye**	**İrem KARADAŞ** **Üye**

8.2. Resume



EMRE TARAKÇIOĞLU

Personal Information

Contact Information

Contact Address	Dokuz Eylül
Phone	
Email	
Web Page	

Education Information

08 September 2017 - Now (7 Year 1 Month)
Doktora, Doktora, DOKUZ EYLÜL ÜNİVERSİTESİ, TÜRKİYE
İZMİR ULUSLARARASI BİYOTIP VE GENOM ENSTİTÜSÜ, MOLEKÜLER BİYOLOJİ VE GENETİK (DR) (İNGİLİZCE)
Diploma Number: -
Cumulative Grade Point Average: 3.96 / 4.0

15 February 2017 - 09 November 2017 (9 Month)
Doktora, Doktora, BAŞKENT ÜNİVERSİTESİ, TÜRKİYE
SAĞLIK BİLİMLERİ ENSTİTÜSÜ, TIBBİ BİYOLOJİ (DR)
Diploma Number: -
Cumulative Grade Point Average: 3.85 / 4.0

01 August 2012 - 01 February 2015 (2 Year 7 Month)
Yüksek Lisans, Tezsiz Program, RİJKSUNİVERSİTEİT GRONİNGEN - HOLLANDA, HOLLANDA
RİJKSUNİVERSİTEİT GRONİNGEN - HOLLANDA, RİJKSUNİVERSİTEİT GRONİNGEN - HOLLANDA

03 September 2007 - 23 June 2011 (3 Year 10 Month)
Lisans, Anadal/Normal Öğretim, BOĞAZİÇİ ÜNİVERSİTESİ, TÜRKİYE
FEN-EDEBİYAT FAKÜLTESİ, MOLEKÜLER BİYOLOJİ VE GENETİK PR. (İNGİLİZCE)
Diploma Number: 11540
Cumulative Grade Point Average: 3.05 / 4.0

Experience Information

September 2017 - Now (7 Year 2 Month) (Tam Zamanlı)
MİSAFİR ARAŞTIRMACI, DOKTORA ÖĞRENCİSİ, İZMİR BİYOTIP VE GENOM MERKEZİ

Foreign Language Information

İNGİLİZCE (Reading: İyi, Writing: İyi, Speaking: İyi)

JAPONCA (Reading: Orta, Writing: Orta, Speaking: Orta)

FRANSIZCA (Reading: Başlangıç, Writing: Başlangıç, Speaking: Başlangıç)

ALMANCA (Reading: Orta, Writing: Başlangıç, Speaking: Başlangıç)

Scientific Technological Activity Fields

Keywords	Mikroglia
	Nöron
	İnflamazom
	İnflamasyon

R&D Competency

Books	B. TAŞTAN, E. TARAKÇIOĞLU, Y. BİRİNCİ KUDU, Y. PARK & Ş. GENÇ, Role of Exosomal MicroRNAs in Cell-to-Cell Communication, M. YOUSEF & J. ALLMER [Editors], miRNomics: MicroRNA Biology and Computational Analysis(269 - 292), ISBN: 978-1-0716-1170-8, AMERİKA BİRLEŞİK DEVLETLERİ: Humana Press, 26 August 2021, Kitapta Bölüm.
Articles	E. TARAKCIOGLU, B. TASTAN, B. ARIOZ, K. U. TUFEKCI & S. GENC, Melatonin Alters the miRNA Transcriptome of Inflammasome Activation in Murine Microglial Cells, NEUROCHEMICAL RESEARCH, 2022, 0364-3190, 47, 10, 10.
	K. U. TUFEKCI, B. ALURAL, E. TARAKCIOGLU, T. SAN & S. GENC, Lithium inhibits oxidative stress-induced neuronal senescence through miR-34a, MOLECULAR BIOLOGY REPORTS, 2021, 0301-4851.
	B. TASTAN, B. I. ARIOZ, K. U. TUFEKCI, E. TARAKCIOGLU, C. P. GONUL, K. GENC & S. GENC, Dimethyl Fumarate Alleviates NLRP3 Inflammasome Activation in Microglia and Sickness Behavior in LPS-Challenged Mice, FRONTIERS IN IMMUNOLOGY, 2021, 1664-3224, 12, 15.
	B. I. ARIOZ, E. TARAKCIOGLU, M. OLCUM & S. GENC, The Role of Melatonin on NLRP3 Inflammasome Activation in Diseases, ANTIOXIDANTS, 2021, 2076-3921, 10, 7, 16.
	B. ARIOZ, B. TASTAN, E. TARAKCIOGLU, K. U. TUFEKCI, M. OLCUM, N. ERSOY, A. BAGRIYANIK, K. GENC & S. GENC et al., Melatonin Attenuates LPS-Induced Acute Depressive-Like Behaviors and Microglial NLRP3 Inflammasome Activation Through the SIRT1/Nrf2 Pathway, FRONTIERS IN IMMUNOLOGY, 2019, 1664-3224, 10.
Conference Papers	E. TARAKÇIOĞLU, B. GENÇ, K. U. TÜFEKCİ & Ş. GENÇ, Perinöronal ağların NLRP3 inflamazom aktivasyonu sonucunda kaybı, Sözlü Sunum, 22. Ulusal Sinirbilim Kongresi, 03 September 2024, 06 September 2024.
	E. TARAKÇIOĞLU, K. U. TÜFEKCİ & Ş. GENÇ, Neuronal Loss of Perineuronal Nets in Response to Microglial NLRP3 Inflammasome Activation, Sözlü Sunum, 6th International Conference on Natural Sciences and Technologies (ICONAT-2024), 30 May 2024, 01 June 2024, 26 - 26.
Projects	BAP, ARAŞTIRMACI, NLRP3 inflamazom aktivasyonunun perinöronal ağlarda yarattığı değişikliklerin incelenmesi, Enforcing Institution: İZMİR BİYOTIP VE GENOM MERKEZİ, Sponsor Institution: DOKUZ EYLÜL ÜNİVERSİTESİ (Yurt İçi) , 01 June 2022, 01 October 2023.

TÜBİTAK Scholarships and Fundings

Project Info

321S141, Mikroglial NLRP3 İnflamazom Aktivasyonunun GABAerjik Ara Nöron Farklılaşmasına, Sağ Kalımına ve Perinöronal Ağlara Etkisinin İncelenmesi, BİDEB Burslusu, Yürürlükte, SBAG - Sağlik Bi?li?mleri? Araştirma Destek Grubu, 3501 - Kariyer, ARDEB, Project Participation/Leave Dates: 7/21/22 - (), Project Start/End Dates: 4/1/22 - 4/1/24.

217S584, Alzheimer Hastalığının Tanısında ve Yayılımında Nöron Kökenli Ekzozomlar, Burslu, Sonuçlandı, SBAG - Sağlik Bi?li?mleri? Araştirma Destek Grubu, 1001 - Araştırma, ARDEB, Project Participation/Leave Dates: 7/23/18 - 10/1/19, Project Start/End Dates: 6/1/18 - 6/1/20.

BIDEB Supports

EMRE TARAKÇIOĞLU, Etkinlik Destekleri ve Eğitim Bursları Müdürlüğü, 2250-Lisansüstü Bursları Performans Programı, Destek Sona Erdi, 2022 - 1.

EMRE TARAKÇIOĞLU, Etkinlik Destekleri ve Eğitim Bursları Müdürlüğü, 2250-Lisansüstü Bursları Performans Programı, Destek Sona Erdi, 2023 - 1.

EMRE TARAKÇIOĞLU, Etkinlik Destekleri ve Eğitim Bursları Müdürlüğü, 2250-Lisansüstü Bursları Performans Programı, Destek Sona Erdi, 2023 - 2.

EMRE TARAKÇIOĞLU, Etkinlik Destekleri ve Eğitim Bursları Müdürlüğü, 2250-Lisansüstü Bursları Performans Programı, Destek Sona Erdi, 2024 - 1.

EMRE TARAKÇIOĞLU, Etkinlik Destekleri ve Eğitim Bursları Müdürlüğü, 2250-Lisansüstü Bursları Performans Programı, Destekleniyor, 2024 - 2.

EMRE TARAKÇIOĞLU, Etkinlik Destekleri ve Eğitim Bursları Müdürlüğü, 2205-Lisans Burs Programı, Bursu Kesildi, 2007, 10/1/07 - 7/6/11.

EMRE TARAKÇIOĞLU, Etkinlik Destekleri ve Eğitim Bursları Müdürlüğü, 2211-A Genel Yurt İçi Doktora Burs Programı, Destekleniyor, 2019 - 3, 10/1/19 - 9/30/24.

Number of Panelist/Observer/Reporter Jobs

Job	ARDEB	BIDEB	SCIENCE SOCIETY	UIDB	TEYDEB	Total
Refereeing/Panelist/Outer Consultant Count	0	0	0	0	0	0
Moderatorships Count	0	0	0	0	0	0
Number of Observer/Consultant Jobs	0	0	0	0	0	0
Number of Reporter Jobs	0	0	0	0	0	0
Not Attended Refereeing/Panelist/Outer	0	0	0	0	0	0

8.3. Publications Linked to the Thesis

Tarakcioglu, E., Tastan, B., Arioz, B.I., Tufekci, K.U., et al. (2022). Melatonin Alters the miRNA Transcriptome of Inflammasome Activation in Murine Microglial Cells. Neurochemical research; 47: 3202-3211.

(Copy of the publication is attached below)

Neurochemical Research (2022) 47:3202–3211
https://doi.org/10.1007/s11064-022-03674-1

ORIGINAL PAPER

Melatonin Alters the miRNA Transcriptome of Inflammasome Activation in Murine Microglial Cells

Emre Tarakcioglu[1,2] · Bora Tastan[1,2] · Burak I. Arioz[1,2] · Kemal Ugur Tufekci[4,5] · Sermin Genc[1,3]

Received: 26 February 2022 / Revised: 13 June 2022 / Accepted: 1 July 2022 / Published online: 16 July 2022
© The Author(s), under exclusive licence to Springer Science+Business Media, LLC, part of Springer Nature 2022

Abstract

Systemic inflammation can have devastating effects on the central nervous system via its resident immune cells, the microglia. One of the primary mediators of this inflammation is inflammasomes, multiprotein complexes that trigger a release of inflammatory proteins when activated. Melatonin, a hormone with anti-inflammatory effects, is an attractive candidate for suppressing such inflammation. In this study, we have investigated how melatonin alters the microRNA (miRNA) transcriptome of microglial cells. For that purpose, we have performed RNA sequencing on a lipopolysaccharide and adenosine triphosphate (LPS + ATP) induced NLR family pyrin domain containing 3 (NLRP3) inflammasome activation model in the N9 mouse microglial cell line, with and without melatonin pre-treatment. We have identified 136 differentially expressed miRNAs in cells exposed to LPS + ATP compared to controls and 10 differentially expressed miRNAs in melatonin pre-treated cells compared to the inflammasome group. We have identified miR-155-3p as a miRNA that is upregulated with inflammasome activation and downregulated with melatonin treatment. We further confirmed this pattern of miR-155-3p expression in the brains of mice injected intraperitoneally with LPS. Moreover, an overexpression study with miRNA-155-3p mimic supported the idea that the protective effects of melatonin in NLRP3 inflammasome activation are partly associated with miRNA-155-3p inhibition.

Keywords Melatonin · Microglia · NLRP3 inflammasome · microRNA · LPS · ATP

Abbreviations

ATP	Adenosine triphosphate
ASC	Apoptosis-associated speck-like protein containing a caspase activation and recruitment domain
CNS	Central nervous system
Ctrl	Control
GAPDH	Glyceraldehyde-3-phosphate dehydrogenase
GSDMD	Gasdermin D
IL	Interleukin
IP	Intraperitoneal
KEGG	Kyoto encyclopedia of genes and genomes
LA	LPS and ATP
LPS	Lipopolysaccharide
miRNA	MicroRNA
MLA	Melatonin and LPS and ATP
MT	Melatonin
NLRP3	NLR family pyrin domain containing protein 3
PBS	Phosphate-buffered saline
qPCR	Quantitative real-time PCR
TLR	Toll-like receptor

✉ Sermin Genc
sermin.genc@deu.edu.tr

[1] Izmir Biomedicine and Genome Center, 35340 Izmir, Balcova, Turkey

[2] Izmir International Biomedicine and Genome Institute, Dokuz Eylul University, 35340 Izmir, Turkey

[3] Department of Neuroscience, Institute of Health Sciences, Dokuz Eylul University, 35340 Izmir, Turkey

[4] Department of Health Care Services, Vocational School of Health Services, Izmir Democracy University, 35290 Izmir, Turkey

[5] Center for Brain and Neuroscience Research, Izmir Democracy University, 35290 Izmir, Turkey

Introduction

Microglia are the primary immune cells in the central nervous system (CNS), responsible for or auxiliary to the inflammatory processes that protect, regulate, and occasionally damage the neuronal milieu [1]. Inflammation in the brain involves a significant degree of inflammasome

activation [2]. Inflammasomes are multiprotein complexes activated in response to certain pathogenic or otherwise harmful molecules and initiate various inflammatory and secretory pathways. NLR Family Pyrin Domain Containing Protein 3 (NLRP3; also known as NALP3) is a well-characterized inflammasome implicated in the pathogenesis of many CNS diseases and injuries [3–5].

Various molecular signals can activate NLRP3, including pathogen-associated molecular patterns, extracellular adenosine triphosphate (ATP), potassium efflux, particulate aggregates, lysosomal or mitochondrial destabilization, and reactive oxygen species [6]. Upon activation on its ligand-sensing leucine-rich repeat domain, NLRP3 self-oligomerizes via its NACHT domain and recruits an adaptor protein called Apoptosis-associated Speck-like Protein containing a caspase activation and recruitment domain (ASC) on its pyrin domain [7]. The ASC proteins clustered on the NLRP3 complex then recruit the inactive enzyme Pro-caspase-1 on their caspase recruitment domains, resulting in proximity-induced cleavage of this enzyme into active caspase-1 [8]. Caspase-1 activates (by cleaving) the inactive forms of inflammatory cytokines Interleukin (IL)-1β and IL-18 and the pore-forming protein Gasdermin-D (GSDMD). Cell contents are secreted outside through pores made by active GSDMD and cause paracrine inflammatory effects [7, 8].

Melatonin is a hormone produced mainly by the pineal gland and conveys light information from the retina to the rest of the body, mediating the circadian rhythm [9]. While it is generally recognized as a hormone, melatonin also functions as a potent antioxidant; and is thought to be produced by any animal cell with mitochondria [10, 11]. In addition to its antioxidant activities, melatonin also has anti-inflammatory, anti-cancer, immune-regulatory, and neuroprotective effects [12]. The anti-inflammatory properties of melatonin also involve inhibition of the NLRP3 inflammasome [13, 14], making melatonin-associated pathways intriguing drug targets for regulation of inflammasome-mediated inflammation.

microRNAs (miRNAs) are small noncoding RNAs involved in the regulation of gene expression and consequently in many inter- and intracellular processes [15]. Several miRNAs have been investigated in the context of inflammation and inflammasomes. Among them, miR-155 and miR-146a have been observed multiple times as being upregulated in response to Toll-like receptor (TLR) signaling, with miR-155 either exacerbating or reducing, and miR-146a reducing inflammation [16]. miR-223, a miRNA that targets NLRP3, is also a crucial player in measures against inflammation [17, 18]. As a highly multifaceted molecule, melatonin influences the miRNA expression of cells and mediates part of its anti-inflammatory and anti-cancer effects through miRNAs [19–22]. Learning how melatonin changes the miRNA repertoire of microglial cells would shed light on how melatonin drives its neuroprotective and anti-inflammatory effects in microglia.

We have previously shown in the N9 microglial cell line that Lipopolysaccharide (LPS) and ATP induce activation of NLRP3 and that melatonin inhibits this induction, as demonstrated by altered levels of NLRP3 and mature caspase-1, IL-1β, and IL-18 [14]. In the current study, we aim to identify how the miRNA transcriptome of microglia changes in response to inflammasome activation and how this change is further altered in melatonin treatment.

Materials and Methods

Cell Culture

The N9 mouse microglial cell line was provided by Dr. Paola Ricciardi-Castagnoli (Cellular Pharmacology Center, Milan, Italy) [23]. Cells were cultured in a growth medium composed of RPMI 1640 with 10% fetal bovine serum, 2 mM L-glutamine, 100 u/ml penicillin, and 100 µg/ml streptomycin (all purchased from Thermo Fisher Scientific) at 37 °C with 5% CO_2. An experiment medium composed of RPMI 1640 with 2 mM L-glutamine (without serum or antibiotics) was used in experimental setups.

In Vitro NLRP3 Inflammasome Activation

Canonical NLRP3 inflammasome activation model was implemented in the study. NLRP3 inflammasome activation was induced by LPS (priming) and ATP (activation), as performed previously [14, 24, 25]. N9 cells were plated on 10 cm cell culture dishes at 3×10^6 cells/dish one day before the experiment. Before the experiment, the growth medium was removed and replaced with the experiment medium. Cells were divided into the following groups: control, LPS+ATP, and melatonin+LPS+ATP (hereafter referred to as Ctrl, LA, and MLA).

The MLA group was pre-treated with 0.5 mM melatonin (Sigma-Aldrich M5250; from an ethanol-dissolved stock of 200 mM), the other groups were incubated with medium without serum or antibiotics for 1 h. Post-incubation, LPS (InvivoGen, LPS from *E. Coli* 0111:B4) was applied at a concentration of 1 µg/ml (from a water-dissolved stock of 5 mg/ml) to the LPS+ groups, and cells were further incubated for 4 h. Finally, ATP (Sigma-Aldrich, A6419) was applied to the ATP+ groups at a concentration of 5 mM (from a Phosphate-buffered Saline (PBS, purchased from

Sigma-Aldrich) dissolved stock of 100 mM), and cells were incubated for 1 h. In all groups, previously added molecules were kept at a constant concentration throughout the experiment.

RNA Isolation

At the end of treatments, cells were scraped and centrifuged at 500 × *g*. Cell pellets were washed with PBS, and total RNA was isolated using a miRNeasy Mini Kit (QIAGEN). Brains from the animal experiment were placed in QIAzol lysis solution (QIAGEN) and homogenized on ice. Total RNA from the brains was also isolated with miRNeasy Mini Kit, according to kit instructions.

RNA Sequencing

Small RNA-seq and the analysis and annotation of the acquired data were performed by Novogene (Novogene (HK) Company Limited, Hong Kong). After passing quality control performed via Agilent 2100 Bioanalyzer (with an average RNA integrity number of 9.99), 3 µg of RNA per sample was used to prepare a small RNA library, using NEBNext Multiplex Small RNA Library Prep Set for Illumina. RNA was sequenced using Illumina SE50, with 10 million reads per sample. The raw data were mapped to the mouse genome using Bowtie [26], and miRNA alignment and annotations were performed via miRDeep2 [27] using miRBase 20 as reference. Expression comparison of groups was performed between normalized read counts of transcripts per million (TPM), where normalized read count is calculated as "mapped read count/total reads* 1,000,000". Differential expression analysis between groups was performed using the DESeq R package (1.8.3). The p-values were adjusted with the Benjamini & Hochberg method [28]. Corrected p-value of 0.05 was set as the threshold for significantly different expression.

Pathway Enrichment Analysis

Kyoto Encyclopedia of Genes and Genomes (KEGG) is a collection of manually curated databases related to genomes, biological pathways, diseases, drugs, and chemical substances [29]. In RNA-seq, KEGG analysis can reveal the main pathways associated with the target gene candidates. We have performed a pathway enrichment analysis using DIANA miRPath v.3 (https://dianalab.e-ce.uth.gr/html/mirpathv3/index.php) [30], which identifies significantly enriched metabolic pathways and signal transduction pathways associated with differentially expressed miRNA target genes, retrieved from TarBase [31]. Genes with adjusted p values smaller than 0.05 were considered significantly enriched.

Quantitative RT-PCR

cDNA for Quantitative real-time PCR (qPCR) was prepared via miScript II RT Kit (QIAGEN), and qPCR was performed using miScript SYBR-Green I kit (QIAGEN) and LightCycler 480 Instrument II (Roche Life Science, USA) according to the manufacturer's recommendations. Relative expression levels were measured by the $2^{-\Delta\Delta ct}$ method [32]. For normalization, U6 small nuclear RNA (Rnu6) was used. As primers, miScript Primer Assays (QIAGEN) were used (No. MS00024255 for miR-155-3p and No. MS00033740 for Rnu6).

In Vivo NLRP3 Inflammasome Activation

Male BALB/c mice, aged 12–16 weeks, were provided by Izmir Biomedicine and Genome Center Vivarium. All animals were maintained and housed in the vivarium under controlled conditions (22 ± 2 °C, 55 ± 10% humidity, 12 h light/dark periods) with access to food and water ad libitum. Mice were randomly divided into three groups with 7 animals per group: Ctrl, LPS, Melatonin + LPS. 5 mg/kg doses of LPS (LPS from *E. Coli* 055:B5) were injected intraperitoneally (IP). Melatonin was injected IP at a 30 mg/kg dose 4 times with 6 h intervals starting 2 h before LPS injection. The LA and Ctrl groups also received equivalent IP PBS injections at corresponding times. 24 h after LPS injection, the mice were sacrificed by decapitation; their brains were collected, flash-frozen in liquid nitrogen, and stored for analysis.

All animal studies and animal care were approved by Dokuz Eylul University Izmir International Biomedicine and Genome Institute Animal Experiments Local Ethics Committee (IBG-AELEC) (Protocol Number: 03/2018).

Transfection

miR-155-3p mimic transfection was performed using products and guidelines by QIAGEN. As mimic, Syn-mmu-miR-155-3p miScript miRNA Mimicy (No. 219600, MSY0000165) was used and as negative control (scramble-miRNA) miScript Inhibitor Negative Control (No. 1027272) was used; both at a final concentration of 20 nM. HiPerFect Transfection Reagent (No. 1029975) was used as the reagent, at double the volume of transfected miRNA. The miRNA-reagent mixture was prepared in growth medium and added dropwise to the growth medium of cells. Cells were then incubated at 37 °C for 48 h. At the end of this procedure, the medium was replaced and further experiments were performed.

ELISA

Secreted IL-1β levels in supernatants of NLRP3 inflammasome induction experiments were determined by mouse IL-1β enzyme-linked immunosorbent assay (ELISA) kits

(No. 88-7013-88, Thermo Fisher Scientific), using F96 Nunc™ Immuno Plates (Thermo Fisher Scientific), according to the manufacturer's instructions.

Statistical Analyses

Statistical analyses of non-RNA-seq data were performed on GraphPad Prism (version 8). Data are presented as mean ± SEM. Normality of the data was assessed by Shapiro–Wilk test. For parametric data with homogeneous variance, comparisons between two groups were analyzed by Student's *t*-test; and comparisons between multiple groups were analyzed by one-way ANOVA with Bonferroni multiple comparison corrections. For parametric data with heterogeneous variance, comparisons between multiple groups were analyzed with Brown-Forsythe ANOVA, with Games-Howell multiple comparison corrections. For non-parametric data, comparisons between two groups were analyzed with the Mann–Whitney *U*-test; and comparisons between more than two groups were analyzed with the Kruskal–Wallis test with Dunn's multiple comparisons. Statistical significance was set at $p < 0.05$.

Results

For miRNA transcriptome data of inflammatory N9 cells treated with melatonin, we performed the LPS+ATP induced NLRP3 inflammasome activation model from our previous study [14]. In brief, N9 cells were pre-treated with 0.5 mM melatonin for 1 h, then with 1 μg/ml LPS for 4 h, and finally with 5 mM ATP for 1 h (while keeping the concentrations of agents added at previous steps constant).

RNA sequencing performed on these cells identified various up- and down-regulated miRNAs in the inflammasome and the melatonin treated groups (Tables 1, 2). In the inflammasome activation group LA, we identified 58 up- and 78 down-regulated miRNAs compared to Ctrl. In contrast, in the melatonin pre-treated group MLA, we identified 43 up- and 55 down-regulated miRNAs compared to Ctrl, and 7 up- and 3 down-regulated miRNAs compared to LA (Fig. 1a). Among the significantly altered miRNAs in the inflammasome group, only one was seen to be significantly altered in the opposite direction in the melatonin group: miR-155-3p, which was upregulated with LPS+ATP treatment and downregulated with the addition of melatonin. The number of uniquely expressed miRNA in the Ctrl, LA, and MLA groups were 41, 5, and 14, respectively (Fig. 1b). A cluster analysis of the miRNA reads of the three groups shows that about 45% of miRNAs that are altered with LPS+ATP (bottom of the chart) are partially reverted to control levels with melatonin treatment (Fig. 1c).

To obtain a broad picture of pathways associated with altered miRNA in the LA and MLA groups (versus Ctrl and LA, respectively), we have performed a KEGG analysis on the RNA-seq results. The KEGG pathway analysis of miRNA reveals multiple common pathways that differentially expressed miRNAs in both LA vs. Ctrl and MLA vs. LA appear in; including inflammation-associated pathways like MAPK and FoxO signaling pathways (Fig. 2).

Table 1 The top ten most up-and down-regulated miRNAs in the LA (inflammasome) group versus the control group, sorted by fold change (n = 4)

miRNA	Fold change	Adjusted p-value
Upregulated in the inflammasome group vs. the control group		
mu-miR-378d	3.72	0.002568
mmu-miR-145a-5p	3.43	0.010218
mmu-miR-155-3p	3.01	7.75E-29
mmu-miR-215-5p	2.89	0.041301
mmu-miR-202-5p	2.88	0.030084
mmu-miR-7012-3p	2.79	0.04497
mmu-miR-215-3p	2.79	0.049725
mmu-miR-3058-3p	2.74	0.04714
mmu-miR-155-5p	2.56	1.96E-13
mmu-miR-96-5p	2.27	0.009007
Downregulated in the inflammasome group vs. the control group		
mmu-miR-27a-5p	0.05	7.32E-272
mmu-miR-6481	0.06	4.38E-29
mmu-miR-26a-2-3p	0.09	6.89E-12
mmu-miR-181b-1-3p	0.11	2.15E-29
mmu-miR-148a-5p	0.12	1.00E-144
mmu-miR-467b-3p	0.13	1.04E-07
mmu-miR-92a-1-5p	0.19	1.07E-43
mmu-miR-30b-3p	0.20	5.28E-46
mmu-miR-16-1-3p	0.21	1.46E-132
mmu-miR-703	0.21	0.000965

Table 2 Significantly up- and down-regulated miRNAs in the MLA (melatonin treatment group) versus the LA (inflammasome) group, sorted by fold change (n = 4; significance cut-off value for p-values is p = 0.05)

miRNA	Fold change	Adjusted p-value
Upregulated in the melatonin group vs. the inflammasome group		
mmu-miR-486a-5p	2.99	0.00013129
mmu-miR-486a-3p	2.98	0.00013129
mmu-miR-486b-3p	2.98	0.00013129
mmu-miR-1a-3p	2.89	0.041575
mmu-miR-1b-5p	2.87	0.041575
mmu-miR-451a	1.95	0.00057708
mmu-miR-363-3p	1.93	0.0051
Downregulated in the melatonin group vs. the inflammasome group		
mmu-miR-155-3p	0.64	4.91E-06
mmu-miR-27b-5p	0.67	0.0051
mmu-miR-21a-3p	0.76	0.04186

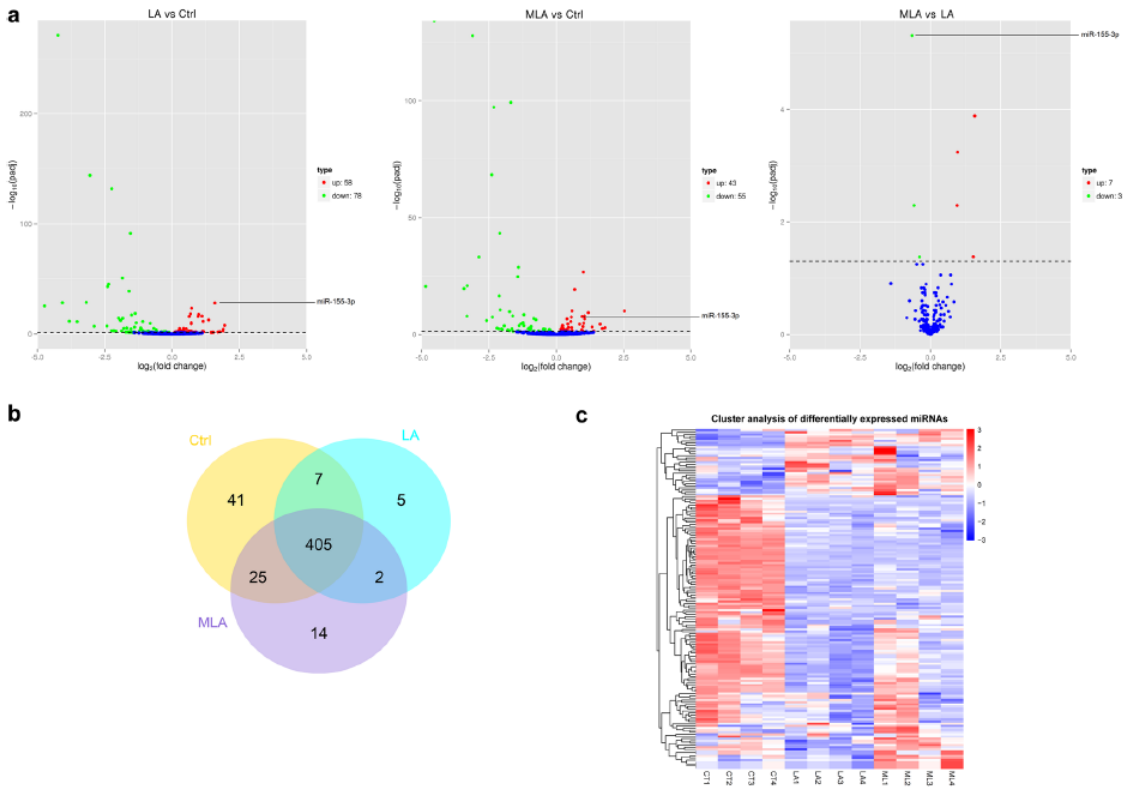

Fig. 1 Differential Expression and clustering analyses from the RNA-seq data of melatonin treatment in NLRP3 inflammasome activation model in N9 microglial cells. **a** Volcano plots of up- (red) and down- (green) regulated miRNAs between the pairs LA vs. Ctrl, MLA vs. Ctrl, and MLA vs. LA. miR-155-3p is indicated in the first and third plots. **b** Venn diagram showing numbers of uniquely expressed miRNAs in each group and co-expressed miRNAs between groups. **c** Cluster analysis of the experimental groups, where each column is a replicate, and each row is a miRNA. miRNAs are hierarchically clustered so that miRNAs that follow similar expression trends are grouped. The spectrum from red to blue represents $\log_{10}$ (TPM+1) values where red indicates upregulation and blue indicates downregulation. (LA: LPS+ATP, Ctrl: Control, MLA: Melatonin+LPS+ATP; cutoff p-value: 0.05)

As miR-155-3p was the only miRNA altered in reverse directions in the LA and MLA groups, we sought to confirm its expression pattern using qPCR. In N9 cells, we observed a rise in miR-155-3p expression in the inflammasome group and the reversal of this rise in the melatonin pre-treated group (Fig. 3a). We also replicated the finding in a mouse model of NLRP3 inflammasome activation: mice that were intraperitoneally injected with LPS had higher levels of miR-155-3p in their brains while this rise was reversed in LPS injected mice that were also injected with four doses of melatonin (Fig. 3b).

To understand the function miR-155-3p in the context of inflammasome activation, we overexpressed miR-155-3p in N9 cells using a miRNA mimic molecule (Fig. 4a). The in vitro NLRP3 activation model was applied post-transfection. At the end of the experiment, supernatants were collected and analyzed by an IL-1β ELISA kit. Overexpression of miR-155-3p reduced the protective effect of melatonin against IL-1β release in a statistically significant manner (from a 55% decrease in IL-1β secretion to 45%; $p = 0.031$), (Fig. 4b).

Discussion

We have shown previously that our LPS and ATP induced inflammasome activation model in N9 cells and LPS-induced in vivo inflammasome model in mice activated the NLRP3 inflammasome at both mRNA and protein levels [14]. In this study, we utilized RNA-seq analysis on the NLRP3 inflammasome activation model in N9 murine microglia to evaluate alterations of miRNA expression profiles. We identified numerous upregulated and downregulated miRNAs in the inflammasome activated group vs. the control group and the

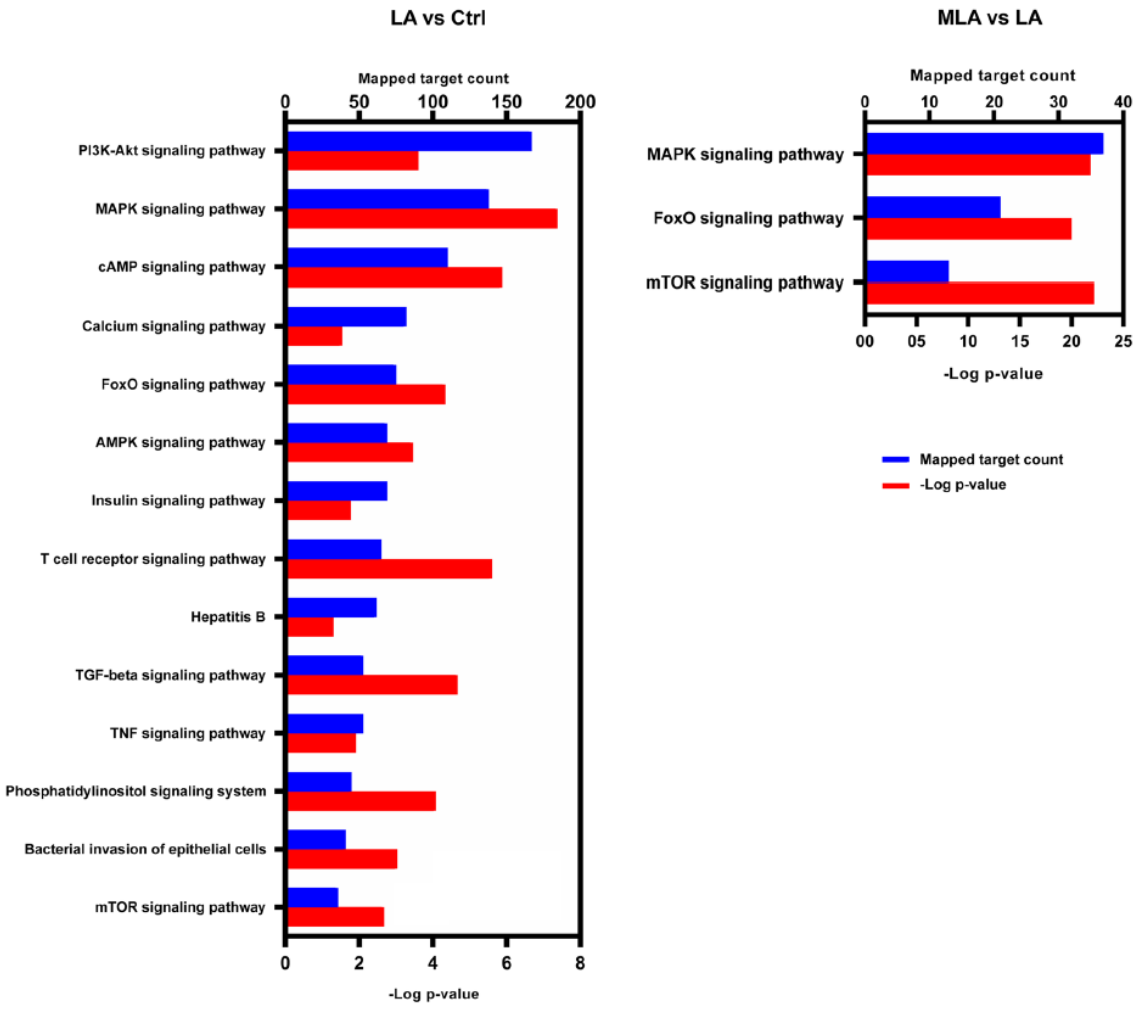

Fig. 2 miRNA target pathway analysis differentially expressed miRNAs in melatonin treatment in NLRP3 inflammasome activation model in N9 microglial cells. An inflammation-related subset of the list of pathways associated with the differentially expressed miRNA in comparisons between LA vs. Ctrl and MLA vs. LA, obtained from KEGG PATHWAY database (14 of 73 pathways in LA vs. Ctrl and 3 of 27 pathways in MLA vs. LA were included). Blue lines indicate the number of associated genes belonging to the corresponding pathway with the differentially expressed miRNAs between the compared groups. Red lines indicate the − log p-value, i.e., the degree of significance. (LA: LPS+ATP, Ctrl: Control, MLA: Melatonin+LPS+ATP; cutoff p-value: 0.05)

melatonin group vs. the inflammasome group (Tables 1, 2). Among them, we identified miR-155-3p as a potent miRNA that was upregulated with inflammasome activation and downregulated with melatonin treatment. Further, we confirmed this NLRP3 inflammasome and melatonin induced deregulation of miR-155-3p in N9 microglial cells and mouse brains via qPCR. Finally, we showed that miR-155-3p overexpression modestly but significantly reversed the protective effect of melatonin treatment against inflammasome activation.

Melatonin, as a multi-functional molecule, is naturally linked with the regulation of numerous miRNAs. Of those, miR-155-3p and miR-155-5p are two different miRNAs, processed from the same primary transcript (pri-mir-155) and generated from the same pre-miRNA molecule. miR-155-5p is more abundant than miR-155-3p in mouse and human tissues, likely due to having a higher affinity to being loaded into Argonaute [33, 34]. This is also the case in our RNA-seq data, where TPM values for miR-155-5p is 30–40 times higher than the values for miR-155-3p. Additionally, both miRs follow an up- and down-regulation pattern with LPS+ATP and melatonin, respectively; but only the changes in miR-155-3p is significant for

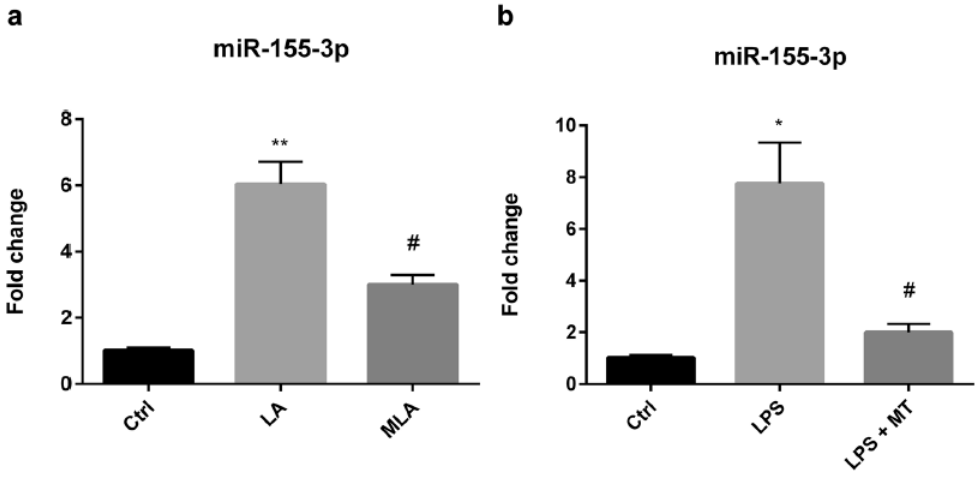

Fig. 3 Confirmation of the protective role of melatonin against LPS-induced miR-155-3p upregulation in N9 cells and mice. **a** Fold change in miR-155-3p expression in N9 cells (n = 7). **b** Fold change in miR-155-3p in brain homogenates of LPS-challenged mice with and without melatonin treatment (n = 7; MT: melatonin). (Data are presented as mean ± S.E.M. *p < 0.05 and **p < 0.01 compared to control; #p < 0.05 compared to the inflammasome group)

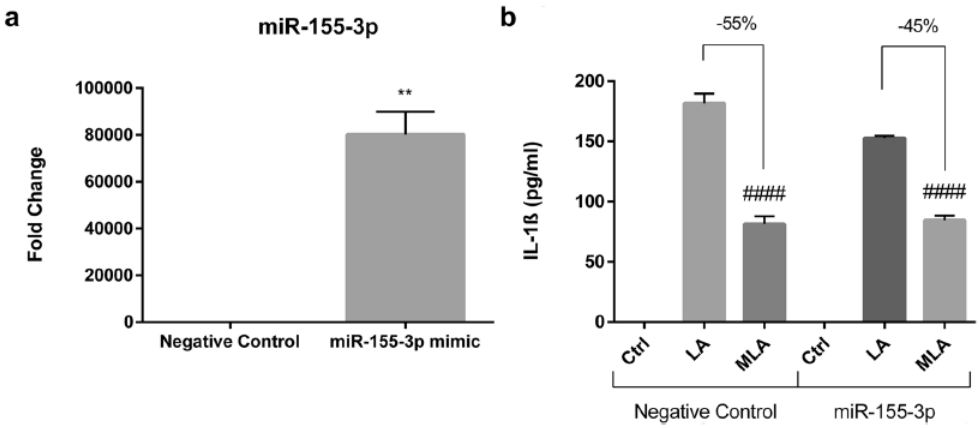

Fig. 4 Protective role of melatonin against inflammasome activation is decreased in N9 cells transfected with a miR-155-3p mimic molecule. **a** Efficiency of miR-155-3p mimic transfection (20 nM, 48 h), as shown by fold change of miR-155-3p in cells transfected with negative control miRNA and miR-155-3p mimic (n = 3). **b** Secreted IL-1β levels in supernatants of N9 cells, as measured by ELISA (n = 7). (Data are presented as mean ± S.E.M. **p < 0.01 compared to negative control; ####p < 0.0001 compared to the inflammasome groups within the respective transfections; control groups in **b** are not included in significance testing since their values are zero)

both interventions. Despite being produced from the same molecule, miR-155-3p is distinct from its partner strand (and not simply a byproduct). Changes in miR-155-3p expression profile can be substantially different from those of miR-155-5p [34]. For example, upon exposure of macrophages to LPS, TNF-α, and IL-1β, miR-155-3p expression peaks about 2–3 h earlier than miR-155-5p. On the other hand, the inflammatory agents poly (I:C) and Pam3Cys induce weaker miR-155 upregulation where both strands increase in a similar fashion[35]. Thus, it can be said that miR-155-3p can act independently from its partner strand. Notwithstanding this distinction, miR-155-5p has been extensively studied as a regulator in inflammatory pathways [36], whereas miR-155-3p remains relatively understudied.

Our data confirm the same LPS-induced expression pattern for miR-155-3p both in vitro and in vivo, pointing to

miR-155-3p as a miRNA potentially responsible for inflammation. Previous literature also lists multiple cases where miR-155-3p's expression is in parallel with induction of inflammation [35, 37–42]. Examples include elevated miR-155-3p in brain tissue in mouse models of multiple sclerosis [37, 38] and higher miR-155-3p expression in M1 vs. M2 polarized macrophages [40]. miR-155-3p is also reported to promote TNF-α expression in human fetal astrocytes and plasmacytoid dendritic cells (PDCs) [39, 41]. Nevertheless, other studies on miR-155-3p have revealed anti-inflammatory roles. In both monocytes and macrophages, it reduces TNF-α expression and upregulates IL-6 [43]. It targets Myd88, a critical player in inflammation via TLR signaling, in breast cancer cells [44]. It also targets lymphotoxin-beta, which contributes to NF-κB mediated inflammation, in mantle cell lymphoma [45]. Moreover, miR-155-3p appears to promote M2-like (anti-inflammatory) polarization in macrophages [46]. It is possible that miR-155-3p acts alongside miR-155-5p as a balancing molecule to the inflammatory effects of the 5p strand. An example of this is seen in, PDCs where the two miRNAs work antagonistically, with miR-155-3p promoting and miR-155-5p suppressing type I interferon production [41]. Ultimately, these contradictory findings in the literature suggest the role of miR-155- in inflammation is dependent on cell type and disease model. To date, no study has shown an effect of melatonin on miR-155-3p in any model. Here, we show for the first time that melatonin downregulates an inflammation-induced increase in miR-155-3p. To examine how miR-155-3p might be affecting the NLRP3 inflammasome model itself, we have performed an overexpression experiment where we measured IL-1β levels in N9 cells transfected with miR-155-3p. The data from this indicate that miR-155-3p reduces the protective effect of melatonin.

The downregulated and upregulated miRNAs in our data were shown in previous studies to be involved in inflammatory pathways in many ways. In a study, small RNA-seq profiling showed that miR-486a-5p may stimulate RAW264.7 murine macrophage cells towards an M2 phenotype [47]. Zhang et al. demonstrated that Kcnq1ot1, a long noncoding RNA, activated pyroptosis in MPC5 mouse podocyte cells by blocking miR-486a-3p, which restrains NLRP3 expression [48]. Moreover, ADAR1 (Adenosine Deaminase RNA Specific)/miR-1a-3p signaling was shown to regulate A20 (TNFα-induced protein 3), which decreases cardiomyocyte inflammation and apoptosis in a viral mouse myocarditis model [49]. A study on miR-451a pointed out that elevated miR-451a levels were detected in the serum of sepsis and septic shock patients, and it was proposed as a sepsis biomarker.[50]. miR-363-3p prevents apoptosis, oxidative stress injury, and inflammatory reactions in a mouse atherosclerosis model and coronary artery endothelial cells [51]. This miRNA is also reported to increase in the plasma exosomes of rats treated with melatonin [52]. In a mouse EAE model, Δ9-Tetrahydrocannabinol and Cannabidiol introduction improved EAE score and repressed neuroinflammation via downregulating miR-27b-5p and other six miRNAs [53]. Lastly, miR-21a-3p was shown to increase the severity of sepsis in a rat CLP model [54].

Melatonin treatment has previously been shown to alter other miRNAs. Its use in non-alcoholic fatty liver disease results in reduced expression of miR-34a, a pro-inflammatory miRNA upregulated in various diseases [22, 55]. Other miRNAs reported to be downregulated by melatonin include miR-23a, miR-155-5p, miR-212 [22]. These three miRNAs, along with miR-34a, suppress the activity of sirtuin-1 (SIRT1), a deacetylase that appears to be a mediator of the anti-inflammatory and antioxidant activities of melatonin [56]. Melatonin also increases miR-223 [57], which targets and downregulates NLRP3 [18, 58].

To attain further insight into the pathways associated with the differentially expressed miRNAs in our study, we performed a KEGG pathway enrichment analysis. The miRNA expression in the LA and MLA groups had significant alterations in the MAPK and FoxO pathways, which are associated with regulation of inflammation [59, 60] and are thus predictable pathways in the context of inflammasome activation or melatonin treatment.

In summary, the role of miR-155-3p in inflammation is ambiguous. In this study, we reproduce its upregulation in response to LPS and we show for the first time its downregulation in response to melatonin. We further show that it reduces, modestly, the protective effect of melatonin against inflammasome activation. Our sequencing has also revealed other, lesser-known miRNAs altered with inflammation or melatonin treatment. Pursuing their targets and functions in the context of inflammation is likely to elucidate the field further.

Acknowledgements The authors would like to thank IBG vivarium members, and Professor Doctor Pembe Keskinoğlu for their contributions.

Author Contributions KUT and SG designed the study. ET, BT, and BIA designed and performed the experiments. ET, BT, BIA, KUT, and SG analyzed and interpreted the data. ET, BT, BIA, KUT, and SG wrote the manuscript. All authors contributed to the article and approved the submitted version.

Funding The study was funded by Dokuz Eylul University Department of Scientific Research Projects (DEU-BAP, Project No: 2018. KB.SAG.078).

Data Availability The RNA-seq datasets analyzed within this study are available upon request to the corresponding author.

Declarations

Conflict of interest The authors declare no financial or non-financial interest regarding this article.

Ethical Approval In vivo studies were performed under the approval of, and following the regulations set by Izmir International Biomedicine and Genome Institute Local Ethics Committee for Animal Experiments (IBG-AELEC, protocol number: 03/2018).

References

1. Kawabori M, Yenari MA (2015) The role of the microglia in acute CNS injury. Metab Brain Dis 30:381–392. https://doi.org/10.1007/s11011-014-9531-6
2. Walsh JG, Muruve DA, Power C (2014) Inflammasomes in the CNS. Nat Rev Neurosci 15:84–97. https://doi.org/10.1038/nrn3638
3. Sarkar S et al (2017) Mitochondrial impairment in microglia amplifies NLRP3 inflammasome proinflammatory signaling in cell culture and animal models of Parkinson's disease. NPJ Parkinson's Dis 3:30. https://doi.org/10.1038/s41531-017-0032-2
4. Song L, Pei L, Yao S, Wu Y, Shang Y (2017) NLRP3 inflammasome in neurological diseases, from functions to therapies. Front Cell Neurosci 11:63. https://doi.org/10.3389/fncel.2017.00063
5. Shi F, Yang L, Kouadir M, Yang Y, Wang J, Zhou X, Yin X, Zhao D (2012) The NALP3 inflammasome is involved in neurotoxic prion peptide-induced microglial activation. J Neuroinflamm 9:73. https://doi.org/10.1186/1742-2094-9-73
6. Jo EK, Kim JK, Shin DM, Sasakawa C (2016) Molecular mechanisms regulating NLRP3 inflammasome activation. Cell Mol Immunol 13:148–159. https://doi.org/10.1038/cmi.2015.95
7. Schroder K, Tschopp J (2010) The inflammasomes. Cell 140:821–832. https://doi.org/10.1016/j.cell.2010.01.040
8. Heneka MT, McManus RM, Latz E (2018) Inflammasome signalling in brain function and neurodegenerative disease. Nat Rev Neurosci 19:610–621. https://doi.org/10.1038/s41583-018-0055-7
9. Claustrat B, Leston J (2015) Melatonin: physiological effects in humans. Neurochirurgie 61:77–84. https://doi.org/10.1016/j.neuchi.2015.03.002
10. Cardinali DP (2019) Melatonin: clinical perspectives in neurodegeneration. Front Endocrinol 10:480. https://doi.org/10.3389/fendo.2019.00480
11. Zhao D, Yu Y, Shen Y, Liu Q, Zhao Z, Sharma R, Reiter RJ (2019) Melatonin synthesis and function: evolutionary history in animals and plants. Front Endocrinol 10:249. https://doi.org/10.3389/fendo.2019.00249
12. Meng X, Li Y, Li S, Zhou Y, Gan RY, Xu DP, Li HB (2017) Dietary sources and bioactivities of melatonin. Nutrients. https://doi.org/10.3390/nu9040367
13. Arioz BI, Tarakcioglu E, Olcum M, Genc S (2021) The role of melatonin on NLRP3 inflammasome activation in diseases. Antioxidants. https://doi.org/10.3390/antiox10071020
14. Arioz BI, Tastan B, Tarakcioglu E, Tufekci KU, Olcum M, Ersoy N, Bagriyanik A, Genc K, Genc S (2019) Melatonin attenuates LPS-induced acute depressive-like behaviors and microglial NLRP3 inflammasome activation through the SIRT1/Nrf2 pathway. Front Immunol 10:1511. https://doi.org/10.3389/fimmu.2019.01511
15. Raisch J, Darfeuille-Michaud A, Nguyen HT (2013) Role of microRNAs in the immune system, inflammation and cancer. World J Gastroenterol 19:2985–2996. https://doi.org/10.3748/wjg.v19.i20.2985
16. Boxberger N, Hecker M, Zettl UK (2019) Dysregulation of inflammasome priming and activation by MicroRNAs in human immune-mediated diseases. J Immunol 202:2177–2187. https://doi.org/10.4049/jimmunol.1801416
17. Zhao G, Jiang K, Yang Y, Zhang T, Wu H, Shaukat A, Qiu C, Deng G (2018) The potential therapeutic role of miR-223 in bovine endometritis by targeting the NLRP3 inflammasome. Front Immunol 9:1916. https://doi.org/10.3389/fimmu.2018.01916
18. Neudecker V et al (2017) Myeloid-derived miR-223 regulates intestinal inflammation via repression of the NLRP3 inflammasome. J Exp Med 214:1737–1752. https://doi.org/10.1084/jem.20160462
19. Chuffa LGA, Carvalho RF, Justulin LA, Cury SS, Seiva FRF, Jardim-Perassi BV, Zuccari D, Reiter RJ (2020) A meta-analysis of microRNA networks regulated by melatonin in cancer: portrait of potential candidates for breast cancer treatment. J Pineal Res 69:e12693. https://doi.org/10.1111/jpi.12693
20. Lu J, Luo Y, Mei S, Fang Y, Zhang J, Chen S (2021) The effect of melatonin modulation of non-coding RNAs on central nervous system disorders: an updated review. Curr Neuropharmacol 19:3–23. https://doi.org/10.2174/1570159X18666200503024700
21. Ferreira LC, Orso F, Dettori D, Lacerda JZ, Borin TF, Taverna D, Zuccari D (2020) The role of melatonin on miRNAs modulation in triple-negative breast cancer cells. PLoS ONE 15:e0228062. https://doi.org/10.1371/journal.pone.0228062
22. Hardeland R (2019) Aging, melatonin, and the pro- and anti-inflammatory networks. Int J Mol Sci. https://doi.org/10.3390/ijms20051223
23. Righi M, Mori L, De Libero G, Sironi M, Biondi A, Mantovani A, Donini SD, Ricciardi-Castagnoli P (1989) Monokine production by microglial cell clones. Eur J Immunol 19(8):1443–1448. https://doi.org/10.1002/eji.1830190815
24. Zha QB, Wei HX, Li CG, Liang YD, Xu LH, Bai WJ, Pan H, He XH, Ouyang DY (2016) ATP-induced inflammasome activation and pyroptosis is regulated by AMP-activated protein kinase in macrophages. Front Immunol 7:597. https://doi.org/10.3389/fimmu.2016.00597
25. Tastan B, Arioz BI, Tufekci KU, Tarakcioglu E, Gonul CP, Genc K, Genc S (2021) Dimethyl fumarate alleviates NLRP3 inflammasome activation in microglia and sickness behavior in LPS-challenged mice. Front Immunol 12:737065. https://doi.org/10.3389/fimmu.2021.737065
26. Langmead B, Trapnell C, Pop M, Salzberg SL (2009) Ultrafast and memory-efficient alignment of short DNA sequences to the human genome. Genome Biol 10:R25. https://doi.org/10.1186/gb-2009-10-3-r25
27. Friedlander MR, Mackowiak SD, Li N, Chen W, Rajewsky N (2012) miRDeep2 accurately identifies known and hundreds of novel microRNA genes in seven animal clades. Nucleic Acids Res 40:37–52. https://doi.org/10.1093/nar/gkr688
28. Chen SY, Feng Z, Yi X (2017) A general introduction to adjustment for multiple comparisons. J Thorac Dis 9:1725–1729
29. Kanehisa M et al (2008) KEGG for linking genomes to life and the environment. Nucleic Acids Res 36:D480–D484. https://doi.org/10.1093/nar/gkm882
30. Vlachos IS, Zagganas K, Paraskevopoulou MD, Georgakilas G, Karagkouni D, Vergoulis T, Dalamagas T, Hatzigeorgiou AG (2015) DIANA-miRPath v3.0: deciphering microRNA function with experimental support. Nucleic Acids Res 43:W460–W466. https://doi.org/10.1093/nar/gkv403
31. Karagkouni D et al (2018) DIANA-TarBase v8: a decade-long collection of experimentally supported miRNA-gene interactions. Nucleic Acids Res 46:D239–D245. https://doi.org/10.1093/nar/gkx1141

32. Livak KJ, Schmittgen TD (2001) Analysis of relative gene expression data using real-time quantitative PCR and the 2(−Delta Delta C (T)) method. Methods 25:402–408. https://doi.org/10.1006/meth.2001.1262
33. Chiang HR et al (2010) Mammalian microRNAs: experimental evaluation of novel and previously annotated genes. Genes Dev 24:992–1009. https://doi.org/10.1101/gad.1884710
34. Dawson O, Piccinini AM (2022) miR-155-3p: processing by-product or rising star in immunity and cancer? Open Biol 12:220070. https://doi.org/10.1098/rsob.220070
35. Simmonds RE (2019) Transient up-regulation of miR-155–3p by lipopolysaccharide in primary human monocyte-derived macrophages results in RISC incorporation but does not alter TNF expression. Wellcome Open Res 4:43
36. Mahesh G, Biswas R (2019) MicroRNA-155: a master regulator of inflammation. J Interf Cytokine Res 39:321–330. https://doi.org/10.1089/jir.2018.0155
37. Gholami S, Mirian M, Eftekhari SM, Aliomrani M (2020) Apamin administration impact on miR-219 and miR-155-3p expression in cuprizone induced multiple sclerosis model. Mol Biol Rep 47:9013–9019. https://doi.org/10.1007/s11033-020-05959-6
38. Mazloumfard F, Mirian M, Eftekhari SM, Aliomrani M (2020) Hydroxychloroquine effects on miR-155-3p and miR-219 expression changes in animal model of multiple sclerosis. Metab Brain Dis 35:1299–1307. https://doi.org/10.1007/s11011-020-00609-z
39. Tarassishin L, Loudig O, Bauman A, Shafit-Zagardo B, Suh HS, Lee SC (2011) Interferon regulatory factor 3 inhibits astrocyte inflammatory gene expression through suppression of the proinflammatory miR-155 and miR-155*. Glia 59:1911–1922. https://doi.org/10.1002/glia.21233
40. Lu L, McCurdy S, Huang S, Zhu X, Peplowska K, Tiirikainen M, Boisvert WA, Garmire LX (2016) Time Series miRNA-mRNA integrated analysis reveals critical miRNAs and targets in macrophage polarization. Sci Rep 6:37446. https://doi.org/10.1038/srep37446
41. Zhou H, Huang X, Cui H, Luo X, Tang Y, Chen S, Wu L, Shen N (2010) miR-155 and its star-form partner miR-155* cooperatively regulate type I interferon production by human plasmacytoid dendritic cells. Blood 116:5885–5894. https://doi.org/10.1182/blood-2010-04-280156
42. Yuan Z et al (2016) TREM-1-accentuated lung injury via miR-155 is inhibited by LP17 nanomedicine. Am J Physiol Lung Cell Mol Physiol 310:L426–L438. https://doi.org/10.1152/ajplung.00195.2015
43. Marques-Rocha JL, Garcia-Lacarte M, Samblas M, Bressan J, Martinez JA, Milagro FI (2018) Regulatory roles of miR-155 and let-7b on the expression of inflammation-related genes in THP-1 cells: effects of fatty acids. J Physiol Biochem 74:579–589. https://doi.org/10.1007/s13105-018-0629-x
44. Zhang L et al (2019) MiR-155-3p acts as a tumor suppressor and reverses paclitaxel resistance via negative regulation of MYD88 in human breast cancer. Gene 700:85–95. https://doi.org/10.1016/j.gene.2019.02.066
45. Yim RL et al (2014) Methylation of miR-155–3p in mantle cell lymphoma and other non-Hodgkin's lymphomas. Oncotarget 5:9770–82
46. Xu J et al (2021) Hypoxic glioma-derived exosomes promote M2-like macrophage polarization by enhancing autophagy induction. Cell Death Dis 12:373. https://doi.org/10.1038/s41419-021-03664-1
47. Zhou X et al (2017) Characterization of mouse serum exosomal small RNA content: the origins and their roles in modulating inflammatory response. Oncotarget 8:42712–42727
48. Zhang C, Gong Y, Li N, Liu X, Zhang Y, Ye F, Guo Q, Zheng J (2021) Long noncoding RNA Kcnq1ot1 promotes sC5b-9-induced podocyte pyroptosis by inhibiting miR-486a-3p and upregulating NLRP3. Am J Physiol Cell Physiol 320:C355–C364. https://doi.org/10.1152/ajpcell.00403.2020
49. Li B, Xie X (2022) A20 (TNFAIP3) alleviates viral myocarditis through ADAR1/miR-1a-3p-dependent regulation. BMC Cardiovasc Disord 22:10. https://doi.org/10.1186/s12872-021-02438-z
50. Wang H, Cui W, Qiao L, Hu G (2020) Overexpression of miR-451a in sepsis and septic shock patients is involved in the regulation of sepsis-associated cardiac dysfunction and inflammation. Genet Mol Biol 43:e20200009. https://doi.org/10.1590/1678-4685-GMB-2020-0009
51. Zhou T, Li S, Yang L, Xiang D (2021) microRNA-363–3p reduces endothelial cell inflammatory responses in coronary heart disease via inactivation of the NOX4-dependent p38 MAPK axis. Aging 13:11061–11082
52. Wang K et al (2020) Melatonin enhances the therapeutic effect of plasma exosomes against cerebral ischemia-induced pyroptosis through the TLR4/NF-kappaB pathway. Front Neurosci 14:848. https://doi.org/10.3389/fnins.2020.00848
53. Al-Ghezi ZZ, Miranda K, Nagarkatti M, Nagarkatti PS (2019) Combination of cannabinoids, delta9- tetrahydrocannabinol and cannabidiol, ameliorates experimental multiple sclerosis by suppressing neuroinflammation through regulation of miRNA-mediated signaling pathways. Front Immunol 10:1921. https://doi.org/10.3389/fimmu.2019.01921
54. Zou Z, Lin Q, Yang H, Liu Z, Zheng S (2020) Nrp-1 mediated plasmatic ago2 binding miR-21a-3p internalization: a novel mechanism for miR-21a-3p accumulation in renal tubular epithelial cells during sepsis. Biomed Res Int 2020:2370253. https://doi.org/10.1155/2020/2370253
55. Stacchiotti A, Grossi I, Garcia-Gomez R, Patel GA, Salvi A, Lavazza A, De Petro G, Monsalve M, Rezzani R (2019) Melatonin effects on non-alcoholic fatty liver disease are related to MicroRNA-34a-5p/Sirt1 axis and autophagy. Cells. https://doi.org/10.3390/cells8091053
56. Hardeland R (2018) Melatonin and inflammation-Story of a double-edged blade. J Pineal Res 65:e12525. https://doi.org/10.1111/jpi.12525
57. Zhang Y et al (2018) Melatonin prevents endothelial cell pyroptosis via regulation of long noncoding RNA MEG3/miR-223/NLRP3 axis. J Pineal Res. https://doi.org/10.1111/jpi.12449
58. Zhu J, Yang J, Xu J (2021) miR-223 inhibits the polarization and recruitment of macrophages via NLRP3/IL-1beta pathway to meliorate neuropathic pain. Pain Res Manag 2021:6674028. https://doi.org/10.1155/2021/6674028
59. Fan W, Morinaga H, Kim JJ, Bae E, Spann NJ, Heinz S, Glass CK, Olefsky JM (2010) FoxO1 regulates Tlr4 inflammatory pathway signalling in macrophages. EMBO J 29:4223–4236. https://doi.org/10.1038/emboj.2010.268
60. Arthur JS, Ley SC (2013) Mitogen-activated protein kinases in innate immunity. Nat Rev Immunol 13:679–692. https://doi.org/10.1038/nri3495

Publisher's Note Springer Nature remains neutral with regard to jurisdictional claims in published maps and institutional affiliations.